# WEARABLE DEVICES FOR PHYSICAL ASSISTANCE: ENHANCING CAPABILITIES AFTER STROKE AND IN RUNNING

A DISSERTATION
SUBMITTED TO THE DEPARTMENT OF MECHANICAL ENGINEERING
AND THE COMMITTEE ON GRADUATE STUDIES
OF STANFORD UNIVERSITY
IN PARTIAL FULFILLMENT OF THE REQUIREMENTS
FOR THE DEGREE OF
DOCTOR OF PHILOSOPHY

Cole Simpson

June 2020



This dissertation is online at: http://purl.stanford.edu/pw966rc4511

I certify that I have read this dissertation and that, in my opinion, it is fully adequate in scope and quality as a dissertation for the degree of Doctor of Philosophy.

**Allison Okamura, Primary Adviser**

I certify that I have read this dissertation and that, in my opinion, it is fully adequate in scope and quality as a dissertation for the degree of Doctor of Philosophy.

**Steve Collins**

I certify that I have read this dissertation and that, in my opinion, it is fully adequate in scope and quality as a dissertation for the degree of Doctor of Philosophy.

**Elliot Hawkes,**

Approved for the Stanford University Committee on Graduate Studies.

**Stacey F. Bent, Vice Provost for Graduate Education**

*This signature page was generated electronically upon submission of this dissertation in electronic format. An original signed hard copy of the signature page is on file in University Archives.*

# Abstract

Exoskeletal robots can augment human motor abilities in tasks such as walking, lifting heavy objects, and performing therapies after motor impairing illness or injury. Yet, developing exoskeletal robots that can safely interact with human operators is a difficult engineering challenge. As a result, many commercially available exoskeletons are expensive, limiting access to them. Limited access implies limited usefulness, particularly for motor impaired populations that might benefit from increased volumes of robot-aided therapies. Exosuits simplify exoskeletal robot development by foregoing the rigid linkages that normally act as a transmission and apply forces generated by actuators directly to the human body. Removing the rigid linkages removes components and mass from the robot, reducing cost and some safety concerns. Passive exoskeletons and exotendons further reduce components and simplify safety considerations using springs and clutches in lieu of electronically controlled motors and pneumatics. In this thesis, we leverage insights from neuromechanics to design, build, and test simple assistive devices that aid post-stroke upper extremity movements and improve running economy.

In the first part of this thesis, we design, build, and test in both unimpaired and stroke impaired populations novel inflatable exosuit actuators to support shoulder abduction which can increase reachable workspace area in the unassisted horizontal plane in stroke survivors. The exosuit actuators, or "exomuscles," we developed are pneumatically actuated bladders that push the arm away from the torso when inflated to support shoulder abduction. We validate that our exomuscles reduce the activity of shoulder abductor muscles without impeding range of motion in healthy operators and that they increase reachable workspace area in the unassisted horizontal plane in

stroke survivors. We provide data demonstrating that some devices might produce the same effect in healthy operators, but show diverging effects in a stroke population – important cautionary data for investigators that primarily validate designs in healthy operators. We also design, build, and characterize in healthy participants an inexpensive passive wearable exoskeleton for shoulder abduction support that can be used for take-home assistance.

In the second part of this thesis, we develop a passive wearable exotendon that improves healthy human running economy. Our exotendon is constructed of a single length of natural latex rubber attached to the shoes, and acts as an energy recycling spring intended to assist the hip muscles in swinging the leg during running. Exotendon use increases the energetically optimal stride frequency of running, allowing runners to select faster stride frequencies that reduce the mechanical effort required to redirect the body's center of mass. This exotendon is a minimally complex, inexpensive device that also sheds light on some of the behavioral adaptations that humans employ to make use of wearable assistive devices.

The work presented in this thesis leverages neuromechanical insights to create wearable, inexpensive devices that aid in post-stroke upper extremity movement and in healthy human running. In turn, some of these devices led to new neuromechanical insights. These low-cost, wearable alternatives to existing assistive devices may enable further discoveries about long-term use of assistive devices and the effects of larger doses of assisted therapies.

# Acknowledgements

There is no standard path that leads from rural towns in the southeastern United States to the elite American universities, such as Stanford. My arrival at Stanford from Bowdon, Georgia was due largely to ignorance of or disregard for this lack of infrastructure and the generosity and kindness of others.

I would like to thank my parents. My disposition has always been one of discontent, which inevitably grows tiresome for those endeavoring to spend significant time with me. For my parents, John and Donna Simpson, in particular, my preferred question, "But why do it this way?" surely has proven particularly irksome. Nevertheless, they have given me every support that they knew how to give. It cannot have been easy to allow and facilitate their eldest son's embarkation at 16 on a series of increasingly far-flung and alien adventures, yet their support has never wavered even if they themselves have begun to wonder, "But why do it this way?"

My brother, aunt, and grandparents (John D. Simpson, Frances Iverson, and Bud and Idell Simpson, respectively) always served as bastions of kindness and generosity. My brother was the scientifically minded person in the family, always closely examining the life and elements around him with such intensity that he often neglected the baseball or football game in which we were engaged. Though we had no examples of professional scientists or engineers in our community, his preoccupation with the concept and his subscription to Popular Mechanics magazine first inspired me to consider this track. My aunt Frances, a longtime elementary and primary school teacher, always encouraged us to pursue our interests, often stepping in with rhymes and songs honed through a long career to encourage focus and motivation. Frances has always enjoyed sharing a private joke with me that rarely phased the stony faces

– variants on American Gothic – that seemed to populate my childhood. My grandparents regarded hard work above all else. As career farmers and factory workers, hard work was the only way to accomplish anything in life. Though my circumstances in the last decade have rarely resembled those of my grandparents, my observations support their convictions.

Without the support of a great community at Georgia Tech, I not be here today. Lena Ting, Hongchul Sohn, and Jeffrey Bingham in particular taught me many lessons about how to do research that I still strive to employ and that have shaped everything that I have done. Karen Adams and Jeffrey Donnell supported my applications for the NSF GRFP and Fulbright Scholarship, which allowed for me to come here and to explore new ideas free from the constraints of a pre-specified project.

A PhD can be a solitary endeavor involving closely just the apprentice and the master. I have been lucky to received the benefits of working with a host of masters, whom generously donated their time, expertise, wisdom, and humor. Thanks very much to Elliot Hawkes, Steve Collins, Scott Delp, Maarten Lansberg, and Jessica Selinger. A special thanks also to my advisor, Allison Okamura, for giving me the opportunity to come to Stanford and for the space to take advantage of the unforeseen opportunities the arose during my time here.

Thanks also to Cara Welker and Sean Sketch, whom have tolerated numerous awful jokes delivered in terribly imitated accents and whom have born the brunt of pilot testing with cobbled together prototypes spawned from hairbrained ideas. I like to think that we all emerged from the experience as more complete people.

Thanks to the members of the Stanford CHARM Lab for providing a diverse community in which to live and work for the last five years. There are pros and cons to working in a lab as large as this, but I have always enjoyed the diversity of ideas and expertise that flourish under one roof – even if it can be a bit cramped at times. Thanks also to the Stanford NMBL and Biomechatronics lab who further extended our community and whom both generously hosted me in numerous capacities.

Thanks to Jim Notwell, Michael Raitor, Sebastian Weingartner, Ravi Haksar, and Massimo Vespignani for making sure that life does not solely revolve around work, for always being supportive yet discerning, and for the numerous adventures to the

mountains and coast. And thanks to Elisa, Emma, Nikki, Daniel, Nova, Lumen, Darrel, Andrew, and Ellen for joining in on said adventures.

To Naike, who has been my partner and greatest supporter through this adventure, thanks for your patience, kindness, and support. We were separated by almost half the Earth for much of this time, but always managed to stay close. I am looking forward to the next great adventure.

# Contents

# List of Tables

# List of Figures

# Chapter 1

# Introduction

## 1.1 Motivation

Producing controlled movement is difficult. Adaptations, both physical and neural, accrued through millions of years of evolution have resulted in a human body able to manage challenges such as uncertainty, nonlinearity, nonstationarity, and noise to produce a diverse set of movements [1]. We can even operate effectively in environments with dynamics in which humans did not evolve, such as viscous underwater environments or the reduced gravity of low-earth orbit or the moon. We have made progress towards understanding the processes involved in producing these controlled movements. Leveraging this understanding, robots can now perform impressive physical feats such as dynamic jumps [2] and manipulation, even in viscous environments [3]. Despite enormous progress, we still do not understand the processes involved in producing controlled movements well enough to automate many tasks.

Though normally exceptional, human movement ability can be impaired by age, injury, and disease. In particular, stroke, the death of brain tissue due to interrupted blood supply, is the leading cause of adult disability [4] and the fifth most common cause of death in the United States [5]. Each year, there are 795,000 strokes in the United States [5]. Relatively new treatment options, such as tissue plasminogen activators (TPA) and mechanical thrombectomies, have drastically improved stroke survival rates. The stark improvement in acute stroke outcomes means that more

than 7 million living Americans have experienced a stroke [5]. The typical stroke survivor regains about seventy percent of lost motor function [6,7,8]. Even so, eighty percent of stroke survivors remain disabled enough to interfere with activities of daily living, with over half of the motor impairments manifesting in the upper limb [9,10].

Luckily, humans are intelligent enough to create tools to augment their abilities. Tools such as the wheel, fire, aeroplanes, computers, and the internet have all revolutionized human capabilities. Specifically, we have developed tools to help us move about, such as bicycles and cars, but these tools are not usable in all environments. We have also developed tools to help those with motor impairments to perform activities of daily living, such as wheelchairs. However, humans have designed our environments around those with no motor impairments. As a result, features designed to facilitate movement, such as stairs, can become major obstacles to those with motor impairments. Assistive devices that mimic both the form and function of a human with no motor impairments, such as exoskeletal robots, are likely best suited to operate in the environments we have designed for ourselves. In this thesis, I leverage insights from human mechanics to create wearable, low-cost exoskeletal robot components and analogs. I validate that these devices aid in human movement and develop models to explain why unexpected human behaviors sometimes arise through their use.

## 1.2 Background

In this section, I briefly describe the current state of exoskeletal robots and discuss efforts to simplify their design and operation to make them more accessible. First, I discuss some exoskeletal robot applications, design considerations needed to ensure safety, and the difficult challenge of exoskeletal robot control. I also describe attempts to simplify the challenge of exoskeletal robot design and construction using soft and passive components.

### 1.2.1 Exoskeletal robots

Exoskeletal robots designed to augment human motor abilities have been in development for more than a century, with patents extending back to 1890 [11]. Historically, exoskeletal robots have been constructed from rigid linkages acting in parallel with the user's skeleton. These linkages are attached at various points on the body by cuffs or straps that transmit forces and torques generated by electric motors or pneumatic actuators. However, movement is a difficult problem that humans accomplish relatively well. To improve on human abilities, exoskeletal robot designers must draw from a wide range of disciplines including advanced materials, electronics, controls, mechanics, and neuroscience, challenging exoskeletal robots' classical form. Common applications for exoskeletal robots today include:

1. **Enhance the operator's physical abilities.** One of the most common applications for exoskeletal robots is to mechanically augment the physical capabilities of the operator. Lower extremity exoskeletal robots have focused primarily on improving economy in walking [12, 13, 14], running [15, 16], or load carriage [17, 18, 19]. Though reduced locomotion economy translates to reduced performance [20], whether increased locomotion economy translates to increased performance has not yet been conclusively shown. Upper extremity and trunk exoskeletal robots are frequently designed to augment the operator's strength [21,22] or to relieve strain due to repetitive task performance in industrial settings [23]. exoskeletal robots also assist movement in motor impaired populations such as stroke survivors [14, 24, 25, 26, 27] and people with spinal cord injury [28].

2. **Provide haptic feedback for operator training or teleoperation.** Due to their ability to both apply forces and moments and measure variables such a position, interaction forces, and biological signals from the operator, exoskeletal robots can be used for kinesthetic haptic communication between the operator and a mechatronic system. Exoskeletal robots can artificially re-create physical interaction that can generate feedback to train the operator's motor skills as in rehabilitation robots or teaching novel skills [29,30]. Haptic feedback exoskeletal

robots can also be used to convey information from a teleoperated system to the physically separated operator [31, 32, 33, 34].

3. **Apply controlled perturbations for scientific experiments.** Scientific studies frequently call for reliable perturbations to be applied to the system being studied. Exoskeletal robots are very good tools for applying reliable perturbations to study how humans adapt to new environments or capabilities. These perturbations can include force fields that can be selectively removed or altered [35], step applications of force [36,37], or targeted assistance or resistance [38, 39]. Many of these devices are still being developed and validated, and a few have led to breakthroughs in understanding how humans control movement and adapt to different conditions [38, 40, 41, 42, 43].

4. **Generate electricity.** exoskeletal robots are typically used to facilitate movement, but one uncommon application of exoskeletal robots actually makes movement more difficult for the operator. Mechanical work done by the operator can be converted into electrical energy with a generator, and doing so creates resistance to motion. Intelligent design of the exoskeletal robot can produce maximal electricity with minimal impact on the operator [44, 45].

In this thesis, I focus on the first application, developing devices to improve human motor ability after stroke and in running.

### 1.2.2 Exoskeletal robot design considerations

#### Transmitting forces and torques to the body

The human body did not evolve to be actuated by an external robot. As such, we have no natural anchor points conveniently placed for a robot to attach and apply forces and torques. Instead, exoskeletal robot designers typically rely on cuffs or straps that distribute the forces applied by the robot over an area of the limb to be actuated to keep pressure concentrations low [17, 47, 48, 49, 50, 51]. Human skin is relatively intolerant to shear loads, so most exoskeletal robots apply forces approximately normally to the skin. Some of work done on the human body by an exoskeletal robot can be

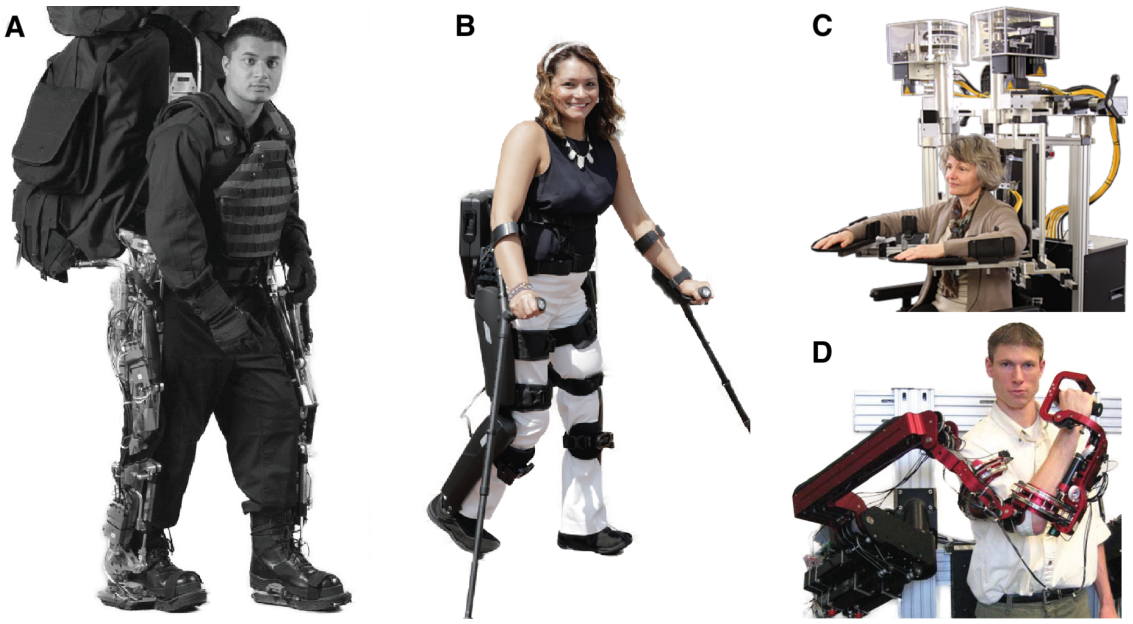


**Figure 1.1: Examples of exoskeletal robots. A.** The Berkeley Lower Extremity Exoskeleton (BLEEX) developed at the Berkeley Robotics and Human Engineering Laboratory [19] (©2006 IEEE). **B.** Personal 6.0 lower limb exoskeletal robot developed by ReWalk®Robotics Ltd. **C.** Kinarm Exoskeleton Lab upper extremity exoskeletal robot from BKIN Technologies [46]. **D.** Upper limb powered exoskeletal robot designed by Joel Perry and colleagues at the University of Washington [47] (©2007 IEEE).

absorbed by soft tissue such as muscle or fat, reducing the efficiency of the robot and potentially causing nonlinear effects [52, 53]. Some advanced systems measure soft tissue compliance to design custom interfaces that reduce discomfort and inefficiencies [54]. Nevertheless, comfortably and safely transmitting forces to the human body remains a difficult challenge.

### Safety

Safety is an important consideration when designing machines that operate in close-proximity to humans. One key safety concern is safely handling the mass added by the exoskeletal robot. Machines with more mass require higher actuator forces to produce the same movement than less massive machines. Distally located mass has a much greater moment of inertia than proximal mass and as such can mean slower response times and greater actuator effort is required. As such, many exoskeletal robots are designed to locate most of the mass of the exoskeletal robot proximally [47, 55]. In some stationary exoskeletal robots, it is practical to mount portions of the exoskeletal robot to an external support, such as the floor or ceiling [24, 56, 57]. Doing so can reduce the loads on the portion of the exoskeletal robot worn by the operator. Soft exosuits, explored in the next section, are another approach to minimizing the mass added by exoskeletal robots.

Another key safety concern is the alignment of the exoskeletal robot's joints with those of the operator. Proper alignment of exoskeletal robot and user joints ensures that the moments applied by the exoskeletal robot directly translate to task accomplishment. Misalignment can result in undesired loads applied to the operator [58] and can be avoided by proper fitting or the design of mechanisms that allow self-alignment [59, 60, 61]. While ensuring proper fitting can be tedious, the alternate approaches can add considerable mass, complexity, and cost to the exoskeletal robot. Care should also be taken to ensure that exoskeletal robots will not hyper extend the operator's joints.

Mechatronic systems can become unstable in some conditions. In robot systems, this usually manifests as oscillations that increase in amplitude that cannot be stopped. Some tasks, such as walking, are passively stable [62] while other tasks,

such as running, require a controller to maintain stability. For tasks that are not passively stable, care should be taken to guarantee that the exoskeletal robot's control policy is stable. In some cases, differences in reaction times between the operator and exoskeletal robot can initiate instabilities. Ensuring that the motions performed by the exoskeletal robot-human operator pair remain stable is an ongoing topic of research [48, 63].

**Exoskeletal robot control**

Seamless robotic assistance requires that both operator and robot agree on the task that is to be attempted. One way to facilitate agreement between operator and robot is to agree on the task beforehand. In the upper extremity, this strategy usually manifests as reaches to defined targets [25, 26]. Using defined targets and models of healthy reaches to targets [64, 65], the exoskeletal robot can either assist the operator in reaching the target or provide strategic resistance with the intent to facilitate motor learning. Repeatedly performing these reaches is a common strategy used in rehabilitation robots to facilitate motor recovery. However, repetition may not be an optimal strategy for motor learning, which appears to benefit from exploration [40, 66, 67]. Generalizing this strategy to accomplish tasks of daily living with the upper extremity is also difficult. Walking, on the other hand is a task where one action, a step or a stride, is performed repeatedly with little variation. Even determining the exoskeletal robot's role in assisting in cyclic locomotion tasks can be difficult. For example, the robot can be used in a position-based control mode to push the operator to follow a prescribed kinematic trajectory or the robot could be used in a torque-based control mode to apply supplemental moments to compensate for known deficits. Determining the best control strategies for gait-assisting exoskeletal robots is an area of active research [13].

Another approach is to automatically infer the operator's intent using information such as neural signals from the brain or periphery or by using unimpaired appendages for control. Brain-computer interfaces are one key technology in this effort, but require invasive surgeries and currently have a maximum communication rate of 3.5 bits per second [68], too slow for natural movement. Non-invasive methods also

exist. These approaches typically measure neural signals on the periphery using electromyography (EMG) [69,70,71] or the cortex using electroecephalography (EEG) [72, 73] and/or the measurement of kinematic and kinetic variables [13, 14]. These areas are topics of active research, and the additional measurement equipment and processing needed to combine all of the measured information rapidly and reliably adds cost and complexity. Many devices also rely on operator inputs from other parts of the body. For instance, many of the lower extremity exoskeletal robots designed to rehabilitate stroke survivors and patients with spinal cord injuries measure trunk movements to cue each step. This approach is effective, simple, transparent, and reliable enough to be made into products. However, this strategy is unlikely to scale to a diverse set of movements. Currently, several of these devices use controls mounted on crutches that accompany the exoskeletal robot to switch between modes. In one mode, a trunk movement cues the exoskeletal robot to stand from a seated position and cues a step in another mode. It is difficult, however, to imagine a system that can switch between all the modes required for activities of daily living.

Rather than inferring operator intent, an exoskeletal robot can provide assistive moments without knowledge of the task. An example of this use-case commonly used in rehabilitation and industrial exoskeletal robots is gravity compensation. These exoskeletal robots provide the vertical forces or related moments to cancel the effects of gravity on the human operator or of the payload being manipulated. Doing so requires only knowledge of the current state of the system and information about the masses being manipulated, which are easily measured with force sensors or adjusted as desired by the operator. Negating the effects of gravity has proven effective in assisting stroke survivors and spinal cord injured patients in movement [14, 24]. Because the forces needed to compensate for gravity only vary with state, it is sometimes possible to accomplish this task mechanically without active control. Many such passive devices are now commercially available to reduce fatigue in industrial applications such as supporting the arms of workers performing overhead work for extended periods of time, such as the EksoVest [74] or the Ottobock Paexo Shoulder.

Exoskeletal robot control can be facilitated or complicated by the fact that the human operator can also learn new control strategies. Adding an exoskeletal robot

might constitute a substantial perturbation to an operator's normal motor patterns. Humans continuously adapt their motor patterns in search of efficient patterns [38]. Yet, the search for efficient patterns takes time and the inherent variability of motor patterns might not always be sufficient to identify optimal motor patterns without an external push [40]. The nature of these learning processes might partially explain why many exoskeletal robots designed to improve walking and running economy based on good rationale returned null or negative results for many years [18,51,75,76]. However, these learning processes may also mean that humans can find ways to compensate for some sub-optimalities in exoskeletal robot design or control.

### 1.2.3 Exosuits – assistance without a skeleton

Exoskeletal robots use rigid linkages to transmit actuator forces to the operator. These rigid linkages also generate reaction forces that limit the loads applied to the operator's skeleton. However, some applications do not require load-bearing beyond the capability of the human skeleton. Exosuits are a class of exoskeletal robots that forgo rigid linkages, applying actuator forces directly to the operator and relying on the operator's skeleton to generate all of the reaction forces. This method limits the maximum forces that can be applied to the body, supplementing rather than multiplying the operator's capabilities. Eliminating rigid linkages allows exosuits to be constructed of primarily compliant materials that can tolerate less precise design and machining than rigid exoskeletal robots, are lightweight, and are generally inexpensive. Safety factors that add considerable cost and complexity such as aligning robot and operator joint axes are eliminated as well because exosuits do not have a center of rotation. However, without rigid linkages, applying forces and torques to the human body can be difficult and factors such as reaction forces must be carefully managed.

A number of creative solutions have been developed to transmit forces to the human operating the exosuit. Early exosuit designs focused on assisting with locomotion. They used inelastic cables to transmit loads applied by remotely located motors to anchor points on the body [14, 16, 77]. Soft exosuits have been used to successfully assist with human walking and running in healthy and motor impaired

populations [14, 16, 78, 79]. The forces needed to actuate the upper extremity to accomplish activities of daily living are generally lower than those needed in the lower extremity. Inelastic cables driven by remotely located motors are also used to actuate the upper extremity [80, 81]. Because the human upper extremity is frequently not habituated to contending with high magnitude forces, standoffs are sometimes implemented in these cable-driven upper extremity exosuits to reduce the forces needed for actuation by increasing the moment arm across the joint to be actuated. These standoffs can create a large device profile and might interfere with objects in the operator's environment in daily life. Other approaches use pneumatically inflated bladders to push against two parts of the body, causing expansive forces and moments that extend the joint [82, 83]. Many of these exosuits have been created to assist with arm movements in stroke survivors [82, 83, 84, 85, 86, 87, 88]. Some of these studies have been validated in healthy users [82, 84, 85, 88], but whether these devices can aid movement in stroke survivors is not yet known.

Though there are many advantages to removing the skeleton from the exoskeletal robot, there is currently not enough data to know whether secondary effects of the applied loads might cause injury in the long term. While exosuit assistance can reduce the forces required of the operator's muscles, the overall forces experienced by the human operator's skeleton can still increase because there is no exoskeletal robot frame to offload reaction forces. These higher forces experienced by the skeleton could lead to faster wear of human joints and higher incidences of arthritis. Additionally, soft tissue is responsible for maintaining integrity in some joints. Exosuit assistance that reduces the activity of certain muscles that also stabilize joints like the knee or shoulder could have unforeseable effects. We cannot yet know how changing muscle activation patterns and applying large loads to specific joints might affect operator safety in the long term.

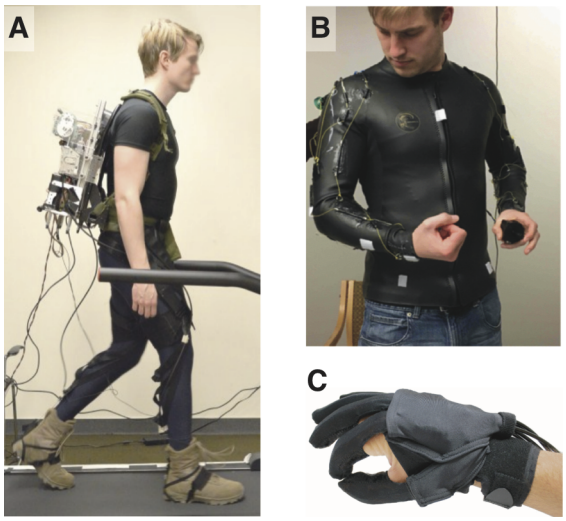


**Figure 1.2: Examples of exosuits. A.** Example of an exosuit for lower extremity assistance during gait developed at the Harvard Biodesign Lab [50] (©2013 IEEE). **B.** Example of an exosuit for post stroke upper extremity assistance developed in the Dynamics, Autonomous Navigation, Surface Engineering and Robotics Lab at University of California Santa Cruz. [86] (©2019 IEEE). **C.** Example of an exosuit for hand assistance and rehabilitation developed at the Harvard Biodesign Lab [89] (©2015 IEEE).

### 1.2.4 Passive exoskeletons – assistance without motors

If exosuits seek to make exoskeleton design easier by removing the skeleton, passive or unpowered exoskeletons seek to simplify the problem by removing the brain, muscles, and energy storage. Given that passive exoskeletons cannot add energy to the coupled system, this approach is analogous to mechanically modifying the human body to be better suited for a specific task. Though no explicit performance limits have yet been identified, passive exoskeletons cannot perform intended tasks for the operator as powered exoskeletal robots can. In the upper extremity, passive exoskeletons have been used to compensate for gravity for both rehabilitation and industrial applications. These devices use stored gravitational or spring potential energy to counter the work done by gravity [74, 90, 91, 92, 93, 94, 95, 96]. In the lower extremity, passive exoskeletons have been developed assist walking by mimicing a spring-clutch behavior identified in the calf muscles [12] and in running by assisting hip muscles with swinging the legs [15, 97].

Some safety concerns are reduced with passive exoskeletons. Because exoskeletons are mechanically programmed to perform a specific task, stability concerns stemming from human inputs to the robotic controller are completely negated. This mechanical programming typically ensures that the exoskeleton's dynamics are more transparent to the operator. Barring mechanical failure, simple passive exoskeletons will almost never behave unexpectedly, facilitating operator training. The removal of expensive components, such as batteries, controllers, and motors, and inherent safety of a passive device mean that passive exoskeletons are a good alternative to powered exoskeletal robots where assistance, rather than the exoskeleton performing the entirety of the task, is acceptable.

### 1.2.5 Exotendons – assistance without a skeleton or motors

In 2003, Antonie van den Bogert published a study suggesting that a simple system of elastic bands and pulleys could reduce the mechanical requirements of walking by as much as 74% *in silico* [99]. This concept combines the properties of passive exoskeletons that do no net work on the operator and of exosuits that do not use a rigid

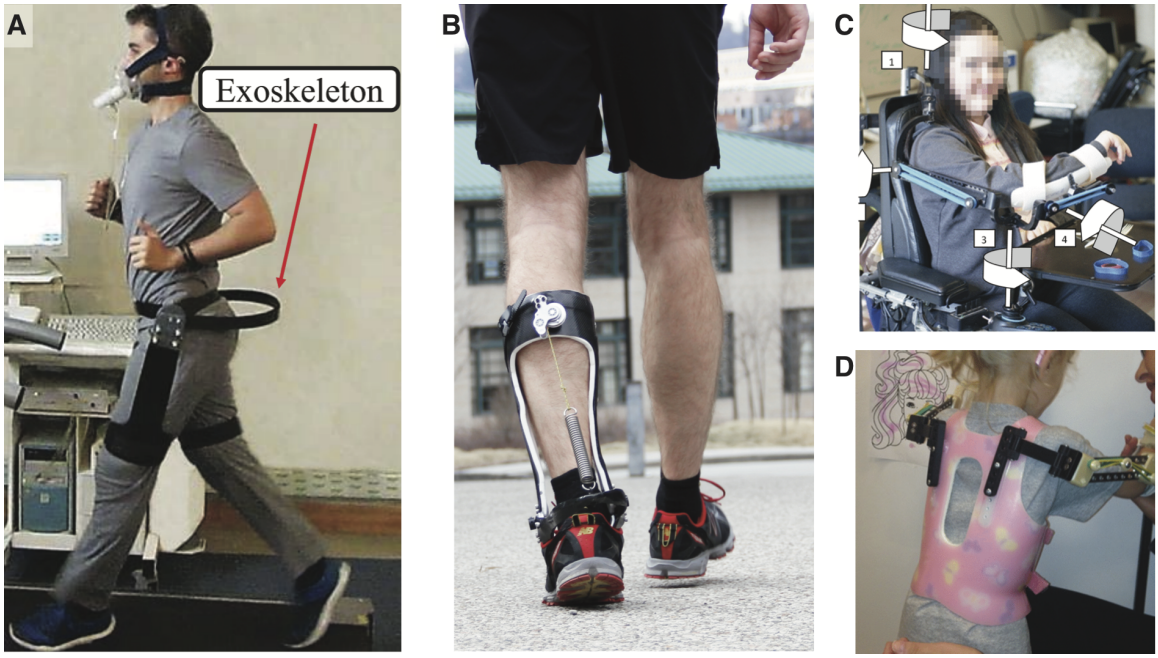


**Figure 1.3: Examples of passive exoskeletons. A.** A passive exoskeleton that improves running economy in humans by assisting the hips with leg swing using a spring mechanism [15] (©2018 IEEE). **B.** A passive exoskeleton that improves human walking economy by supplementing a clutch-spring mechanism identified in the calf muscles [12] (photo credit: Carnegie Mellon Engineering). **C. and D.** Wilmington Robotic EXoskeleton (WREX), a passive exoskeleton that uses springs to support the weight of the arm and can attach to the back of a wheelchair (C) or to a trunk-mounted brace (D) [98] (©2015 IEEE).

frame. Van den Bogert called these externally mounted elastic bands "exotendons" in reference to the hypothesis that tendons act as springs that recycle energy in animals. If proven to be effective *in vivo*, these exotendons have the potential to be even more lightweight and less expensive than passive exoskeletons, which require extra components to create the exoskeleon frame. Due to their low mass, exotendons might be well-suited for applications such as running, in which mass imposes a significant metabolic penalty [20, 100].

### 1.2.6 Access

Though a number of exoskeletal robots are commercially available, one of the primary factors limiting the impact of exoskeletal robots in society is cost. Commercial versions of traditional exoskeletal robots cost on the order of hundreds of thousands of dollars. Devices such as the BKin Technologies' Kinarm and the Hocoma Lokomat may be important tools for rehabilitation. Yet the price of these exoskeletal robots mean that only well-funded health care institutions can afford one or two examples, which limits both the number of patients that can benefit and the amount of time each patient can access these devices. The problem of limited access is critical given that dosage may be a key limiting factor in motor recovery after events such as stroke [101, 102]. Primary contributors to these costs are high performance components, engineering required to ensure safety, and the absence of manufacturing at scale. By removing some of the high-cost components, exosuits can be an order of magnitude less expensive than traditional rigid exoskeletal robots. However, commercial exosuits are still rare. Passive exoskeletons can be another order of magnitude less expensive than traditional exoskeletons, with offerings priced under 10,000 USD. Passive exoskeletons forego some of the most expensive components of a traditional exoskeleton and because range of motion and applied forces are mechanically prescribed, control and safety considerations are greatly simplified or nullified. Because thousands of dollars is still very expensive for most patients, most passive rehabilitation exoskeletons, such as the Saebo Mobile Arm Support or Hocoma ArmeoSpring,

are marketed towards clinics. These clinics in turn typically acquire only a few systems, again limiting patient access to these tools.

Prosthetic limbs are one example of an assistive, wearable device commonly prescribed to alleviate disability. Like exoskeletal robots, prosthetic limbs can be simple, inexpensive passive devices or high performance active limbs. Most insurance companies in the United States will only pay for passive prosthetic legs for most users, citing a lack of clinical evidence for the benefits of active prostheses for many users [103]. Currently, the clinical evidence in support of exoskeleton devices for motor-disabled assistance or recovery is contested [104, 105] and insurance companies are unlikely to pay for exoskeletal robots for individuals. This creates a chicken-and-egg problem in which testing the efficacy of exoskeletal robot devices for motor recovery is difficult until exoskeletal robots are built down to an accessible price point. Building to an accessible price point will be beneficial for widespread adoption by unimpaired individuals who are unlikely to pay thousands of dollars for an exoskeletal robot to improve running efficiency.

## 1.3 Contributions

In addition to this introduction (Chapter 1) and a conclusion (Chapter 6), this thesis consists of four chapters in two parts. Part I focuses on design, characterization in healthy subjects and on the bench top, and validations in stroke survivors of three simple exoskeletons/exosuits/exotendons that support shoulder abduction. Each of these exoskeletons/exosuits/exotendons and related experiments are described in its own chapter (Chapters 2-4). Part II focuses on the design and validation of a simple-as-possible passive exotendon that improves efficiency in running humans, described in full in Chapter 5. The contributions of the thesis are presented chapter-wise below:

- **Chapter 2**: We describe in detail **a new type of exosuit actuator** designed specifically to actuate shoulder abduction, which is commonly associated with reduced reachable workspace in stroke survivors. This soft exosuit actuator lifts the arm from below using pushing forces rather than pulling from above with

tensile elements or directly applying bending moments. We characterize this actuator on the benchtop and in healthy human subjects to demonstrate its effectiveness. We then perform one of the first pilot studies in a stroke survivor of an upper extremity exosuit and **demonstrate that reachable workspace is increased with our actuator.** The material cost of our actuator, which does not include a compressor or controller, is less than 20 USD. While no upper extremity exosuits are commercially available, some lower extremity offerings for walking cost approximately 30,000 USD.

- **Chapter 3**: We describe in detail an **updated design for our exosuit actuator to actuate shoulder abduction,** based on a new class of growing robots [106, 107]. We demonstrate in healthy operators that the exosuit actuator provides the intended support without interfering with other joints. We then **demonstrate increased reachable workspace** in 4 out of 6 stroke survivors using this type of support, and provide data supporting the hypothesis that abnormal activation of the flexor synergy causes reduced upper extremity workspace. We repeated these assessments using a ceiling-mounted device as a positive control and found much better performance using the positive control. This inconsistency demonstrates that **two devices can show the same outcomes in healthy users but very different outcomes in the target impaired population.** Many similar studies test only in healthy users to validate their designs; we contribute data that cautions against extrapolating these results to stroke survivors.

- **Chapter 4**: We describe in detail **a passive exoskeleton to assist shoulder abduction.** We characterize the new exoskeleton on the benchtop and in healthy operators, demonstrating that the exoskeleton **provides the intended assistance without impeding range of motion in any other upper extremity joint.** However, the results in Chapter 3 demonstrate that results in a stroke population cannot be extrapolated from unimpaired participants, so we also present a protocol for assessing this exoskeleton's usefulness in aiding stroke survivors with activities of daily living, rather than specialized subtasks

such as reachable workspace area. The material costs of this exoskeleton were less than 100 USD, while similar commercially available passive exoskeletons for industrial applications are typically priced between 5,000 and 8,000 USD. Because of its effectiveness, simplicity, and price point, this design could be a powerful tool for studying the effects of gravity compensation on stroke recovery with higher dosages than existing devices.

- **Chapter 5**: We describe the design of **an exotendon that demonstrably improves human running economy by 6%**, exceeding the performance of many powered exoskeletons. We provide **a theoretical biomechanical framework that explains the mechanism of energetic savings.** This framework predicts changes in mechanical effort required in specific phases of gait that we verified. We also perform ancillary tests to demonstrate that the benefits of our device are not due to the placebo effect and that it can be effectively used in unstructured environments, such as suburban streets. Our device is manufacturable for approximately 1 USD.

Note that we compare the material cost of each of our designs to the retail price of existing devices. The retail price encapsulates marketing, logistics, labor, profit margins, and other costs that are not considered in this thesis. We are not able to accurately estimate the retail price of any of our devices, because the only cost for which we can accurately account is the material cost. Though we made an effort to limit the number and cost of the components used in our designs, readers should be mindful of the differences between material cost and retail price in our comparisons.

# Part I

# Upper extremity: Stroke application

# Chapter 2

# Inflatable exomuscle for shoulder abduction support

## Summary

Stroke is the leading cause of adult disability. Many robots have been developed to administer movement therapies or provide physical assistance to stroke survivors suffering from movement deficits. One effective approach has been to support the weight of the arm, offloading shoulder abductor muscles that have become coupled to elbow muscles. However, patients have limited access to such robots due to the robots' complexity, cost, and bulk. To counter this problem, we developed a lightweight (350 g), inexpensive external actuator, which we call an exomuscle. We constructed a prototype exomuscle by reinforcing a plastic bladder with a fabric bag that is sewn to supporting straps. The bladder can then be inflated with pressurized air to provide expansive forces between the user's torso and arm, supporting shoulder abduction. A seam acting as a hinge joint connects the exomuscle to the torso. We demonstrate that our exomuscle reduces muscular effort by 74% in isometric tasks and 72% in dynamic reaching tasks while minimally affecting the range of motion of the shoulder and elbow (average 4% reduction) on three users ranging from 165 to 188 cm tall. We also show in a pilot test on a stroke survivor that exomuscle assistance can increase reachable workspace. This chapter was adapted from Simpson, C.S., Okamura, A.M.,

and Hawkes, E.W., 2017. Exomuscle: An inflatable device for shoulder abduction support. IEEE International Conference on Robotics and Automation, pp. 6651-6657 [84]. We describe a new experiment in Section 2.5 that was not included in that publication.

## 2.1 Introduction

Stroke results from significantly reduced blood supply to part of the brain and is one of the leading causes of long-term adult disability [4]. Stroke survivors can suffer from a large range of negative effects such as pain, spasticity (continuous contraction of some muscles), muscle weakness, hemineglect (unawareness of half of space), and cognitive deficits. Some researchers believe that the main cause of post-stroke motor impairment is abnormal muscle co-contractions [108]. These abnormal muscle co-contractions were first observed as the coupling of shoulder abductor with elbow flexor muscles and shoulder adductor with elbow extensor muscles [109]. Since then, post-stroke abnormal muscle co-contraction patterns have been observed for a range of upper extremity tasks [110], as well as for walking [111]. While there is a highly nonlinear relationship between the electromyographical (EMG) signals on which these analyses are based and the resultant joint torques, abnormal joint torque couplings have been found that match the EMG-based results [112]. These researchers have also demonstrated substantial improvements in motor function, achieved by supporting the weight of the hemiparetic arm with an air bearing, which unloads the shoulder abductor muscles [113].

Many researchers are developing robots to work with humans with neuromotor impairments for assistance or rehabilitation. A large number of these robots are designed to help users repeatedly perform a task [25,26], but this approach might not be optimal for stroke rehabilitation [66,114]. Building on the results from [113], Ellis et al. [24] designed and built an impairment-specific rehabilitation robot, ACT$^{3D}$, to provide shoulder abduction support. They then administered a therapy in which shoulder abduction support was gradually reduced over a period of eight weeks and found several motor improvements [24,115]. However, the level of motor recovery is

tied to the intensity of therapy, and most rehabilitation robots are expensive, unwieldy devices confined to the lab or clinic where patients have limited access to them.

Many of the robots currently being developed for rehabilitation are *exoskeletal* robots. Typical exoskeletal robots are constructed from rigid linkages acting in parallel with the user's skeleton. These linkages are then attached at various points on the body by cuffs or straps to transmit forces and torques. Motors or hydraulic actuators then actuate these linkages. By including linkages acting in parallel with the user's skeleton, an exoskeleton transmits many of the forces that would otherwise need to be transmitted through the user's skeleton. Such exoskeletal robots have already been developed for stroke rehabilitation [24, 25, 115]. These robots show promise in taking state-of-the-art rehabilitation out of the clinic. However, there are many difficulties associated with the design and operation of traditional exoskeletal robots, including cost, aligning operator and robot joint axes [58], safely handling the mass added by the exoskeleton, and ensuring stable interactions with human users [48, 63]. Further, exoskeletal robots might be excessive for tasks that do not require load-bearing beyond the capability of the human skeleton.

To address the problems associated with traditional exoskeletal robots, several groups have recently built *soft exosuits* that forgo rigid linkages and directly apply forces and torques to the user's skeleton instead. Eliminating rigid linkages allows exosuits to be constructed of primarily compliant materials that require less precise design and machining, are lightweight, and are generally inexpensive. However, without rigid linkages, applying forces and torques to the human body can be difficult. Some designs use inelastic cables intelligently placed on the body and anchor points to transmit loads to specific body parts [49, 50]. While these designs have proven effective, they increase the compressive load on the joints. Another take on this approach uses cuffs as attachment points for cables driven by motors located elsewhere (typically in a backpack or offboard) [80, 81]. However, this design requires large standoffs to increase the moment arm across the joint to be actuated that create a large device profile and might interfere with objects in the users' environments in daily life. Other approaches use pneumatically inflated bladders to push against two parts of the body, causing expansive forces and moments that extend the joint [82,83].

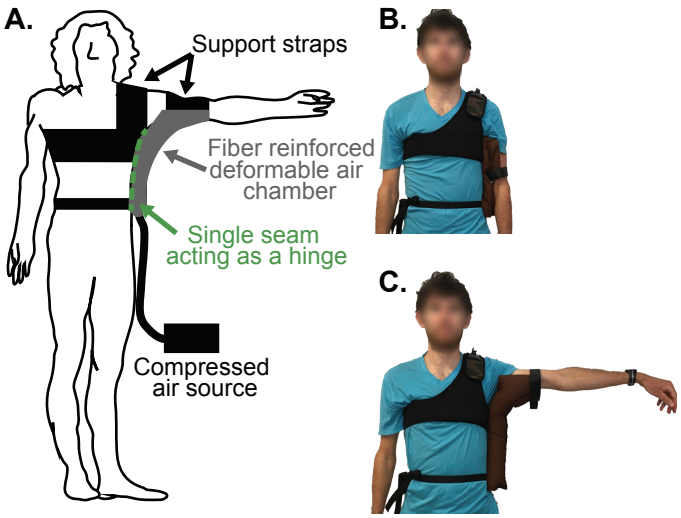


**Figure 2.1: Exomuscle schematic and prototype images. A.** Schematic of our exomuscle, which attaches under the arm and against the torso and is held in place with assorted straps. A single seam running down the torso acts as a hinge to allow free shoulder horizontal abduction. The exomuscle is inflated by a compressed air source. Inflating the exomuscle causes expansive forces between the seam against the torso and the arm. **B.** A user wears the exomuscle in its uninflated state. **C.** A user wears an inflated exomuscle. ©2017 IEEE [84].

Only a couple of these devices currently exist and they tend to focus on simple, single degree-of-freedom joints, such as the elbow.

Our goal is to assist people with post-stroke motor impairments by providing shoulder abduction support with a wearable, affordable, and soft device. To keep costs low, we forgo the rigid linkages of a traditional exoskeleton. Since we are only seeking to actuate a single degree of freedom, we only need one actuator, which we call an external muscle or *exomuscle*. Here we discuss the design and evaluation of our exomuscle. We experimentally verify that the device minimally impacts the user's range of motion in shoulder internal/external rotation, horizontal abduction/adduction, and elbow flexion/extension. We also demonstrate that the exomuscle reduces muscular effort in select shoulder abductor muscles while performing a series of isometric and dynamic tasks. We also show in a pilot test on a stroke survivor that exomuscle assistance can increase reachable workspace.

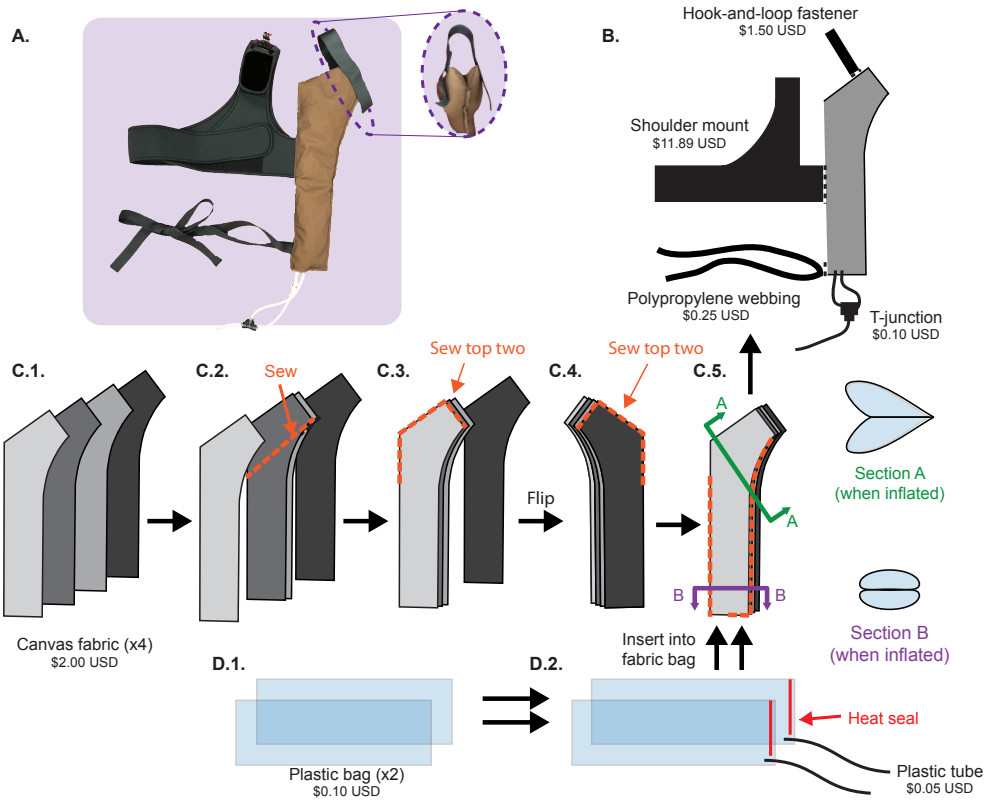


**Figure 2.2: Exomuscle construction. A.** Photograph of a completed exomuscle. Inset: V-shaped part that supports the arm. **B.** Diagram of a finished exomuscle. **C.** The construction process of the fabric bag used to reinforce plastic bladders to create the exomuscle. First, four pieces of canvas fabric are cut to the shape shown in C.1. Two of these pieces are sewn together with the seam shown in C.2. A third piece of canvas is placed on top of the two previously sewn together and the top two canvas pieces are sewn together with the seam shown in C.3. That assembly is then flipped over and the fourth piece of canvas added and sewn to the piece directly under it as shown in C.4. This series of steps creates a stable V-shaped support for the arm. Finally, all four pieces of canvas are sewn together with the seam shown in C.5. **D.** The construction process for twin bladders that line the exomuscle. The bladders are created from plastic bags (D.1.). Plastic tubes are inserted into one end of the plastic bags. The bags are then heat sealed around the plastic tubes to ensure that air cannot escape as shown in D.2. The two bladders are then inserted into the fabric bag previously sewn to create a finished exomuscle. The exomuscle is then sewn to various straps to attach it to the user (B). Note that the single seam attaching the exomuscle to the torso acts as a hinge joint. The price of each component is listed in United States Dollars. These components total $16.34 USD.  [84].

## 2.2 Device design and construction

We designed and built a prototype exomuscle from fabric reinforced inflatable bladders to provide low-cost shoulder abduction support that minimally interferes with range of motion for stroke rehabilitation and assistance. The exomuscle consists of twin plastic bladders that have been reinforced by fabric bags sewn to the desired final shape of the device. A flow chart of the construction process is shown in Fig. 2.2. The final exomuscle is roughly triangular when viewed from the user's front or back, and has a Y-shape when viewed from the side (Fig. 2.2, top left). The V-shape at the top of the Y creates a stable support for the arm that prevents the arm from falling off the support during movements. The completed exomuscle was then sewn onto a shoulder mount that holds the exomuscle next to the torso and under the arm of the user with a single seam that acts as a hinge joint. The exomuscle is attached to the user's waist by a polypropylene waistbelt. Elastic straps help to hold the arm in place on top of the exomuscle. Compressed air is pumped into the exomuscle to provide expansive forces between the attachment points on the human body: the seam along the torso and the underside of the arm. We used a portable compressor to inflate the exomuscle. While 27.5 kPa was sufficient pressure to provide significant support to our users, we inflated the exomuscle to 55 kPa without failure.

## 2.3 Experimental methods

### 2.3.1 Device characterization

To control the exomuscle, we need to know the relationship between the input air pressure and the resulting shoulder abduction angle. Thus, we measured the relationship between air pressure in the bladder and shoulder abduction angle by inflating the exomuscle to air pressures of 0, 6.9, 13.8, 20.7, and 27.5 kPa while recording the shoulder abduction angles at each pressure with a visual tracking system for each of three users.

To ensure comfortable and safe interactions, we need to understand the interaction forces between the exomuscle and the arm. We measured the relationship between

shoulder abduction angle and the interaction forces between the exomuscle and the upper arm by attaching the exomuscle to a one-degree-of-freedom test apparatus. The test apparatus consisted of two linkages connected by a hinge joint. The exomuscle was connected to the two linkages of the test apparatus so that one linkage acted as a torso and the other acted as an arm. The hinge joint acted as a simple shoulder. The exomuscle was inflated to 6.9, 13.8, 20.7, or 27.5 kPa and then compressed by rotating the two linkages of the test apparatus towards each other (similar to shoulder adduction). We recorded the deflection angle with a visual tracking system and the interaction forces between the exomuscle and the test apparatus linkage representing the arm with a three-axis force transducer (ATI Mini45) connected between the two.

### 2.3.2 Range of motion

Traditional exoskeletons limit the user's range of motion, which limits their utility. To determine how our device affects upper extremity range of motion, we used a goniometer to measure the extrema of shoulder internal/external rotation, shoulder horizontal abduction/adduction, and elbow flexion/extension for three users, under two conditions: (1) with the exomuscle inflated to approximately 27.5 kPa, and (2) with no exomuscle.

### 2.3.3 Muscular effort

*Isometric task:* To determine whether our exomuscle can reduce shoulder abductor muscle effort in an isometric task, we recorded neural activity in both the anterior and medial components of the deltoid muscle in three users during a series of isometric arm holds using electromyography (EMG). Each isometric hold was performed in one of three postures (Fig. 2.3, top left): (1) shoulder horizontally abducted to 90° (straight in front of the torso), (2) shoulder horizontally abducted to 45°, or (3) shoulder horizontally abducted to 0° (straight out to the side) with the elbow fully extended and the arm raised to shoulder height. EMG data was collected for ten seconds at 25 Hz using a Delsys Bagnoli 2 EMG system read by a Tektronix oscilloscope for each of these three postures with and without exomuscle support.

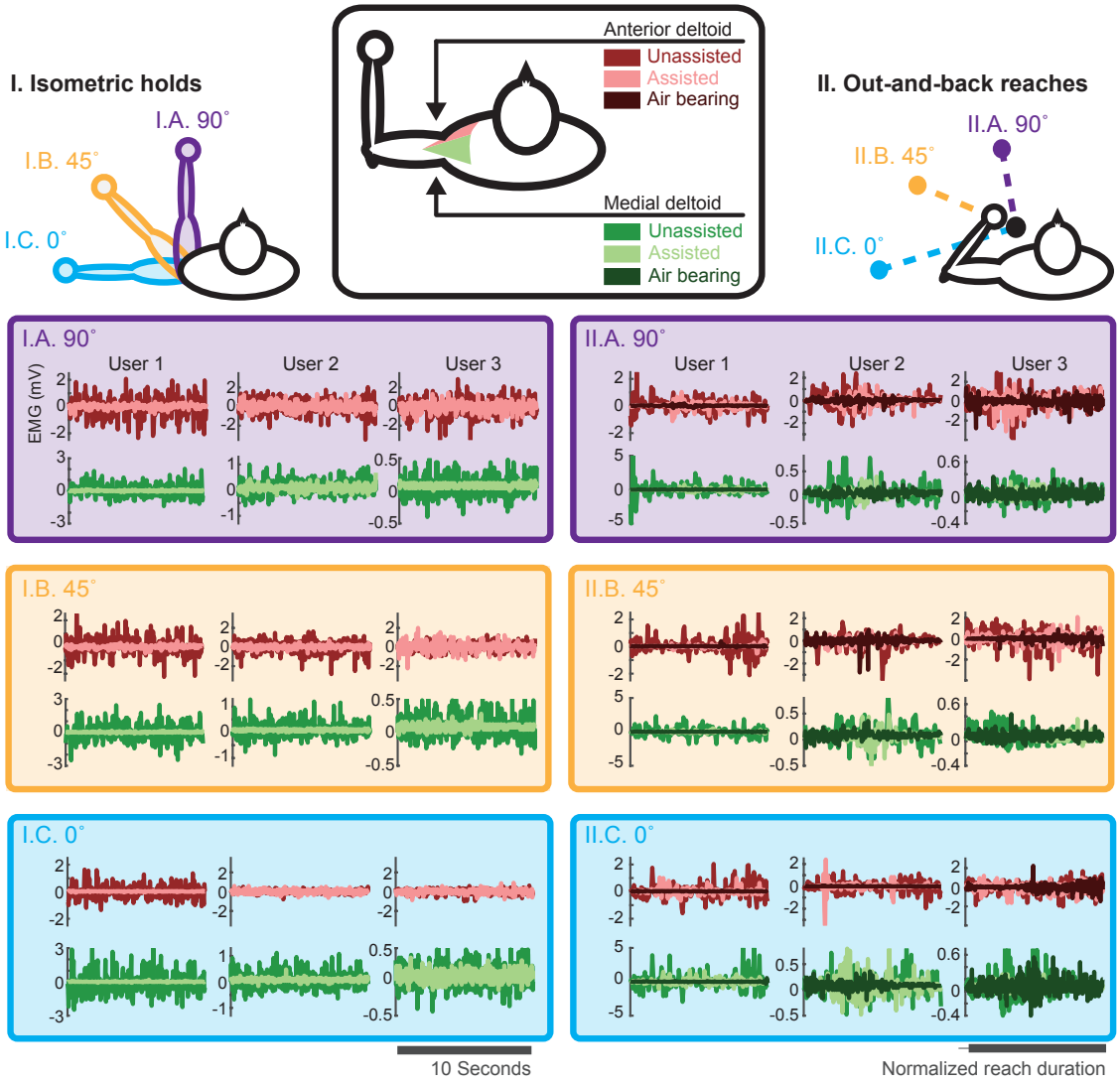


**Figure 2.3: Electromyographical (EMG) data recorded during isometric (left column) and dynamic (right column) tasks (n=3).** EMG data was recorded from both the anterior and medial deltoid while each task was performed in different conditions: (1) unassisted, (2) with exomuscle assistance, and (3) for the reaches with assistance provided by an air bearing. In most cases, exomuscle assistance significantly reduced muscular effort. On average, the exomuscle does not achieve the performance of the air bearing, but in some cases, such as user 3's medal deltoid for all reaches, the exomuscle outperforms the air bearing. ©2017 IEEE [84].

*Dynamic task:* To determine whether our exomuscle can reduce shoulder abductor muscle effort in a dynamic task, we again recorded EMG data from the anterior and medial components of the deltoid muscle in three users during a series of out-and-back reaches. Each reach began in the same posture: arm raised to shoulder height and elbow maximally flexed so that the hand was in front of the shoulder. Users then reached to one of three target points (Fig. 2.3, top right): (1) shoulder horizontally abducted to 90° (straight in front of the torso), (2) shoulder horizontally abducted to 45°, or (3) shoulder horizontally abducted to 0° (straight out to the side) with the elbow fully extended and the arm raised to shoulder height. After reaching a target posture, users returned their arm to the initial posture. EMG data was recorded throughout the reach, and kinematics were recorded by a visual tracking system. Users performed each reach in three support conditions: (1) unaided, (2) shoulder abduction supported by our exomuscle, or (3) arm weight supported by a custom air bearing. The air bearing allowed users to rest their arms on a table, but minimized friction forces in the plane of the tabletop. The air bearing support was included here to see whether the exomuscle could approach the performance of other established upper extremity support mechanisms in a dynamic task. The air bearing support was not included in the isometric task because there should be no neural activity in the deltoid muscles when the arm is fully supported in an isometric task. With our first user, we verified that the variance of resting noise was less than 0.22% of the signal variance from the unsupported case.

### 2.3.4 Users

We recruited three volunteer users for our air pressure verses abduction angle, range of motion, and muscle effort studies. These users consisted of two right-handed males (height 171 and 188 cm) and a left-handed female (height 165 cm). All users wore the same exomuscle supporting the left arm with only the supporting straps adjusted for each individual.

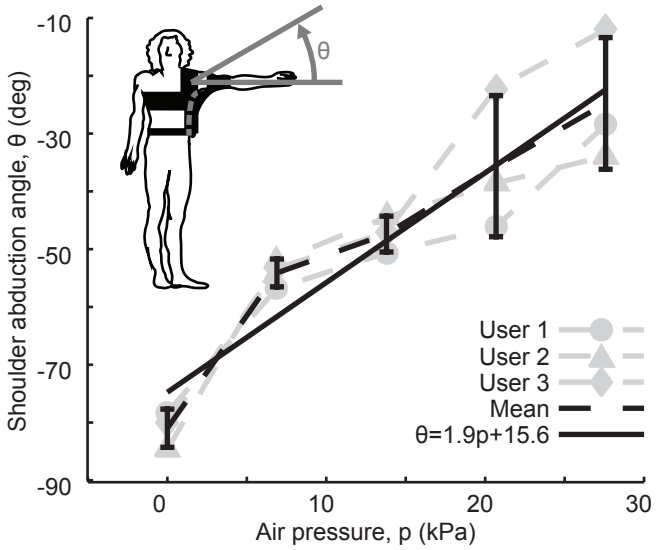


**Figure 2.4: Abduction angle verses air pressure (n=3).** Shoulder abduction angle increases nearly linearly with pressure for three different users (gray dashed lines). The black dashed line and error bars show the mean and standard deviations of the experimental data from each of the three users. ©2017 IEEE [84].

## 2.4 Results

We designed and constructed a prototype exomuscle that assists users in shoulder abduction. The prototype is inexpensive ($16.34 USD), lightweight (350 g), and made from entirely soft materials. While the prototype was made to the specifications of a 173 cm tall individual, we demonstrated its effective use on users ranging from 165 to 188 cm tall.

### 2.4.1 Device characterization

The exomuscle exhibits a linearly increasing relationship between air pressure and shoulder abduction angle (Fig. 2.4). This linear relationship is promising for future development of a feedback control system for arm positioning.

Interaction forces increase as shoulder abduction angle decreases and as air pressure increases (Fig. 2.5). In this way, the exomuscle behaves as a nonlinear spring whose resting position is maximal shoulder abduction and whose stiffness is tunable

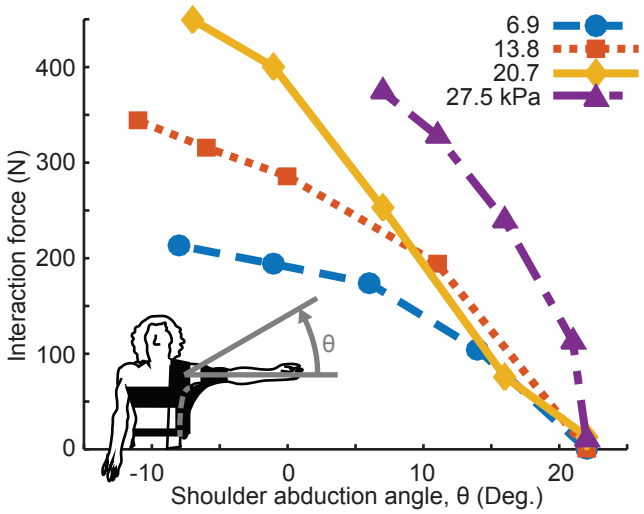


**Figure 2.5: Abduction angle verses interaction force.** Force exerted on the arm by the exomuscle plotted against the shoulder abduction angles for a range of different air pressures. The exomuscle's behavior resembles a nonlinear torsional spring whose resting position is the maximal shoulder abduction angle of the exomuscle and whose stiffness is tunable by modulating air pressure. ©2017 IEEE [84].

by modulating air pressure, which is analogous to impedance control.

### 2.4.2 Range of motion

We compared the user range of motion with the exomuscle inflated to approximately 27.5 kPa and without the exomuscle. We found that shoulder internal/external rotation increased by 8%, shoulder horizontal abduction decreased by 13%, and elbow flexion/extension decreased by 8% (Fig. 2.6).

### 2.4.3 Muscular effort

*Isometric task:* To determine whether the forces applied by our exomuscle reduced users' muscular effort, we recorded neuronal activity in select shoulder abductor muscles during a series of isometric holds and out-and-back reaches. We compared the variance of the electromyographical (EMG) signals when users were wearing the exomuscle inflated to approximately 27.5 kPa to that from unsupported trials (combined

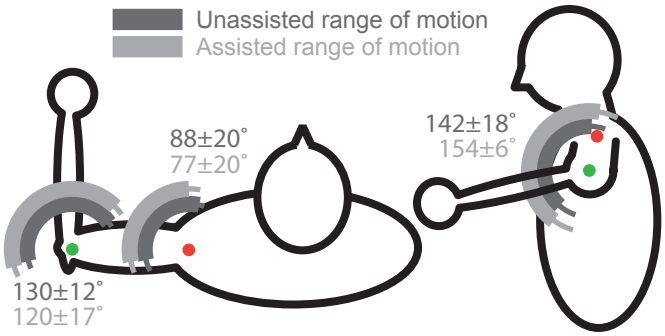


**Figure 2.6: Comparative range of motion (n=3).** The left silhouette presents the range of shoulder horizontal abduction/adduction and elbow flexion/extension, and the right silhouette presents the range shoulder inter/external rotation demonstrated by our users. Ranges of motion are presented as mean plus one standard deviation both without assistance and with the exomuscle inflated with approximately 27.5 kPa of pressure. ©2017 IEEE [84].

isometric and out-and-back reaches). Our results show that, on average, anterior and medial deltoid muscle activity decreased 73% (74% for isometric tasks, 72% for out-and-back reaches). In some cases, such as User 2's anterior deltoid during a 0 degree hold (Fig. 2.3), muscle activity increased with exomuscle support. However, this phenomenon was usually observed when the muscle in question was not active in the unsupported case.

*Dynamic task*: We compare users' muscular effort when using our device to that of another device designed to provide similar support in dynamic tasks. On average, using our exomuscle reduced the variance of recorded EMG signals by 72% from the unsupported case while the air bearing reduced the variance by 86% from the unsupported case.

## 2.5 Effect on workspace of a stroke survivor

Shoulder abduction support can increase stroke survivor's reachable workspace in the horizontal plane [116]. To determine whether our exomuscle can produce a similar effect, we recruited a chronic stroke survivor (male, 3.5 years post-stroke, affected side

= right, height = 175 cm, weight = 63.5 kg, age = 48 years, upper extremity Fugl-Meyer score = 36) who provided informed consent prior to participation in accordance with the policies of the Stanford University Internal Review Board.

We followed the protocol used to measure the reachable workspace in stroke survivors from Sukal et al. [116] with small modifications to accommodate our device. The participant was instructed to individually flex and extend the elbow and shoulder to trace the largest possible circle that he could reach while keeping the hand and elbow raised to the height of the shoulder. To ensure that the full reachable workspace area was achieved during the experiment, the motions were demonstrated by experimenters and the participant was coached by the experimenters during the trial. The participant was then fitted with the exomuscle and repeated the same workspace measurement procedure. In each trial, arm kinematics were recorded using motion capture (Impulse X2E, Phasespace, San Leandro, CA, USA) at 135 Hz with LED markers placed on the C7 vertebrate, acromion, clavicle, olecranon, lateral humeral epicondyle, radial styloid, ulnar styloid, and first knuckle. Workspace area greatly increased through exomuscle use (Fig. 2.7), demonstrating the potential of our exomuscle to improve post-stroke motor abilities.

## 2.6 Discussion

The exomuscle is a one-size-fits-many device that has little impact on healthy users' range of motion. While most exoskeletons require many adjustments for each new user due to the need to align joint axes, the exomuscle was effective on users ranging in height from 165 to 188 cm with minimal adjustments. The exomuscle greatly reduced muscular effort in both isometric and dynamic tasks (74% and 72% reduction of EMG variance from unassisted condition, respectively). In dynamic tasks, the exomuscle performed nearly as well as an air bearing (72% and 86% reduction from unassisted condition, respectively). We also demonstrated a linear relationship between air pressure in the exomuscle and shoulder abduction angle as well as a nonlinear spring behavior that can be used for position or impedance feedback control in future work. Exomuscle use also increased reachable workspace in a stroke survivor.

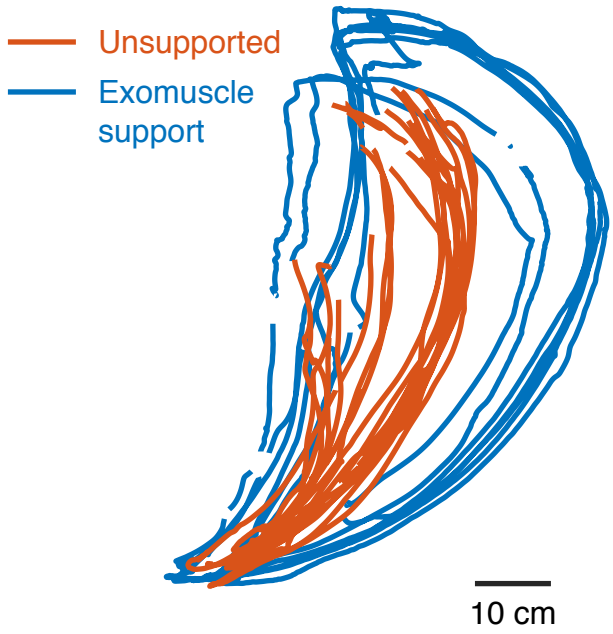


**Figure 2.7: Reachable workspace comparison (n=1).** Comparison of reachable workspace measured in a stroke survivor without assistance (red) and with exomuscle support (blue).

We have demonstrated promising performance of our device with healthy users; future work aims to achieve improved performance and rehabilitative outcomes in motor impaired populations. Prior work shows that individuals with chronic post stroke motor impairment frequently have abnormal co-activations of the medial and anterior components of the deltoid muscle with other muscles [109, 117]. These studies also indicate that when shoulder abduction (which is largely performed by the deltoid) was supported by a robot, motor performance markedly increased [113]. Therapies in which robots gradually decrease the amount of support they provide have also yielded improved motor performance even without further robotic support [115]. Combining the reductions in muscular effort that we observed in the deltoid muscles with the largely preserved range of motion of other upper extremity degrees of freedom suggests that future studies involving users with chronic post-stroke motor impairments will yield similar results to those found in [113] and [115]. The low cost and high portability of our exomuscle might give patients the opportunity have their own exomuscle at home that they can use daily to get much higher volumes of therapy. Therefore we might even see better results than traditional rehabilitation studies such as [115].

Several attempts have been made to make soft wearable assistive robots. Many of them are gait-assist devices worn on the lower extremities [49, 50], but a few have also been developed for upper extremities [82, 83]. Like our device, Natividad and Yeow's device [82] provides shoulder abduction assistance. However, their device behaves like a cantilever beam when inflated. While this device might yield some benefits to stroke patients, such as preventing stiffness in the shoulder, its usefulness for assisting patients to perform activities of daily living is limited. Our device, like another push from below device developed at the same time in the Harvard Biodesign Lab [85], supports shoulder abduction while leaving the remaining degrees of freedom unhindered. With a competent controller incorporated, exomuscle users would be able to perform a wide range of tasks.

Future iterations of our exomuscle will focus on hardware improvements and controller development. Donning and doffing the prototype described here requires the attachment of several sets of straps. A complicated attachment procedure might

prevent people with motor impairments from using our exomuscle, regardless of how effective it proves to be. We plan to streamline the attachment procedure by reducing the number of straps or incorporating the exomuscle into a shirt. Depending on the initial state of the device, we occasionally observe that the exomuscle buckles and provides less support or pushes the arm in an undesired direction. This problem can usually be corrected by increasing the air pressure. However, we prefer to operate the exomuscle at lower pressures to minimize required energy inputs. We believe that a wider exomuscle will be less likely to buckle, but at the expense of a larger profile and a larger amount of air required for operation. We also want exomuscle operation to be as intuitive as possible. Possible approaches include connecting the tube that inflates the exomuscle to another closed reservoir that can be operated by another limb or using electromyography-based controllers [118].

A key criticism of pneumatic devices is that they are reliant on a supply of compressed air or other fluid. While we used a grounded air supply for most of our experiments, we have also used a battery powered portable compressor to inflate the exomuscle. While noisy, the portable compressor inflates the exomuscle beyond the maximum air pressure used in testing within three seconds. Compressed gas reservoirs, such as those used to power paintball guns or quickly inflate bicycle tires, can also be used to repeatedly inflate the exomuscle due to the low air pressures required. While these devices have limited capacity, they are compact, lightweight, quiet, and many are refillable. The exomuscle can also be constructed as a closed system, in which air can pass from another reservoir into the exomuscle. The external reservoir could be actuated by another of the user's limbs.

Design principles similar to those employed for the exomuscle could be used to develop a modular exosuit. While some exosuits that operate across multiple joints have already been developed [49, 50], these designs rely on multi-joint connections. The exomuscle, on the other hand, operates on a single degree of freedom without impinging on other degrees of freedom. Much like the human muscular system, which is made up of muscles specialized for their function, additional exomuscles could be developed with properties to fulfill specialized roles in a larger exomuscle "suit."

The exomuscle increased shoulder internal/external rotation range of motion in

healthy users. While this increase might be an artifact of low user numbers, many researchers have demonstrated that certain muscles consistently act together even in healthy users [119]. As a result, the unloading of certain muscles in healthy users can result in an increase in range of motion [113].

The exomuscle increased reachable workspace area in the unactuated horizontal plane in a stroke survivor. However, more studies are needed to know if more stroke survivors might receive the same benefit. The workspace assessment in this study was performed at a fixed exomuscle pressure and thus a fixed arm elevation. Adding active control to the exomuscle to allow for online adjustments of shoulder elevation might also increase range of motion in the actuated degree of freedom after a stroke.

While we designed our exomuscle for the needs of post-stroke motor impaired individuals, other populations might also benefit from this device. Several professions involve large amounts of time spent raising the hands above the head, which can be extremely fatiguing. One example is a grocery store employee who must repeatedly raise his or her arms overhead with a payload in order to restock shelves. By offloading shoulder adbuctor muscles, our exomuscle might increase endurance and decrease discomfort during such activities. In addition, our exomuscle could be used to augment the user's strength.

# Chapter 3

# Growing exomuscle for shoulder abduction support

## Summary

Assistive devices may aid motor recovery after a stroke, but access to such devices is limited. Exosuits may be a more accessible alternative to current devices and have been used to successfully assist movement after a variety of motor impairments, but we know little about how they might assist post-stroke upper extremity movement. Here, we designed an exosuit actuator to support shoulder abduction, which we call an "exomuscle" and is based on a form of growing robot known as a pneumatic-reel actuator. The length of our device and therefore height of the arm can be increased by growing the robot and reduced by retracting it. We also assembled a ceiling-mounted support to serve as a positive control. We verified that both supports reduce the activity of shoulder abductor muscles and do not impede range of motion in healthy participants (n=4). Then, we measured reachable workspace area in stroke survivors (n=6) with both supports and without support. Our exomuscle increased workspace area in four participants (180±90 $cm^2$) while the ceiling support increased workspace area in five participants (792±540 $cm^2$). Design decisions that make the exomuscle wearable, such as leaving the forearm free, likely contribute to the performance differences between the two supports. Heterogeneity amongst stroke survivors' abilities

likely contribute to a high variability in our results. Though both supports resulted in similar performance for healthy participants, the performance differences in stroke survivors highlight the need to validate assistive devices in the target population. This chapter was adapted from Simpson, C., Huerta, B., Sketch, S., Lansberg, M., Hawkes, E., and Okamura, A., 2020. Upper extremity exomuscle for shoulder abduction support. bioRxiv [120].

## 3.1 Introduction

Stroke, the death of brain tissue due to interrupted blood supply, is the leading cause of adult disability [4]. While the typical stroke survivor regains about 70% of lost motor function [6, 7, 8], stroke remains the most common cause of adult disability in the United States [121]. Due to aging populations and changing lifestyles, the incidence and impact of stroke is expected to increase. Post-stroke permanent disability might be reduced by increasing therapy dosage [101, 102], but rigorously testing large dosages in humans is difficult due to the commitment required of both therapist and patient and the likelihood of interfering with standard care. Assistive devices may help patients to perform more and longer therapies with less therapist involvement.

Assistive devices can be designed to aid patients in a number of ways; one promising approach is to compensate for the effects of gravity. Compensating for gravity has been shown to increase stroke survivors' reachable workspaces [116], theoretically increasing the number of tasks that can be performed. The relationship between gravity compensation and increased reachable workspace is attributed to abnormal flexor synergy activation, in which stroke survivors lose the ability to independently control the shoulder abductor and elbow flexor muscles [110, 112]. Unloading the shoulder abductor muscles by providing gravity compensation reduces activity in the elbow flexor muscles, increasing elbow range of motion [113]. This gravity compensation strategy has been used in an eight-week therapy in which support was gradually removed, and motor improvements were found [24, 115]. Because of the simplicity and effectiveness of this approach, gravity compensation or shoulder abduction support is the goal of many assistive devices.

Exoskeletal robots, which use motors and rigid linkages to transmit forces to the user, have been used extensively in research applications [24, 116]. However, widespread adoption of rehabilitation exoskeletal robots by practicing healthcare providers has not yet taken place. Some commercially produced passive exoskeletal devices, which use stored potential energy to compensate for gravity, are used in the clinic. Examples of such devices include the Hocoma ArmeoSpring and the SaeboMAS. These commercial devices are rarely used outside the clinic. One key factor limiting adoption may be that existing devices are too expensive and complex to operate. Much cost and complexity stems from safety considerations such as aligning robot and operator joints [58], compensating for the additional mass of the robot, and ensuring stable interactions with users [48, 63]. These devices are limited by the workspace of the device, which is usually grounded to a table, the floor, or a wheelchair. Wearable devices, grounded to the body instead of the environment, may diversify the contexts in which assistive devices can used.

Soft exosuits can address many challenges associated with traditional exoskeletal robots. While exoskeletal robots use rigid linkages to generate reaction forces, exosuits forgo rigid linkages, relying instead on the user's skeleton for that purpose [77]. Doing so removes components and therefore mass from the system, allowing exosuits to be constructed of primarily compliant materials that are lightweight, inexpensive, and require less precise manufacturing. While early exosuit designs focused on assisting with locomotion [14, 16, 77], several recent examples actuate the upper extremity [122, 123]. Specifically, exosuits have been created to assist with arm movements in stroke survivors [82, 83, 84, 85, 86, 87, 88]. In particular, several of these studies have examined how exosuit use affects muscular activity in healthy users and whether the exosuit limits the user's range of motion [82, 84, 85, 88]. Only one recent study has examined the effects of an upper extremity exosuit on stroke survivors. In that study, exosuit use increased shoulder abduction and flexion range of motion, the degrees of freedom supported by their exosuit, in five stroke survivors [124]. O'Neill et al. [124] do not investigate whether unsupported degrees of freedom, such as the elbow, benefit from exosuit assistance of shoulder abduction support as suggested by previous studies of gravity compensation after stroke. No validations in healthy users

were reported in that study.

Here, we design and build a novel inflatable actuator for shoulder abduction support, analogous to gravity compensation (Fig. 3.1A). We show in healthy participants that the device does not impede range of motion and supports the anterior and medial components of the deltoid muscles in abducting the shoulder, previously shown to be related to post-stroke reachable workspace. We then test in stroke survivors whether exomuscle assistance increases reachable workspace area in the transverse plane (orthogonal to exomuscle support), and whether a ten-minute assisted therapy session changes reachable workspace area. We perform the same set of evaluations using a ceiling-mounted arm support for a positive control. We show an increase in reachable workspace area in the transverse plane in 4 out of 6 stroke survivors. Exomuscle support correlated with increased elbow range of motion, which is not supported by our exomuscle. Although the ceiling-mounted support and exomuscle produced the same results in healthy participants, we show that they produce very different outcomes in stroke survivors, highlighting the need to validate assistive devices in the target population.

## 3.2 Shoulder abduction support device design

Complexity, weight, cost, and safety considerations all limit access to robot-aided therapies. Our goal is therefore to create a simple, lightweight, inexpensive, wearable device capable of aiding in stroke rehabilitation by supporting shoulder abduction. We also constructed a ceiling-mounted support for use as a positive control. These two devices are shown in Fig. 3.1.

### 3.2.1 Exomuscle design – experimental device

Exosuits are frequently made using multiple actuators that apply compressive loads on the user's joints [49,80,81]. However, in early pilot testing, we determined that the forces required to fully support the weight of the arm without standoffs resulted in uncomfortably high compressive loads on the shoulder. Rather than adding standoffs

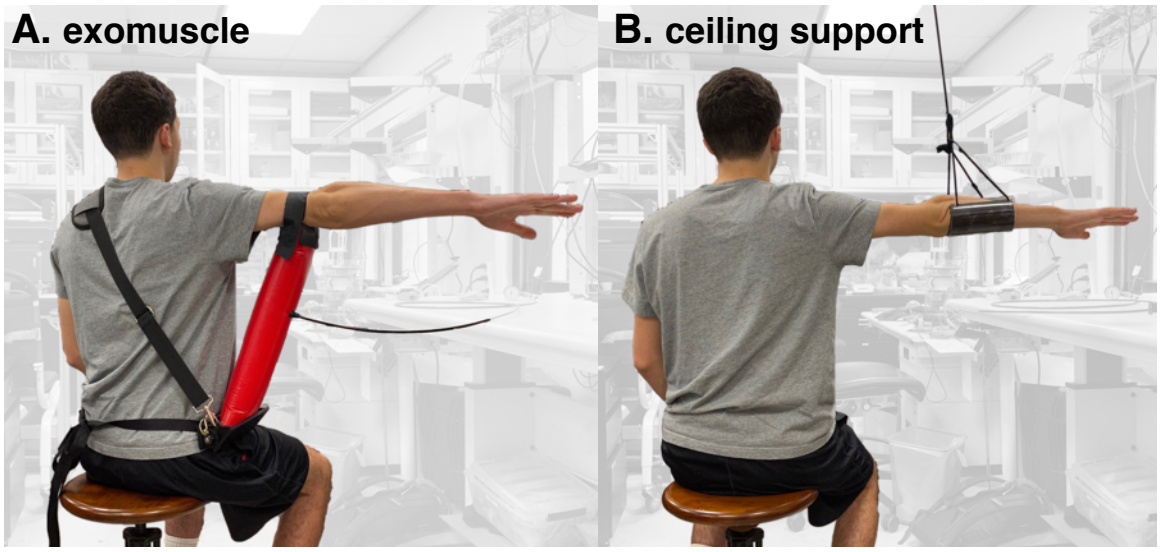


**Figure 3.1: User with (A) an exomuscle and (B) a ceiling support. A.** The exomuscle is the experimental device in this study. Its design is based on a type of growing robot [106] called a pneumatic-reel actuator [107]. **B.** The ceiling support is used as a positive control in this study.

that might catch on objects in the environment to reduce these loads, we designed our device to push the arm from beneath rather than pull from above. Additionally, because our device comprises a single actuator rather than a suit of actuators, we refer to it as an "exomuscle" rather than an "exosuit."

In Simpson et al. [84], we described a compliant inexpensive wearable exomuscle with a single controlled degree of freedom that assists shoulder abduction in healthy users without restricting motion in other joints. That device controls shoulder abduction angle by modulating the air pressure in a bladder sewn with a hinge-like seam to a chest harness and resting under the arm. That device is effective at lifting the arm and supporting movement while pressurized, but can buckle at small shoulder abduction angles/low air pressures. Here we describe a new actuator that uncouples air pressure and shoulder abduction angle.

Our updated design, based on the pneumatic reel actuators developed by Hammond et al. [107], consists of a plastic bladder reinforced by a fabric tube sewn out of thermoplastic polyurethane (TPU)-coated polyester cloth. The fabric reinforced tube

is then wrapped around an axle mounted to the base assembly shown in Fig. 3.2. In this study, we use a locking disk and pin to fix the shoulder abduction angle so that the elbow rests at shoulder height. For active length control, the lock disk can be replaced with a transmission to a motor as described in Hammond et al. [107]. The base assembly is held in place on the wearer's side by a waist strap and a contralateral shoulder strap, which supports the vertical forces required to support the arm. Our prototype base is made out of polyoxymethylene plastic. The supported arm is held in place on top of the inflated bladder by a hook-and-loop fastener strap. A flow chart of the construction process is shown in Fig. 3.2.

When completed, this exomuscle has convenient properties for interfacing with human operators. The height of the support can be adjusted without changing the air pressure by growing or retracting the robot by spooling and unspooling the bladder on the axle. The arm rests on the inflated tube, which is compliant enough at operational air pressures of 25-50 kPa to provide a comfortable support. Additionally, extra material at the top and bottom of the inflated tube where it transitions from a rectangular cross section (at the ends where the tube is rolled about the axle or sewn with a straight seam) to a circular cross section creates pivot points that act as ball joints. These natural pivots combine with soft tissue compliance from the wearer resulting in a flexible support. Because the exosuit should not interfere with other joints, we attach the exomuscle under the upper arm to avoid crossing the elbow joint, which would require additional compliance about the long axis of the bladder to preserve full elbow range of motion.

### 3.2.2 Ceiling support – positive control

To examine the effectiveness of the wearable exomuscle design, we need a good-as-possible support to serve as a positive control for comparison. Previous studies examining the effects of gravity compensation in stroke use robotic exoskeletons [115] or low-friction air sleds to support the arm [113]. In both cases, the workspace of the exoskeleton or table supporting the air sled requires that the workspace task be broken into segments with the robot or table repositioned in the middle to complete

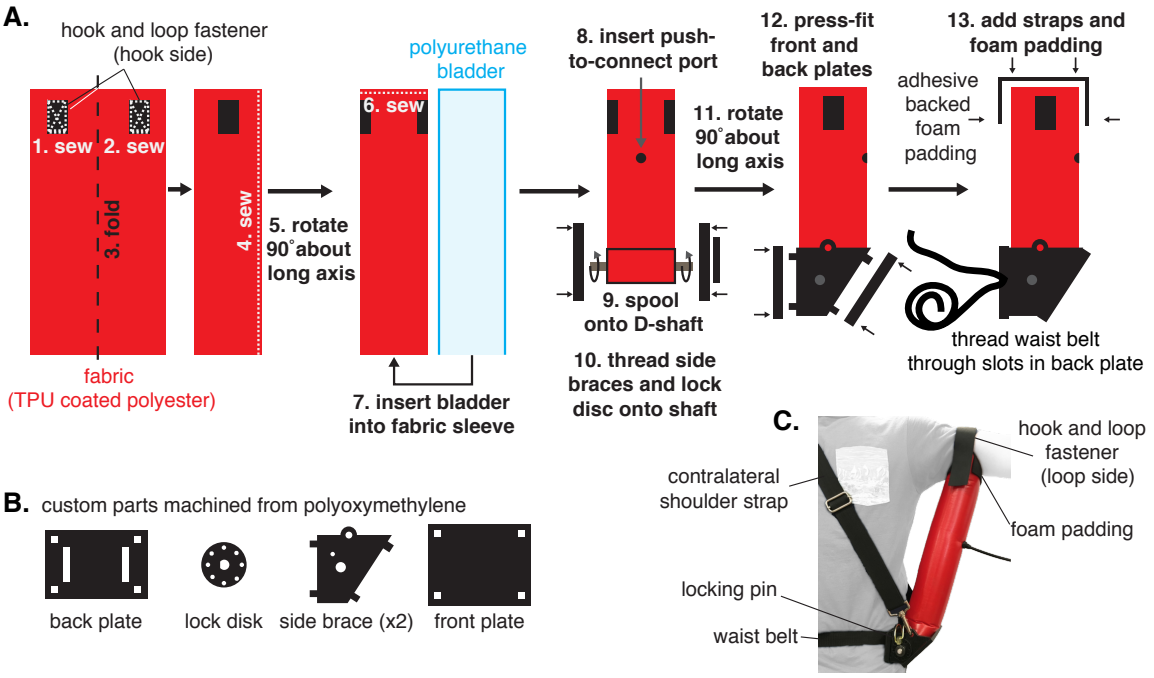


**Figure 3.2: Exomuscle design.** **A.** The pneumatic reel exomuscle consists of two main parts, a long bladder and a base that contains the reel. The bladder is constructed of a single piece of TPU coated polyester with hook and loop fasteners sewn near the tip to hold the strap that will later hold the arm in place. The fabric is then sewn into a tube and then twisted one quarter turn around the long axis such that the hook and loop patches are on the sides. The end of the tube is then sewn shut and a polyurethane bladder inserted. A push-to-connect port is then inserted through the first layer of fabric and one side of the bladder to allow for inflation. **B.** The base station is constructed out of four custom parts machined from polyoxymethylene, a back plate with slots for a waist belt, two side braces that include holes for a shoulder strap to attach, a front plate, and a disk brake. The bladder is spooled onto a D-shaft, and the side braces and disk brake are inserted onto the ends of the D-shaft. Shaft collars can be added for extra stability. The back and front plates are then press fit onto the notches on the side braces. Then foam padding and straps can be added as desired. **C.** When completed, the exomuscle base rests against the wearer's side, supported by the contralateral shoulder strap and waist belt, and underneath the upper arm, supported by another strap.

the workspace measurement. These devices also add inertia to the arm, a potential confound.

Instead, we constructed a low-inertia, large workspace sling support [125, 126]. We suspended an arm rest from the ceiling using 165 cm of high-strength nylon rope. The arm rest was placed under the forearm as close as possible to the center of mass of the arm for each participant. We positioned each participant such that their elbow was directly beneath the attachment to the ceiling.

## 3.3 Device effects in unimpaired population

Before testing in a vulnerable population such as stroke survivors, we wanted to ensure that the exomuscle produces the intended effects and test for confounding effects in unimpaired participants. To that end, we recruited four participants with no indicated musculoskeletal deficits or injuries (3 males, 1 female; age: 26±4 yrs; height: 180±6 cm; mass: 72±10 kg; all right-hand dominant). Participants gave their informed consent in accordance with the policies of the Stanford Internal Review Board. We tested if the exomuscle was able to offload the effort of the shoulder abductor muscles most commonly affiliated with abnormal flexor synergy activation. We also conducted a test to examine whether the exomuscle limits the range of motion of healthy users.

### 3.3.1 Deltoid muscular effort

To determine if our exomuscle assists the user's muscles with shoulder abduction, we measured muscle activity in the shoulder muscles related to post-stroke workspace impairments while participants performed isometric and dynamic tasks. We measured muscle activity from the anterior and medial components of the deltoid muscle using a Delsys Bagnoli 2 EMG system (Natick, MA, USA) read with a National Instruments USB-600X DAQ (Austin, TX, USA) at 1000 Hz. In the isometric tasks, participants were asked to hold their right arm at the height of the shoulder (90° shoulder abduction) with elbow fully extended for three seconds in each of three postures: (1) hand directly in front of the shoulder (90° shoulder flexion), (2) hand directly out to the

side (0° shoulder flexion), and (3) halfway in between those postures (45° shoulder flexion). In the dynamic tasks, participants were asked to start in an initial posture in which the arm is raised to the height of the shoulder (90° shoulder abduction), the elbow fully flexed, and shoulder rotated such that the hand is directly in front of the shoulder. Participants were then asked to reach to each of the three target postures described in the isometric tasks (shoulder abducted 90°, elbow fully extended, shoulder flexed to 90°, 0°, and 45°) before returning to the initial posture. Each task was demonstrated first by the experimenter, participants were asked to confirm they understood the instructions, and the experimenter monitored performance of each task to ensure the correct postures were attained. Each participant completed both isometric and dynamic tasks in three conditions: (1) unassisted, (2) exomuscle support, and (3) support from the ceiling support described in Section 3.2.2.

Electromyograms (EMG) from each muscle were high-pass filtered with a cutoff frequency of 30Hz, rectified, and then low-pass filtered with a cutfoff frequency of 6Hz to create linear envelopes. All filters were 8th order, zero-phase shift Butterworth filters (butter.m and filtfilt.m in MATLAB, Natick, MA, USA). We then computed the average muscle activation in each trial and muscle and compiled all average muscle activations resulting from a given support condition (unsupported, exomuscle, or ideal) and task condition (isometric or dynamic) into a set. Because a one-sample Kolmogorov-Smirnov test showed that the data in some sets were not normally distributed, we used the non-parametric Kruskal-Wallis test followed by Tukey's test to compare muscle activation across support conditions.

Exomuscle use reduced muscle activity by 79.5% ($p = 1.7 \times 10^{-9}$) and 58.6% ($p = 9.6 \times 10^{-6}$) on average in the isometric and dynamic tasks, respectively (Fig. 3.3). The ideal support reduced muscle activity by 83.5% ($p = 6.1 \times 10^{-11}$) and 52.9% ($p = 4.6 \times 10^{-7}$) on average in the isometric and dynamic tasks, respectively (Fig. 3.3). The average muscle activity during exomuscle use was not significantly different from that measured while using the ideal support use in either isometric or dynamic tasks with an $\alpha = 0.05$ confidence level. Both assistive devices support shoulder abduction as intended.

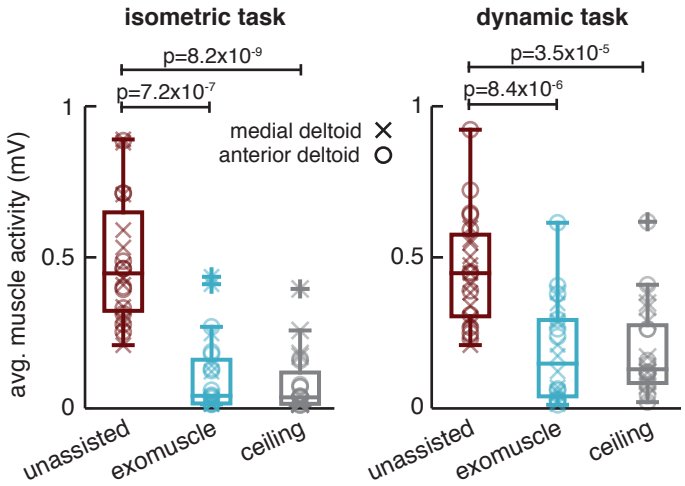


**Figure 3.3: Healthy participant muscular effort in different support conditions (n=4).** The average anterior and medial deltoid muscle activations were computed for each trial of the isometric and dynamic tasks. These were combined into sets according to support type: unassisted, exomuscle, or ceiling support. In both isometric and dynamic tasks, muscle activity decreased with both exomuscle and ceiling support use. There was no difference between the muscle activations recorded in the two support conditions at an $\alpha = 0.05$ confidence level in either task.

### 3.3.2 Range of motion

To be useful in a wide range of tasks, the exomuscle should not impede the motion of the upper extremity while supporting shoulder abduction. To measure upper extremity range of motion, we used motion capture (Impulse X2E, Phasespace, San Leandro, CA, USA) to measure body kinematics at 135 Hz while participants were instructed to move to the extrema of elbow flexion and shoulder flexion with no assistance, with exomuscle support, and with the ceiling support. We also assessed shoulder rotation with no assistance and with exomuscle support. We did not test shoulder rotation with the ceiling support because it attaches at the forearm and thus does not allow shoulder rotation.

Motion capture data was low-pass filtered at 20 Hz using an 8th order, zero-phase shift Butterworth filter (butter.m and filtfilt.m in MATLAB, Natick, MA, USA). Any gaps in the marker trajectories caused by temporary occlusions of the marker were filled using cubic interpolation (interp1 function in MATLAB). We computed the elbow angle using the angle between the forearm vector (vector connecting the LED markers placed on the lateral humeral epicondyle to the ulnar epicondyle) and upper arm vector (vector from the acromion to the lateral humeral epicondyle). We computed the shoulder flexion angle as the angle between the trunk vector (vector connecting the acromion with the C7 vertebrate) and the upper arm vector. We computed the shoulder internal/external rotation angle as the angle between the forearm vector and the vertical axis of the motion capture coordinate frame. For comparison across conditions, we compute the range of motion as the difference between each extrema. For example, the elbow range of motion is the difference between the peak elbow flexion angle and the peak elbow extension angle. We then grouped the ranges of motion for elbow flexion/extension and shoulder flexion/extension into a single set for each support condition. Because a one-sample Kolmogorov-Smirnov test showed that the data in some of these sets were not normally distributed, we used the non-parametric Kruskal-Wallis test to compare range of motion across support conditions. We used the non-parametric Wilcoxon signed-rank test to compare shoulder internal/external rotation in the unassisted and exomuscle support conditions because the ceiling support does not allow for this motion.

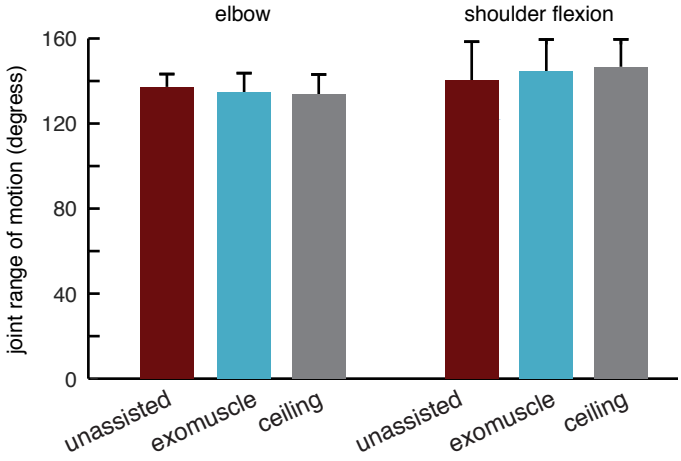


**Figure 3.4: Healthy participant range of motion in different support conditions (n=4).** In addition to supporting shoulder abduction, the exomuscle is designed to minimize its impact on other upper extremity degrees of freedom. Here, we measured range of motion in the shoulder and elbow in the unassisted case (red), while using an exomuscle (blue), and with support from the ceiling-mounted device (gray). The range of motion did not change across the conditions ($p = 0.97$, Kruskal-Wallis test).

The results of the range of motion analysis are shown in Fig. 3.4. Neither the exomuscle nor ceiling support changed the range of motion for shoulder flexion/extension or elbow flexion/extension ($p = 0.97$, Kruskal-Wallis). The exomuscle did not reduce the shoulder internal/external rotation range of motion ($p = 0.89$, Wilcoxon signed-rank test). Thus the exomuscle and ceiling support do not impede the motion of the unsupported joints.

## 3.4 Effects on post-stroke motor performance

Our device was designed to support shoulder abduction, previously shown to increase the reachable workspace area in stroke survivors [113, 116] by offloading abnormal flexor synergy effects [110, 112]. To determine whether the shoulder abduction assistance from our device increases post-stroke reachable workspace as expected, we recruited 6 stroke survivors with upper extremity motor impairments. We screened participants during the recruitment process to include those with arm weakness whose

stroke occurred more than 6 months before the study date and exclude those with conflating health problems, sensory deficits, or that experience pain during passive movements of the arm. All participants gave their informed consent in accordance with the policies of the Stanford Internal Review Board. We administered the upper extremity portion of the Fugl-Meyer exam and tested for visual and tactile neglect in all participants. We also administered the manual muscle test (MMT) and modified Ashworth Scale (MAS) on the biceps, triceps, and deltoids of each participant. Because of safety concerns in lifting the arm, we also checked all participants for scapulo-humeral rhythm. The results of these assessments as well as demographic information are shown in Table 3.1. We measured the reachable workspace of all participants in 3 support conditions: unassisted, exomuscle support, and ceiling support. We also tested an indicator of flexor synergy activation in each condition and tested for session effects.

### 3.4.1 Methods

We designed our exomuscle to aid shoulder abduction and thus increase the reachable workspace of post-stroke users while wearing the device. In pilot studies, however, one participant's unassisted reachable workspace appeared to increase immediately after a short period of exercise with exomuscle support when compared to unassisted reachable workspace before the exercise. Such session effects are rarely reported [127, 128] and the neurophysiological mechanisms for such spontaneous recovery, if they exist, could be useful to investigate. We thus designed a protocol to not only assess (1) reachable workspace and (2) flexor synergy activation in each support condition, but also (3) whether a short period of assisted exercise could produce short-term motor improvements.

Our protocol consists of a set of assessments performed with each of the 3 support conditions. In each assessment, the reachable workspace was measured using the protocol described below in Section 3.4.1 and a proxy for flexor synergy activation was measured using the protocol described below in Section 3.4.1. Each participant completed the first set of assessments unassisted to get baseline measurements.

**Table 3.1: Stroke survivor demographics and clinical assessment scores.**

| ID | Age | Sex | Dominant arm | Affected arm | Years since stroke | FMA UE | MAS | MMT | Neglect | Rhythm |
|---|---|---|---|---|---|---|---|---|---|---|
| 1 | 48 | M | R | R | 3.5 | 36 | [1+, 1+, 2] | [2, 4, 4] | N/N | Y |
| 2 | 53 | M | R | L | 3 | 25 | [0, 0, 0] | [5, 4, 4] | N/N | Y |
| 3 | 70 | M | R | L | 11 | 14 | [0, 1, 0] | [2-, 2-, 2+] | N/N | Y |
| 4 | 44 | F | R | L | 2 | 21 | [0, 0, 2] | [2-, 4, 2] | N/N | Y |
| 5 | 50 | F | R | L | 1 | 17 | [4, 1+, 2] | [4, 2+, 3+] | N/N | Y |
| 6 | 41 | M | R | L | 20 | 47 | [0, 2, 0] | [4, 4, 5] | N/N | Y |

Abbreviations: M = male, F = female, R = right, L = left, N = no, Y = yes
FMA UE = upper extremity portion of the Fugl-Meyer assessment, MAS = modified Ashworth scale,
MMT = manual muscle test
Neglect = visual and tactile neglect, Rhythm = scapulohumeral rhythm.
Scores on the MAS and MMT are presented in the order: [deltoid, biceps, triceps].
Visual and tactile neglect results are presented are presented in the order: visual/tactile.

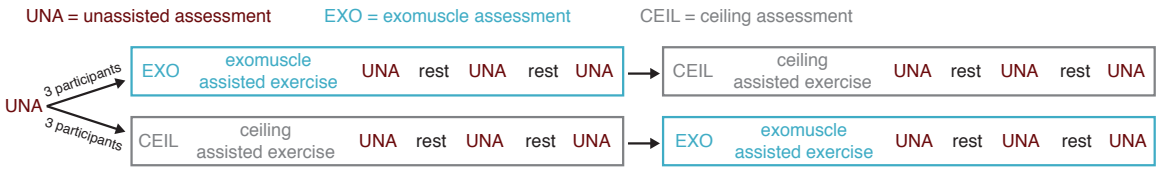


**Figure 3.5: Experimental protocol followed by stroke survivors.** Participants performed a baseline assessment without support from either test device. Participants were then randomly assigned to use the exomuscle or ceiling support first. They performed an assessment with that support followed by a 10-minute supported exercise. Follow-up assessments punctuated by 10-minute rests were performed after each exercise to gauge residual effects of device use. Participants then repeated this set of tests with the other support. Each assessment consists of a workspace measurement and the recording of a proxy for flexor synergy activation.

Participants were then randomly assigned a support condition (exomuscle or ceiling support) and completed a trial with that support condition followed by a trial with the other support condition as shown in Fig. 3.5. Each trial consists of a workspace and flexor synergy evaluation with the assigned support followed by a ten-minute intervention trial designed to replicate the exercise that appeared to produce a session effect in a pilot study. In this intervention trial, participants performed the same clockwise and counterclockwise circular movements with the hand used to measure the reachable workspace (see Section 3.4.1). The direction of the circular movements was randomly determined and repeated for 1 minute. Up to three 1-minute rest periods were allowed as needed. The support was then removed and participants performed another workspace and flexor synergy assessment with no support to test for any effects of the exercise. Participants then rested for ten-minutes before performing another workspace and synergy assessment to determine whether any exercise effects had worn off. Participants were given one more ten-minute rest before a final assessment. Participants then completed the same set of tests with the other support condition, exomuscle or ceiling support.

### Workspace assessment

We followed the protocol used to measure the reachable workspace in stroke survivors from Sukal et al. [116] with small modifications to accommodate our devices and equipment. In every case, participants were instructed to individually flex and extend the elbow and shoulder to trace the largest possible circle that they could reach while keeping the hand and elbow raised to the height of the shoulder. In order to record the largest workspace, participants performed 6 circles per measurement, 3 in each direction with the order randomly determined, and were coached by the experimenter who demonstrated the ideal form throughout. In each trial, arm kinematics were recorded using motion capture (Impulse X2E, Phasespace, San Leandro, CA, USA) at 135 Hz with LED markers placed on the C7 vertebrate, acromion, clavicle, olecranon, lateral humeral epicondyle, radial styloid, ulnar styloid, and first knuckle.

Motion capture data was low-pass filtered at 20 Hz using an 8th order, zero-phase shift Butterworth filter (butter.m and filtfilt.m in MATLAB, Natick, MA, USA). Any gaps in the marker trajectories caused by temporary occlusions (less than 0.2 seconds) of the marker were filled using cubic interpolation (interp1 function in MATLAB). Any occlusions lasting longer than 0.2 seconds were ignored in our analyses rather than interpolated to avoid generating incorrect data. We computed the reachable workspace of the hand using the boundary function in Matlab, which computes a concave boundary around the input data and computes the area of that boundary. However, because the original task described by Sukal et al. [116] required that the arm remain at the height of the shoulder throughout the experiment, we disregarded datapoints in which the hand (defined as the marker on the ulnar epicondyle) or elbow (defined as the marker on the lateral humeral epicondyle) fell below 20 cm below the height of the shoulder (defined as the marker on the acromion). Due to occlusions in some participants, we substituted the acromion for the C7 marker in all trials. Because the 20 cm threshold selected has the potential to impact the results, we performed a sensitivity analysis of this value presented in the Appendix.

We also computed the range of elbow and shoulder flexion/extension achieved during the workspace recordings using the same method described in Section 3.3.2.

#### Flexor synergy assessment

The increase in workspace that normally occurs with gravity compensation is thought to be due to unloading of the flexor synergy. To estimate the relative magnitude of the flexor synergy effect, Ellis et al. [129] developed an experiment to approximate flexor synergy activation in which the affected arm is placed in a posture that activates the deltoid muscles – and thus the flexor synergy in those that express abnormal flexor synergy – while measuring the activity of the biceps muscles. We copied this experiment with each of our support conditions by asking each participant to hold a posture for three seconds in which the hand and elbow were raised to shoulder height with the hand resting in front of the shoulder and the elbow flexed approximately 70° while the activity of the biceps was measured using a Delsys Bagnoli 2 system (Natick, MA, USA) read with a National Instruments USB-600X DAQ (Austin, TX, USA) at 1000 Hz.

EMG from each participant were high-pass filtered with a cutoff frequency of 30Hz, rectified, and then low-pass filtered with a cutfoff frequency of 6Hz to create linear envelopes. All filters were 8th order, zero-phase shift Butterworth filters (butter and filtfilt functions in MATLAB). We then computed the average muscle activation in each trial.

### 3.4.2 Results

#### Workspace

Workspace area increased with exomuscle support in 4 out of 6 participants compared with 5 out of 6 with ceiling support (Fig. 3.6). The two participants who did not increase in workspace with exomuscle support were the two participants with the largest baseline workspace area (S2 and S6, Fig. 3.6). Only participant 4 did not increase in workspace area with ceiling support. This participant also exhibited the most fatigue and spasticity effects. Note that we present the workspace area change relative both to the baseline measurement and relative to the previous unassisted trial in Fig. 3.6B. We discuss the comparison against the previous unassisted trial here because it is likely the more accurate measurement due to the effects of fatigue

and spasticity discussed in Section 3.4.2.

Changes in workspace area were strongly correlated with changes in elbow range-of-motion (r=0.84), while shoulder range-of-motion was weakly correlated with workspace area (r=0.34, Fig. 3.6C.), consistent with Sukal et al.'s findings [116].

### Flexor synergy

Biceps activation during a shoulder abduction task, a proxy for flexor synergy activation, decreased in 4/6 and 5/6 participants using the exomuscle and the ceiling support, respectively. Biceps activations were weakly correlated with elbow range of motion (r=0.31) and workspace area (r=0.41) (Fig. 3.7). Though the correlations shown in Fig. 3.7 are weak, they show the expected trend: that reductions in flexor synergy activation will lead to increased elbow range of motion and increased reachable workspace. This correlation might be weak due to our limited ability to screen for participants with abnormal flexor synergy activation, adding noise to this measurement.

### Session effects

We did not see single-session increases in workspace area after our intervention. Rather, we saw short-term decreases in workspace related to use of the arm, likely due either to fatigue or use-dependent effects of spasticity (Fig. 3.8). Workspace area decreased more after exomuscle exercise than after exercise with the ceiling support (p= 0.03, Wilcoxon rank sum), suggesting exomuscle use was more fatiguing than use of the ceiling support. Because participants did not recover these losses in workspace area between the first and third unassisted assessments (p=0.79, Wilcoxon sum rnk), this time-dependent effect is likely to have impacted our results. If we compare workspace area while using the exomuscle to the previous trial in which assistance was not used rather than the baseline measurement, 4/6 participants increase in workspace by an average $180 \pm 90$ cm$^2$.

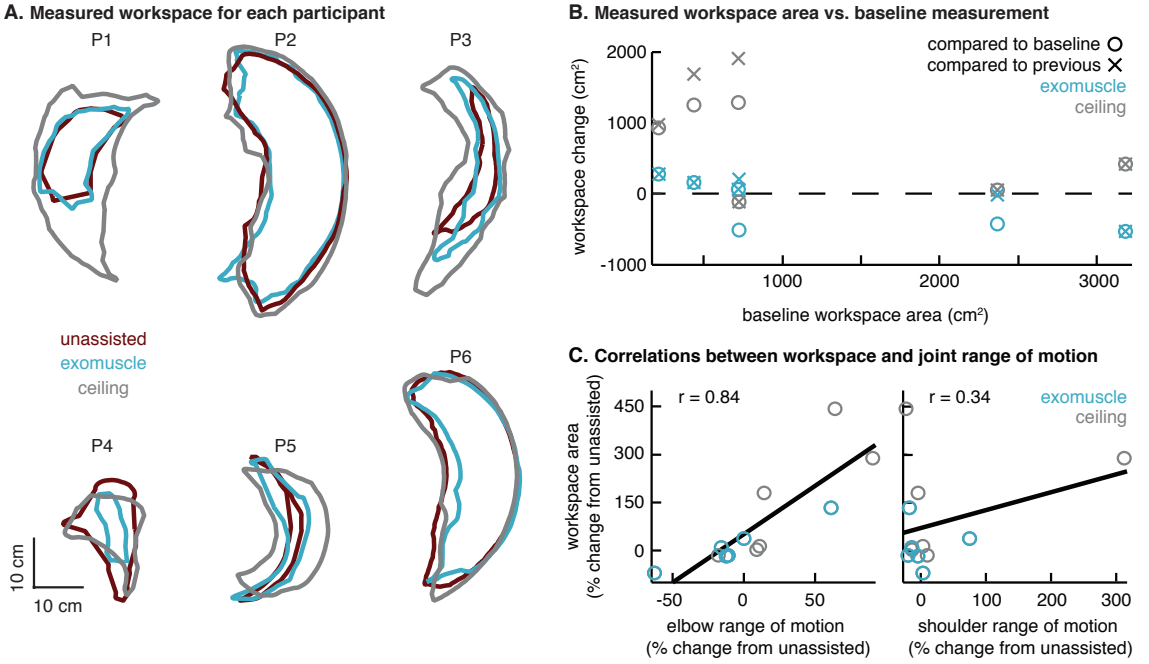


**Figure 3.6: Stroke survivor workspace measurements with different support conditions (n=6). A.** Workspace area measured in each participant in three support conditions: unassisted, exomuscle, and ceiling support. **B.** Workspace area increased for only three participants using the exomuscle (blue hollow circles) while the ceiling support increased workspace in five participants (gray hollow circles). Pariticpants with small unassisted workspaces received more benefit from both devices. Four participants increased in workspace when compensating for fatigue by comparing against the previous unassisted trial, rather than the first. **C.** Elbow range of motion was strongly correlated with workspace area (r=0.84). This correlation supports the argument that the support devices offload the flexor synergy, which constrains elbow range of motion. Shoulder range of motion was weakly correlated with workspace area (r=0.34).

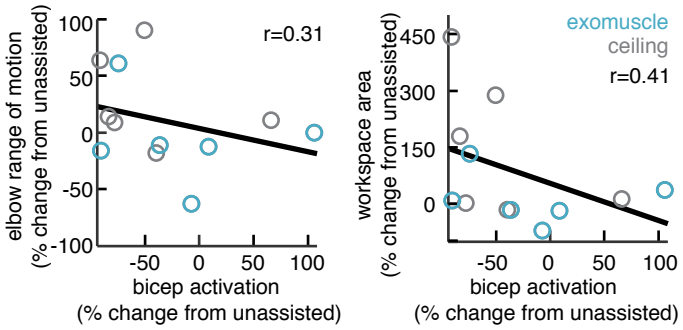


**Figure 3.7: Correlations between biceps activation and elbow range of motion and workspace area.** We measured biceps muscle activation as a proxy for flexor synergy activation [129]. Changes in bicep activation were weakly negatively correlated with both elbow range of motion (left) and workspace area (right).

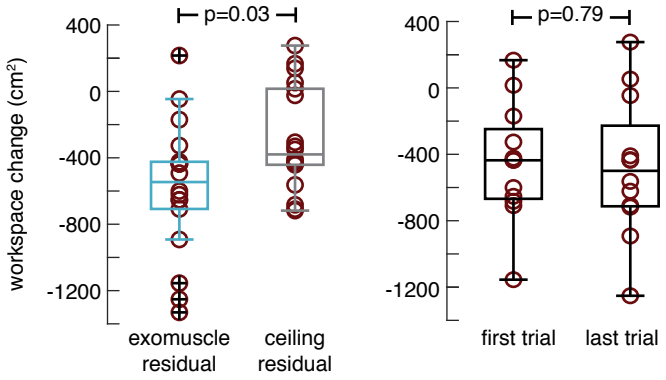


**Figure 3.8: Session effect on unassisted workspace area.** Workspace area decreased more after exercise with the exomuscle than with the ceiling support (left, p=0.03, Wilcoxon rank sum test), suggesting that exomuscle use was more fatiguing than the ceiling support. Workspace area did not return to baseline after the two ten-minute rest periods (right, p=0.79, Wilcoxon rank sum test), suggesting that fatigue or spasticity may have played a role in decreasing workspace measurements in the second half of the experiment. To control for this, we compared workspace measurements to the most recent unassisted trial in addition to the baseline trial in Fig. 3.6.B.

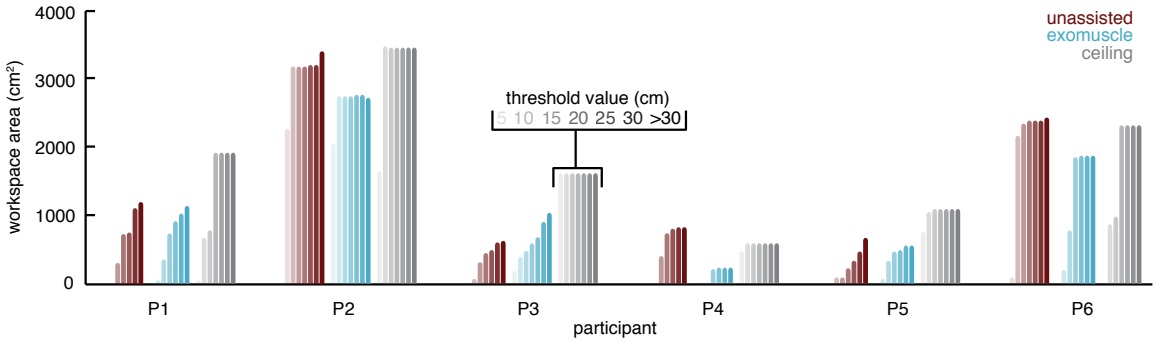


**Figure 3.9: Sensitivity of workspace area measurement to the threshold value.** We computed the reachable workspace area using data in which the hand and elbow were within a thresholded height of the shoulder of 20 cm. Here we compute the reachable workspace area for different threshold values ranging from 5 cm to considering all points (>30 cm) for each participant in each support condition.

### 3.4.3 Sensitivity to selected threshold value

To estimate the workspace area at the height of the shoulder in our experiment, we disregarded datapoints in which the hand or elbow markers dropped below the shoulder marker by threshold of 20 cm (Fig. 3.6). However, because this threshold has the potential to influence our results, we perform a parameter sweep on the value of the threshold. Our parameter sweep shows that workspace measurements using the ceiling support are insensitive to the selected margin, likely due to the forearm support provided.

## 3.5 Discussion

We designed a single degree-of-freedom exosuit actuator that we call an exomuscle to support shoulder abduction, verified that it performs as intended in healthy participants, and tested its efficacy in increasing a motor performance metric in stroke survivors. Several recent devices incorporate multiple controlled degrees of freedom to command a larger range of actions in the wearer. We take the opposite approach in attempting to assist only a single degree of freedom shown in other works to be effective in improving a measure of post-stroke motor capability, reachable workspace

area. We verified in healthy subjects that our exomuscle reduces the activity of shoulder abductor muscles required for support against gravity and implicated in reduced workspace area. We also verified that the exomuscle does not impede joint range of motion of the shoulder or elbow. We then measured workspace area in six stroke survivors, finding an increase in workspace area in four with exomuscle support. We compared the exomuscle with a ceiling support serving as a positive control, which increased workspace area in five participants. Though the two performed similarly in healthy participants, the ceiling support outperformed the exomuscle in every measure in stroke survivors. This result highlights the need to study device effects in the target population.

Several design factors may contribute to the difference in performance between the two devices in stroke survivors. Certain design concessions that were made to make the exomuscle wearable are not necessary for the ceiling support. The most noticeable of these is that the ceiling support lifts the user's forearm while the exomuscle supports the wearer's upper arm, leaving forearm support to the user. This concession enables exomuscle users to internally rotate the shoulder and allows for a simpler design than would be required to support the forearm throughout the full range of shoulder-plus-elbow motion. This concession made little difference to healthy users, who were able to support their own forearms while exploiting the exomuscle for support. Stroke survivors, on the other hand, frequently needed the additional forearm support provided by the ceiling support to maintain the experiment posture.

Stroke survivors have different levels of motor ability depending on the size and location of the lesion and on treatment. Stroke survivors frequently experience a combination of sensorimotor deficits including abnormally coupled joints [109, 112, 113], increased noise in sensing and estimation [130], muscular weakness [131], and spasticity [132]. Our exomuscle was designed to assist individuals with abnormally coupled joints in the form of the flexor synergy [133]. Our screening procedure, however, likely failed to distinguish between individuals with an abnormal flexor synergy and those with muscular weakness for example. These sensorimotor deficits can have very different effects on motor performance [134], which might explain in part why some of our participants increased in reachable workspace by 130% while

others decreased by up to 70%.

Exosuits, which have no rigid frame, require that the user's musculoskeletal system must support the additional loads generated by the device. In many cases, these loads are compressive [49,80,80,81,86]. However, our device can produce tensile loads on the shoulder complex, which must be supported by soft tissue. Some stroke survivors have difficulty supporting tensile loads in the shoulder, even in unloaded scenarios, resulting in subluxation. Though commercial braces exist to support against subluxation in stroke survivors that could be used in parallel with our device, a better approach might be to design assistive devices that either generate compressive loads on the shoulder in a comfortable range or those that add no net resultant force to the shoulder as in traditional exoskeletons whose frames support their own reaction forces.

Open challenges for this device include active control necessitating transparent intent recognition and onboarding of all actuators and power sources. Simple, inflatable devices such as ours still require an actuator, compressor, power supply, controller, and sensing for transparent untethered operation. Given that our device is meant to compensate for gravity, a predictable force whose effects vary only with body state, purely mechanical devices can be designed to accomplish the same thing with 0 controlled DOFs [74, 94, 135, 136]. Such mechanisms, can provide shoulder abduction support that varies with posture to negate the effects of gravity on a wearer's arm without actuators, compressors, power supplies, controllers, or sensing. These mechanisms' rigid frames react applied loads, meaning that no net force is applied to the shoulder complex that may cause discomfort in stroke survivors.

While our exomuscle is designed for the needs of stroke survivors, other populations might also benefit from similar devices. Gravity supported therapy has shown to improve clinical measures of motor ability in participants with cerebral palsy [137]. Gravity-compensating devices can also provide movement benefits to individuals with muscular dystrophy [138], though most extant examples are mounted to wheelchairs and are not wearable.

# Chapter 4

# Passive exoskeleton for shoulder abduction support


## Summary

Assistive devices can aid stroke survivors in upper-extremity movements by supporting shoulder abduction. These devices are typically world-grounded, limiting the contexts in which they can be effectively used. Wearable devices might allow stroke survivors to benefit from assistance in a wider range of activities, but must be inexpensive to be widely useful. In this chapter, we develop a wearable passive exoskeleton similar to those used to support overhead industrial work, verify its effectiveness for shoulder abduction support, and that it does not interfere with upper extremity range of motion in healthy participants. We outline an experiment to test whether stroke survivors receive any clinically relevant benefits while wearing the exoskeleton, and discuss future experiments that could be enabled by such devices.


## 4.1 Introduction

In Chapters 2 and 3, we designed and tested two exosuit actuators. Both of these devices were able to decrease shoulder abductor muscle activity while preserving active range of motion in healthy participants and both increased reachable workspace

area in some stroke survivors. The devices presented in the earlier chapters are made from inexpensive components and are relatively easy to manufacture, keeping costs low. However, these devices only function as the actuator and frame of the exoskeleton. In our experiments, we used these exosuit actuators in a passive mode with the shoulder abductor position fixed by the experimenter. For the exosuit actuators to raise and lower the arm actively for the operator, difficult challenges such as control and onboarding of power sources (batteries and compressors) must be resolved. While numerous technologies exist to both perform autonomous intent recognition and control [13, 14, 69, 70, 71, 72, 73] and to onboard all components, a more elegant solution might be to obviate these challenges through mechanical design.

In previous chapters, we have simplified our designs by focusing on the actuation of a single degree of freedom: shoulder abduction. We elected to support shoulder abduction because it is a particularly problematic joint to control for stroke survivors. Though the neural mechanisms governing that phenomenon are still being investigated, interventions that support shoulder abduction have proven effective [115, 116, 139]. The primary force to be countered in shoulder abduction is the effect of gravity on the arm. The moment needed to counter gravity varies sinusoidally with shoulder abduction angle. A number of passive mechanisms have been developed to support the weight of the arm using this approach [74, 90, 91, 92, 93, 94, 95, 96]. Few of these devices are wearable. Most of the wearable devices are developed for industrial applications and do not support low angles of shoulder abduction ($<60°$) – making them less useful for stroke survivors that need help lifting to that height.

## 4.2 Design

Because complexity, weight, cost, and safety considerations all limit access to robot-aided therapies, our goal was to design a lightweight, low-cost, wearable, passive exoskeleton to support shoulder abduction. Existing wearable devices that passively compensate for the weight of the arm use counterweights [90] or springs with variable moment arms [74, 91, 92, 93]. To keep exoskeleton mass low, we chose the latter approach. Our exoskeleton is wearable, inexpensive to manufacture, lightweight, and

supports the full range of shoulder abduction, where other existing devices only offer a subset of these features.

### 4.2.1 Components

Each force acting on the body must have an equal and opposite reaction. Many world-grounded upper extremity exoskeletons use a frame mounted to the ground, a table, or a wheelchair to react the forces applied to the human operator. In a wearable device, both the intended force and the reaction force must be applied to the operator. We elected to exploit the operator's torso to resist forces needed to support the arm. Attaching to the torso allows for a large contact area that reduces pressure on the body exerted by the exoskeleton frame. Our exoskeleton then consists of three subsystems: the connection to the arm, the connection to the torso, and the exoskeleton frame.

#### Connection to arm

We designed a custom 3D printed arm cup to interface between the exoskeleton frame and the operator's arm. The arm cup is designed with a cylindrical profile in which the arm rests. Slots allow for hook and loop fasteners to be inserted to securely fasten to the arm (Fig. 4.1D). Counterbored holes on both ends of the arm cup allow for a quick release push pin connection to holes in the arm linkage of the exoskeleton frame (Fig. 4.1C). The quick release pin is connected to the distal of the two counterbored holes on the arm cup. The single pin connection allows for the arm cup to rotate, which can reduce pressure concentrations on the upper arm in case of misalignments. The counterbored holes on both ends of the arm cup allow for the quick release pin to be attached at either end of the cup to allow for use of the same arm cup on either arm. The arm cup is lined with 3 mm thick neoprene padding for comfort.

#### Connection to torso

We sewed daisy chains to a neoprene posture vest using 1 and 1.5 inch (2.5 and 3.8 cm) wide nylon webbing. A vertical daisy chain was sewn on the lateral inferior posterior

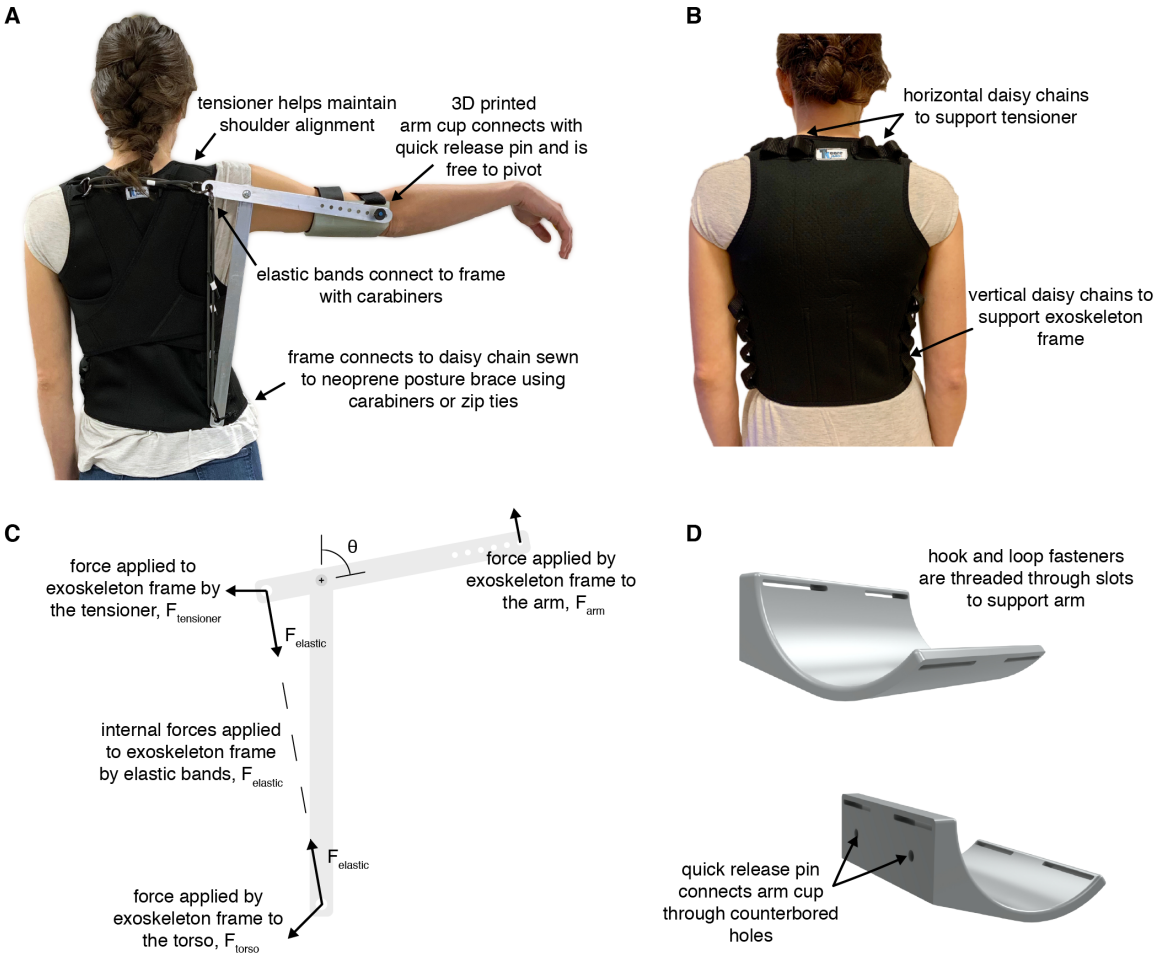


**Figure 4.1: Passive exoskeleton design.** **A.** Photograph of a user wearing the exoskeleton. **B.** Detailed view of vest. Vertical daisy chains were sewn to the lateral inferior posterior aspects of a neoprene vest to support the exoskeleton frame. Horizontal daisy chains were sewn to support a tensioner intended to maintain alignment. **C.** Exoskeleton frame. Internal forces produced by the elastic bands produce an upward force to lift the arm. The forces applied to the arm are reacted at the inferior end of the exoskeleton frame by the attachment to the vest on the torso. The tensioner applies a horizontal force to help maintain alignment between the exoskeleton frame pivot point and the shoulder. **D.** Detailed view of the custom 3D printed arm cup.

aspect of the vest to support the vertical loads applied by the exoskeleton frame. The exoskeleton frame connects to whichever loop in the daisy chain best aligns the frame to the shoulder joint via a carabiner or zip tie. To allow for support of either arm or both arms simultaneously, we sew these vertical daisy chains to both sides of the vest. We constructed three sizes of vest to suit a larger range of operators. Horizontal daisy chains were sewn to the lateral superior posterior aspects of the vest near the shoulders to support a contralateral tensioner that helps to maintain alignment between the exoskeleton and operator's shoulder joint (Figs. 4.1A and B). In the current design, the tensioner attaches to the arm linkage of the exoskeleton frame, producing an undesired torque that pushes the arm towards horizontal (abducted to 90°). When the shoulder is abducted more than 90°, the torque generated by the tensioner is in the opposite direction from the torque generated by the vertical elastic bands. Though the magnitude of this undesired torque is small compared to the torque caused by the vertical elastic bands, future design iterations might remove this torque altogether by moving the connection point of the tensioner to the torso linkage or axle.

**Exoskeleton frame and springs**

The exoskeleton frame supports the elastic bands that act as springs and reacts the forces generated by the bands to generate a pure moment. The frame is constructed of 1 × 1/4 inch (2.5 × 0.6 cm) aluminum bars. Two bars form the frame, the torso linkage and the arm linkage. The two linkages are connected by a pin joint made from a barrel screw serving as the axle and a flanged bearing to reduce friction. Quarter-inch (0.6 cm) holes were drilled in the arm linkage through which quick release pins connect to the arm cup. The exoskeleton can be adjusted to different arm lengths by connecting through different holes. Half-inch (1.3 cm) holes are drilled in the proximal end of the arm linkage and the inferior end of the torso linkage to accept carabiners. The frame is then attached to the vest by the carabiner on the torso linkage and by zip ties to the daisy chains on the vest, providing ball joints that allows unimpeded motion for the operator. The elastic bands can be added or removed to adjust the supportive moment to suit individual needs. Similarly, the length and stiffness of

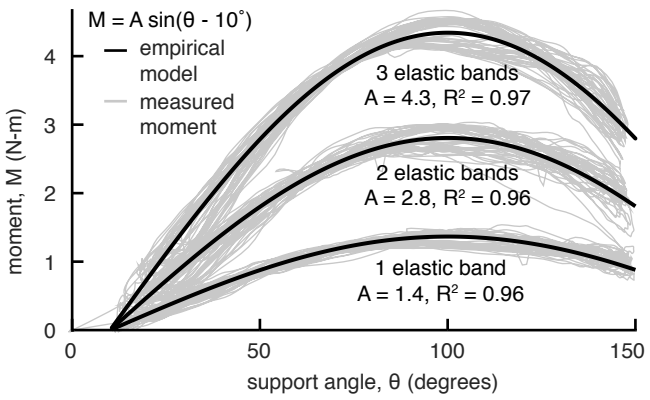


**Figure 4.2: Device angle-moment relationship.** Experimentally measured moments vary sinusoidally with support angle. The amplitude of the sinusoidal fit, A, varies linearly with the number of elastic bands. The exoskeleton moment can be reliably estimated from two parameters, exoskeleton state, $\theta$, and number of elastic bands.

the tensioner can also be adjusted to suit individual needs. The exoskeleton frame is shown in Fig. 4.1A as a part of the full assembly.

### 4.2.2 Angle-moment relationship

In order to support the arm against gravity, the shoulder muscles must exert a moment that varies with posture and external loads. By neglecting external loads and modeling the arm with the elbow fully extended as a pendulum, we determine that our support needs to generate moments that vary sinusoidally with shoulder abduction angle, $M \propto \sin\theta$.

We measured the moment generated by our device as we swept the support through a range of angles. We measured the applied force using a force gauge (Mark-10, Copiague, NY, USA) and the exoskeleton's state and the applied force's line-of-action using motion capture (PhaseSpace, San Leandro, CA, USA). A sine function with a phase-shift of 10° explains $\geq$96% of the variance in our data (Fig. 4.2). The moment linearly increases with the number of rubber bands loaded onto the exoskeleton.

## 4.3 Device effects for unimpaired users

Before testing in a vulnerable population such as stroke survivors, we verify that our exoskeleton provides the intended support and test for confounding effects in unimpaired participants. We tested whether the exoskeleton can reduce shoulder abductor muscle effort and whether the exoskeleton limits the users' joint range of motion in six participants with no musculoskeletal deficits or injuries (3 males, 3 females; age: 30±2 yrs; height: 170±6 cm; mass: 66±9 kg; all right-hand dominant). Participants gave informed consent in a study approved by the Stanford Internal Review Board before completing the study.

### 4.3.1 Deltoid muscle activation

To determine whether the moments applied by the exoskeleton reduce muscular effort, we performed the same experiments as Chapters 2 and 3 in which we measured muscle activity in the shoulder muscles related to post-stroke motor impairments while participants performed isometric and dynamic tasks. We measured activity from the anterior and medial components of the deltoid muscle using a Delsys Bagnoli 2 EMG system (Natick, MA, USA) read with a National Instruments USB-600X DAQ (Austin, TX, USA) at 1000 Hz. In isometric tasks, participants were asked to hold their right arm at the height of the shoulder (90° shoulder abduction) with elbow fully extended for three seconds in each of three postures: (1) hand directly in front of the shoulder (90° shoulder flexion), (2) hand directly out to the side (0° shoulder flexion), and (3) halfway in between those postures (45° shoulder flexion). In dynamic tasks, participants were asked to start in an initial posture in which the arm is raised to the height of the shoulder (90° shoulder abduction), the elbow fully flexed, and shoulder rotated such that the hand is directly in front of the shoulder. Participants were then asked to reach to each of the three target postures described in the isometric tasks (shoulder abducted 90°, elbow fully extended, shoulder flexed to (1) 90°, (2) 0°, and (3) 45°) before returning to the initial posture. Each task was demonstrated first by the experimenter, participants were asked to confirm they understood the instructions, and the experimenter monitored performance of each task to ensure

the correct postures were attained. Each participant completed both isometric and dynamic tasks in two support conditions: (1) unassisted and (2) with exoskeleton support.

Electromyograms from each muscle were high-pass filtered with a cutoff frequency of 30Hz, rectified, and then low-pass filtered with a cutfoff frequency of 6Hz to create linear envelopes. All filters were 8th order, zero-phase shift Butterworth filters (butter and filtfilt functions in MATLAB, Natick, MA, USA). We then computed the average muscle activation in each trial and computed the average muscle activation for each subject across resulting from a given support condition (unassisted or exoskeleton assisted) and task condition (isometric or dynamic). A one-sample Kolmogorov-Smirnov test showed that the data was normally distributed, so we used paired t-tests to compare muscle activation between support conditions.

Exoskeleton use reduced muscle activity by 51% ($p = 0.0044$, paired t-test) and 63% ($p = 0.0035$) on average in the isometric and dynamic tasks, respectively (Fig. 4.3.A).

### 4.3.2 Range of motion

For maximal utility, the exoskeleton should not impede the motion of the upper extremity while supporting shoulder abduction. To test whether the exoskeleton impedes upper extremity range of motion, we performed the same experiments as Chapters 2 and 3 in which we measured body kinematics using motion capture (Impulse X2E, Phasespace, San Leandro, CA, USA) at 135 Hz while participants moved to the extrema of elbow flexion/extension, shoulder flexion/extension, shoulder medial/lateral rotation, and shoulder abduction/adduction in two conditions: (1) unassisted and with (2) exoskeleton support.

Motion capture data was low-pass filtered at 20 Hz using an 8th order, zero-phase shift Butterworth filter (butter and filtfilt functions in MATLAB, Natick, MA, USA). Any gaps in the marker trajectories caused by temporary occlusions of the marker were filled using cubic interpolation (interp1 function in MATLAB). We computed the elbow angle using the angle between the forearm vector (vector connecting the

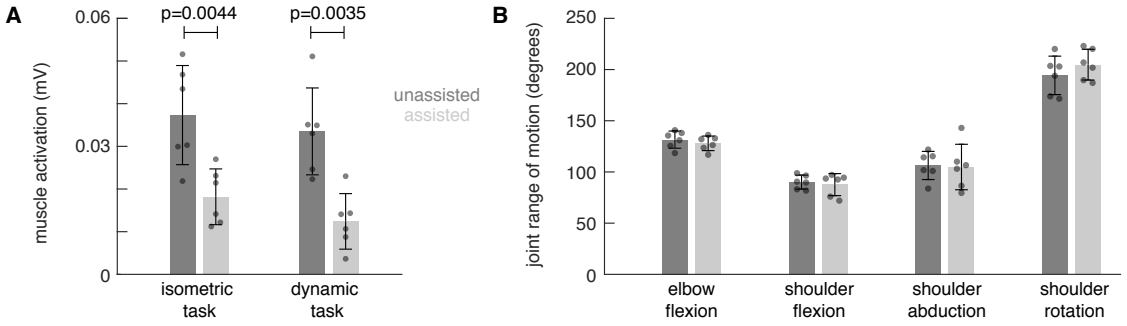


**Figure 4.3: The exoskeleton reduces shoulder abductor muscle activity while not limiting range of motion of any upper extremity joint (n=6). A.** Muscle activity measured from the anterior and medial heads of the deltoid muscle were reduced with exoskeleton support in both isometric tasks ($p = 0.0044$, paired t-test) and in dynamic reaches ($p = 0.0035$). **B.** The exoskeleton provides this support without limiting the range of motion of the elbow or any of the shoulder degrees of freedom (p=0.97, Kruskal-Wallace test).

LED markers placed on the lateral humeral epicondyle to the ulnar epicondyle) and upper arm vector (vector from the acromion to the lateral humeral epicondyle). We computed the shoulder flexion angle as the angle between the trunk vector (vector connecting the acromion with the C7 vertebrate) and the upper arm vector. We computed the shoulder internal/external rotation angle as the angle between the forearm vector and the vertical axis of the motion capture coordinate frame and shoulder abduction angle as the angle between the upper arm vector and the vertical axis of the motion capture coordinate frame. For comparison across conditions, we compute the range of motion as the difference between each extrema. For example, the elbow range of motion is the difference between the peak elbow flexion angle and the peak elbow extension angle. Because a one-sample Kolmogorov-Smirnov test showed that the data were not normally distributed, we used the non-parametric Kruskal-Wallis test to compare range of motion between support conditions.

The results of the range of motion analysis are shown in Fig. 4.3.B. The exoskeleton did not change the range of motion for shoulder flexion/extension or elbow flexion/extension ($p = 0.97$, Kruskal-Wallis test).

## 4.4 Planned experiments in stroke survivors

Studies of the impacts on post-stroke motor performance of assistive devices typically employ targeted measurements of joint-level performance. For example, the devices described in Chapters 2 and 3 and the most recent published study on exosuits for upper extremity [124] assistance measured the range of motion of specific joints or of multiple joints used in coordination as in the reachable workspace area assessments we performed. While joint range of motion and reachable workspace area affect the ability to perform activities of daily living, they are not necessarily perfectly correlated. It is important to consider how an assistive device might impact a stroke survivor's ability to perform activities of daily living directly.

Standardized measurements of functional ability are commonly used to assess functional ability and recovery in stroke survivors. One of the most common of these assessments is the Fugl-Meyer test [140]. We administered the upper extremity portion of the Fugl-Meyer assessment in Chapter 3 because the assessment's ubiquity makes it possible to compare the motor ability of stroke survivors across studies. The Fugl-Meyer test, however, primarily assesses the ability to move outside of certain movement synergies commonly observed after a stroke. Other tests, such as the Wolf Motor Function Test (Wolf) and Action Research Arm Test (ARAT) [141, 142], focus on stroke survivors' abilities to accomplish activities of daily living. These tests may not be good indicators of motor recovery because increased reliance on compensatory movements might give false positives [143]. However, these tests might be well suited to examining the functional benefits of exoskeleton or exosuit assistance on activities of daily living. Because the ARAT test is much quicker to administer, limiting the effects of fatigue, shown to be an important considerations in Chapters 3 and because results on the Wolf and ARAT tests are highly correlated [144], we propose using the ARAT to examine whether a given exoskeleton or exosuit can improve an operator's abilities to complete activities of daily living. The minimum clinically relevant difference in ARAT scores is 5.7 points [145]. If a stroke survivor improves by at least 6 points on the ARAT scale with exoskeleton assistance, that operator can be considered to be functionally less disabled than when not receiving

exoskeleton assistance. We propose running randomized trials in which 5-10 stroke survivors complete ARAT assessments with and without exoskeleton assistance in randomized order in a single session with a short stretching break in between the assessments to counter fatigue and spasticity effects.

Unfortunately, these planned experiments were placed on hold indefinitely due to the COVID-19 pandemic.

## 4.5 Discussion

In this chapter, we design, construct, and test in healthy volunteers a fully wearable lightweight passive exoskeleton. This exoskeleton can fit a range of body sizes due to design considerations such as different sizes of vests, daisy chains that allow for attachment at different heights, and multiple contact points along the arm linkage to allow for different arm lengths. The moment provided by the exoskeleton is linearly related to the number of elastic bands attached, it can be predictably titrated by adding and removing elastic bands. We demonstrated that the exoskeleton offloads shoulder abductor muscle effort without impeding range of motion in any upper extremity degree of freedom in six healthy participants. We also motivate an experiment to determine whether the exoskeleton can improve stroke survivors' performance on standardized assessments of activities of daily living.

Simplifications make our exoskeleton easier to use and manufacture, but can negatively impact performance. For instance, we modeled the arm with the elbow extended as a simple pendulum that requires a sinusoidal torque to counteract gravitational forces. However, the elbow is unlikely to remain locked in place during activities of daily life and the actual moment needed to support the arm will be a function of both shoulder abduction angle and elbow angle. The forearm's relatively light and proximally located mass mean that our simple exoskeleton provides reasonable assistance in many conditions and the additional performance gained by compensating for elbow motion may not be worth the additional complexity. However, some improvements to the exoskeleton might be warranted. Our current design employs an elastic tensioner routed from the contralateral shoulder to the arm linkage of the exoskeleton frame.

This tensioner produces an undesired torque that could be avoided by moving the attachment point from the arm linkage to the axle or torso linkage. This modification would improve performance with negligible additional complexity.

Validations in benchtop tests and on healthy operators verified that we achieved our design goals of providing low-cost, wearable shoulder abduction support that does not limit range of motion. However, in the previous chapter we demonstrate that these validations are not sufficient to know whether this exoskeleton is well suited for post stroke assistance. The results from Chapters 2 and 3 as well a recent results from O'Neill et al. [124] suggest that we can expect stroke survivors to receive some benefit from the provided support. The magnitude and ubiquity of that benefit will have to be determined through future experimentation.

Post-stroke permanent disability might be reduced by increasing therapy dosage [101,102], but rigorously testing large dosages in humans has been difficult due to the commitment required of both therapist and patient and the likelihood of interfering with standard care. Assistive devices might be able to increase therapy dosage by aiding stroke survivors in completing therapies. So far, limited access to assistive devices due primarily to cost and limited use cases have been limitations in assisted therapy dosage. Our exoskeleton is untethered and passive, meaning that operators can use the exoskeleton for hours at a time without concerns about battery life or fuel and that the exoskeleton can be worn anywhere. Because of its low cost and portability, our exoskeleton might be a useful tool in studying whether assistance leads to increased use of the impaired arm and if so, whether that increased use translates to improved rehabilitation outcomes. The idea that assistance might lead to increased use and improved outcomes is related to the concepts behind constraint-induced movement therapy (CIMT) [146] in which the unaffected arm is restrained, typically with a sling or oven mitt, so that stroke survivors must use the impaired arm to perform tasks. While CIMT has shown to be effective for motor recovery [147], forced use of the impaired arm can be frustrating for stroke survivors. Assisting the impaired arm with an exoskeleton might encourage its use without the frustrations stemming from constraining the unimpaired arm.

# Part II

# Lower extremity: Running application

# Chapter 5

# Passive exotendon for running assistance

## Summary

Human running is inefficient. For every ten calories burned, less than one is needed to maintain a constant forward velocity—the remaining energy is, in a sense, wasted. The majority of this wasted energy is expended to support the bodyweight and redirect the center of mass during the stance phase of gait. An order of magnitude less energy is expended to brake and accelerate the swinging leg. Accordingly, most devices designed to increase running efficiency have targeted the costlier stance phase of gait. An alternative approach is seen in nature: spring-like tissues in some animals and humans are believed to assist leg swing. While it has been assumed that such a spring simply offloads the muscles that swing the legs, thus saving energy, this mechanism has not been experimentally investigated. Here we show that a spring, or 'exotendon', connecting the legs of a human reduces the energy required for running by 6.4 $\pm$ 2.8%, and does so through a complex mechanism that produces savings beyond those associated with leg swing. The exotendon applies assistive forces to the swinging legs, increasing the energy optimal stride frequency. Runners then adopt this frequency, taking faster and shorter strides, and reducing the joint mechanical work to redirect their center of mass. Our study shows how a simple spring improves

running economy through a complex interaction between the changing dynamics of the body and the adaptive strategies of the runner, highlighting the importance of considering each when designing systems that couple human and machine. This chapter is adapted from Simpson, C.S., Welker, C.G., Uhlrich, S.D., Sketch, S.M., Jackson, R.W., Delp, S.L., Collins, S.H., Selinger, J.C. and Hawkes, E.W., 2019. Connecting the legs with a spring improves human running economy. Journal of Experimental Biology, pp. jeb-202895 [148].

## 5.1 Introduction

Running expends more energy than any other commonly used form of locomotion, including walking, swimming, and flying [149,150,151] (Fig. 5.1A). In running humans, only a small amount of the metabolic energy expended does net external work on the environment; this energy is used to overcome aerodynamic drag and represents less than 8% of the total energy expended (Fig. 5.1B) [152, 153]. The remaining energy is 'wasted' in the sense that it is expended by processes that do no useful external work on the environment. According to studies that attempt to partition the energy expended by these processes, most of the wasted energy (65-82%) is used to brake and accelerate the center of mass, both vertically and fore-aft, a process that occurs each stance phase [154]. A smaller portion is used to swing the legs [154, 155, 156], with the current best estimate at 7% [154].

Given the inefficiency of running, many devices have been designed to reduce a runner's metabolic energy expenditure, with most targeting the largest costs—redirecting the center of mass and supporting the weight during the stance phase of gait. These devices can be either active or passive. Active devices inject energy from an external source to reduce the amount of energy expended by the human, even while the total energy expended by the human-plus-device may increase. For example, exoskeleton robots use motors in parallel with human muscles [13, 16]. However, these active exoskeleton robots usually use offboard motors and power sources, which prevent them from being autonomous. Other examples of active devices include mechanisms with accelerated masses [159] and jet packs [160]. No actively powered device, however,

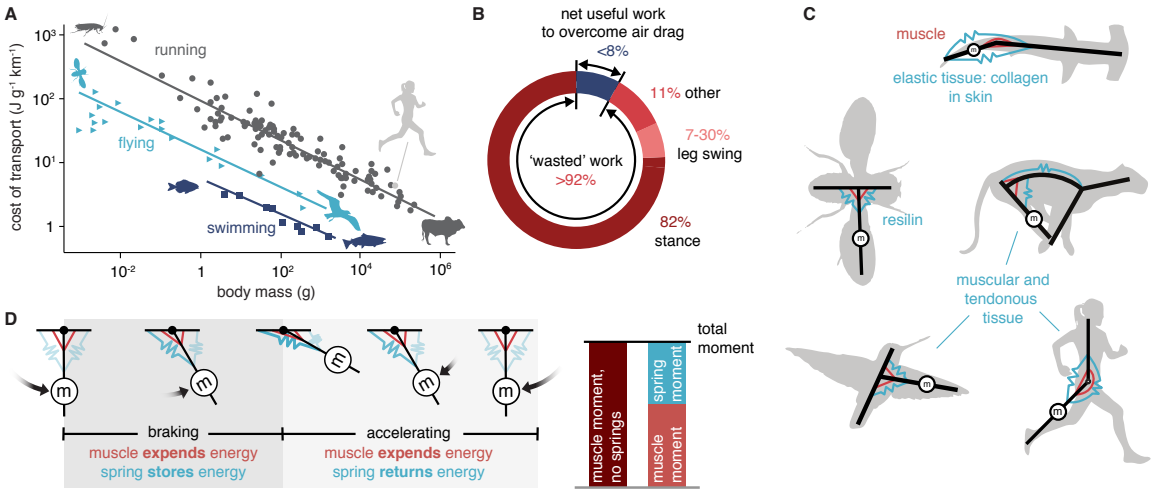


**Figure 5.1: Energetics and mechanics in running animals. A.** Cost of transport as a function of body mass [151, 157, 158] shows that running (grey circles) is less efficient than swimming (dark blue squares) and flying (light blue triangles). **B.**. Only a small fraction of the energy expended in running does useful work on the environment to move against air resistance [152,153]; the remainder is expended primarily to accelerate the center-of-mass, both vertically and fore-aft, during stance. Much less is used to swing the legs [154, 155, 156]. **C.** Elastic tissues are hypothesized to reduce the energy required to swing limbs. **D.** A pendular model of limb oscillation showing that a parallel spring (elastic tissue) can store energy during braking and return energy during acceleration, reducing required muscle moments.

has consistently reduced the energy required for a human to run while carrying the full weight of the device. Passive devices, in contrast, seek to reduce the energy required by the human to run by storing and returning energy to create a more efficient human-plus-device system. An early example is a running surface with stiffness tuned to minimize energy lost during impacts [161, 162]. Another passive assistance strategy involves using springs in parallel with the legs [51, 75], but this approach has yielded mixed results. Most recently, a shoe with spring-like foam and an assistive carbon fiber plate resulted in a 4% improvement in running economy [163, 164], the largest savings for a self-contained system across all devices that target costs primarily occurring during stance.

Notably, few devices have been designed that specifically target the metabolic energy expended for leg swing during running, even though numerous researchers hypothesize that passive elastic tissues in animals may reduce the energy required to oscillate limbs. Many quadrupeds have elastic tissues running along the top of the spine and front of the hip that are thought to assist spinal extension and hip flexion [165, 166] (Fig. 5.1C). Analogous passive elastic tissues are also in the skin of some fishes [167] and the wings of birds and insects [168, 169]. While no such mechanisms have been identified in humans, studies have correlated less flexibility in the legs and lower back with improved running economy [170, 171, 172]. This decreased flexibility might result from increased stiffness of passive elastic tissue spanning the relevant joints. For all of these examples, it is thought that the passive elastic tissues store and return energy during the oscillation of a limb, reducing the effort required to actively brake and accelerate the limb with muscles (Fig. 5.1D) [165,166,167,168,169,170,173]. Interestingly, recent work both in simulation [97] and in experiments with a hip-mounted metal torsional spring device [15] suggest that the savings resulting from assisting swing in humans are comparable to those seen when assisting stance. This is despite the fact that the energy expenditure associated with stance is an order of magnitude larger [154]. Moreover, the savings associated with assisting swing may actually exceed the expected expenditure associated with swing [154], suggesting that the mechanism of savings when assisting swing is not understood.

Here, we first test if a simple spring, or 'exotendon,' connecting the legs of a

human can reduce whole-body metabolic energy expenditure during running. Next, to elucidate the underlying mechanism of savings, we test the hypothesis that applying moments to assist moving the legs back and forth during swing may in fact reduce costs associated with performing work on the center of mass, incurred during the stance phase of gait (Fig. 5.2). This hypothesis can be explained as follows. During natural running, we expect certain costs to increase with increasing stride frequency, such as costs associated with swinging the legs back and forth at rates higher than the natural frequency [174, 175]. Other costs we expect to decrease, such as costs associated with performing mechanical work on the center of mass, to redirect the body in both the vertical and fore aft directions [175,176,177]. Therefore, the optimal stride frequency is dictated by a tradeoff between the marginal costs of each. We thus hypothesize that when a device assists leg swing to reduce energy expenditure at a higher stride frequency, the optimal stride frequency will increase. Adopting this new higher stride frequency will reduce costs that decrease at higher stride frequencies, such as redirecting the body during stance.

## 5.2 Materials and Methods

### 5.2.1 Device design

We constructed our exotendons out of natural latex rubber surgical tubing (hollow cylindrical tubing, 0.95 cm outer diameter, 0.64 cm inner diameter). Each exotendon consists of a single length of tubing with a 1 cm loop at each end for attachment purposes. To make each loop, we folded the tubing, stretched the loop by hand, and wrapped the looped tubing tightly with electrical tape. Once released, the forces provided by Poisson expansion of the tubing supplement the adhesive, forming a secure connection. We then attached each loop to a 1.6 by 0.5 cm s-shaped stainless-steel carabiner that was clipped to the shoelaces of each participant. The length of each exotendon from end to end of each attachment loop was set to 25% of the participant's leg length, measured as the distance from the top of the anterior superior iliac spine to the medial malleolus of the ankle. Through pilot testing, we found that

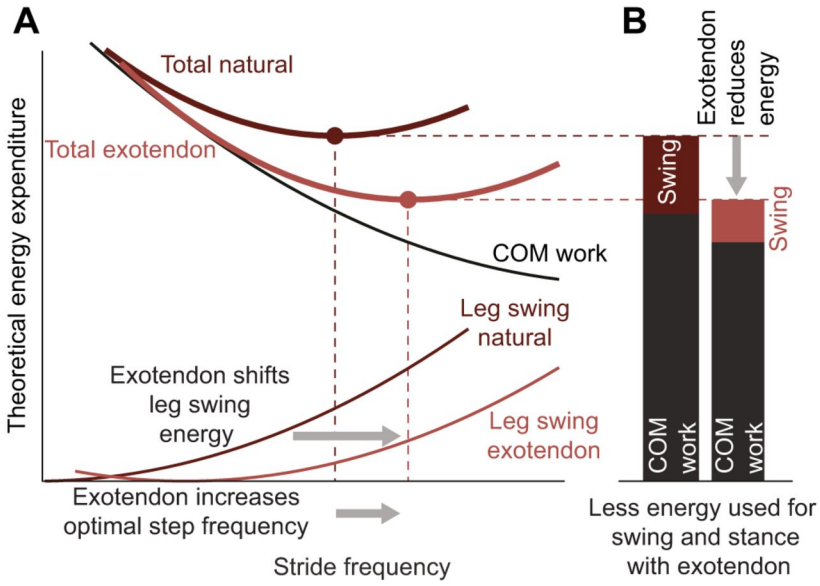


**Figure 5.2: Exotendon hypothesized mechanism of savings. A.** Runners choose an energetically optimal stride frequency (dark-red circle), which results from a combination of processes that require more energy with increasing stride frequency, such as leg swing (dark-red thin line), and those that require less energy with increasing stride frequency, such as the work performed to redirect the center-of-mass during stance (black thin line). We hypothesize that the exotendon shifts the leg swing curve rightward (light-red thin line), increasing the optimal stride frequency, and reduces total energy expenditure (including expenditure associated with work on the center-of-mass). **B.** Note that at this new optimal stride frequency, the costs associated with performing work on the center-of-mass can be reduced by an amount that is comparable to, or even exceeds, reductions associated with swinging the legs.

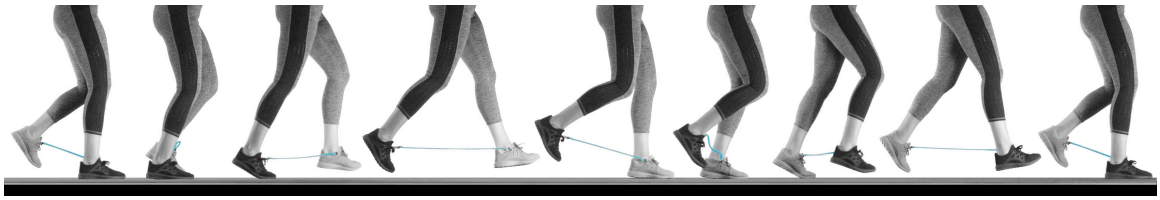

**Figure 5.3: Time-lapse photographs of a runner using the exotendon.** The length of the exotendon is tuned so that the device is long enough that it does not apply forces when the feet cross each other and does not break when the feet are far apart, yet short enough that it does not become entangled when the feet pass each other. Images span one complete gait cycle.

this length was long enough to avoid breaking and short enough to avoid tripping during running. As this work was our first proof-of-concept for the device, we did not develop a systematic method for determining the optimal stiffness of the device. Instead, we heuristically chose a single stiffness for the device that was stiff enough in piloting to exert noticeable assistive forces, yet compliant enough that it did not highly constrain gait. An exotendon device is shown in Fig. 5.3.

Designing devices that reliably and accurately apply forces to the human body is a challenge. It often requires overcoming a myriad of difficulties including: aligning device and joint axes [178], limiting added mass and materials to the body, and comfortably transferring force from rigid devices to often soft and deforming body segments [179]. While we could have designed our device to attach more proximally, at the knee or hip for example, we found in piloting that the aforementioned challenges could be largely avoided by affixing our device to the shoes. In addition, attaching more distally on the leg offered two further advantages. First, due to a longer moment arm about the hip, the forces necessary to provide assistive moments to the limb were smaller than if the attachment points were more proximal. Second, more distal placements ensure the line-of-action of the spring is predominantly along the flexion-extension axis of the hip, minimizing adduction moments on the leg. We note Nasiri et al. [15] have created an effective hip-mounted device, although the current, largely metal, design must contend with the challenges of added mass and comfortably transferring force from the device to the user.

### 5.2.2 Device characterization

To determine the force-length relationship of our device, we applied six known forces to one end of a 23 cm exotendon five times each using a pull-linear scale while the other end was fixed. At the same time, the length was recorded with a motion capture system at 270 Hz (Impulse X2E, PhaseSpace, San Leandro, CA, USA). We insured that the displacements achieved exceeded 30 cm (that expected during exotendon running at our experimental speeds). We then fit a linear model to the force-displacement data using least squares regression and computed the coefficient of determination. We found that the forces applied by the exotendon vary nearly linearly with displacement. A linear model fit to the recorded force-displacement data (Fig. 5.4) was able to account for most of the variance ($R^2 = 0.96$).

To determine how much of the energy stored in a stretched exotendon is returned, we suspended a 2.3 kg mass from one end of a 30 cm exotendon with its other end fixed to a table. We stretched the exotendon to 70 cm (for 40 cm of displacement beyond its free length) and after releasing, measured displacement. We computed the stored potential energy in the stretched exotendon and the gravitational potential energy at the apex of the motion. Comparing these two values gave an energy return of 97%.

### 5.2.3 Participants

A total of 19 healthy young adults, with no known musculoskeletal or cardiopulmonary impairments, participated in the study (8 females; age: 24.9±2.7 years; height: 174.4±6.9 cm; mass: 67.3 ± 11.0 kg). The study was approved by the Stanford University ethics board and all participants provided written informed consent prior to testing.

### 5.2.4 Experimental protocols

We conducted four separate experiments to: determine if the exotendon improves running economy (Experiment 1), test for the possibility of a placebo effect (Experiment 2), investigate the mechanism of energy savings (Experiment 3), and test the

safety of the device during over-ground running (Experiment 4).

**Experiment 1 – Running economy**

To determine if the exotendon improves running economy, we conducted an experiment to compare metabolic energy expenditure with and without the exotendon. Twelve participants (5 females; age: 24.7±2.9 years; height: 177.0±6.7 cm; mass: 69.3±11.4 kg) completed a two-day running protocol. On the first day of testing, we measured participants' leg lengths and constructed personalized exotendons (25% of leg length). Participants were told that the exotendon was designed to improve running efficiency and were told to 'relax into running with the device' and try to 'think about something else' while running. The exotendon was then attached to the participant's shoes (see Device design for attachment location rationale). To habituate participants to the device, they completed a minimum of four 15 m over-ground walking and running trials until they verbally confirmed they were comfortable walking and running with the exotendon. Participants were then instrumented with indirect calorimetry equipment (Quark CPET, Cosmed, Rome, Italy) and completed a 5-minute quiet standing trial, during which baseline metabolic energy expenditure was measured. Participants then completed four 10-minute runs, with 5-minute rests between each, on a treadmill (Woodway, Waukesha, WI) at 2.67 m/s (10 minutes/mile). Though slow for competitive runners, this pace allows a larger pool of potential participants than a faster pace and is similar to that used in other studies of assistive devices for running [15, 16]. The runs alternated between 'natural running' (without an exotendon) and 'exotendon running' (with an exotendon), with the first running condition randomly assigned. The second day of testing was identical to the first for each participant. We define a trial as the comparison between consecutive natural and exotendon runs resulting in four trials over the two-day experiment. During runs, we recorded sagittal plane video, which we later used to determine runners' stride frequencies. However, in 5 of 12 participants, due to equipment availability, we recorded stride frequency using an accelerometer (Trigno IM, Delsys Inc., Natick, MA, USA) mounted on the dorsal surface of the foot.

**Experiment 2 – Placebo effect**

To determine if a placebo effect could explain the changes in running economy observed in Experiment 1, we conducted a separate experiment to compare metabolic energy expenditure during running with and without a placebo exotendon. Four naïve participants (2 females; age: 24±2.2 years; height: 168.3±2.5 cm; mass: 60.1±10.8 kg) completed a two-day running protocol that was identical to Experiment 1. The only difference was that participants ran with an exotendon that had a stiffness two orders of magnitude lower than the original exotendon (5 N/m versus 120 N/m, respectively), and therefore provided negligible assistive moments to the limbs. The length of each placebo exotendon was still set to 25% of participant leg length.

**Experiment 3 – Mechanism**

To investigate how the exotendon reduces energy expenditure, we conducted an experiment to test how running mechanics, energetics, and muscle activity change during exotendon running. Four participants (2 females; age: 25.0±1.6 years; height: 179.5±7.4 cm; mass: 75.3±13.7 kg), randomly selected from the 12 that participated in Experiment 1, completed an additional third day of testing. During this testing day, kinematic, kinetic, electromyographical (EMG), and metabolic data were recorded during running with and without the exotendon at a range of stride frequencies.

All runs were completed at 2.67 m/s on an instrumented treadmill (Bertec Corporation, Columbus, OH, USA) to allow for collection of ground reaction forces (2000 Hz). Kinematic data were recorded at 100 Hz using a 9-camera optical motion tracking system (Motion Analysis Corporation, Santa Rosa, CA, USA). Anatomical reflective markers were placed bilaterally on the 2nd and 5th metatarsal heads, calcanei, malleioli, femoral epicondyles, anterior and posterior superior iliac spines, and acromion processes, as well as on the C7 vertebrae. An additional 16 tracking markers, arranged in clusters, were placed on the shanks and thighs of both legs. Markers on the medial malleoli and femoral epicondyles were removed following the static trial. EMG data were recorded (Trigno IM, Delsys Inc., Natick, MA, USA) at 2000

Hz from the following 15 muscles of a single limb: peroneus, soleus, medial and lateral gastrocnemii, tibialis anterior, medial and lateral hamstrings, gluteus medius and maximus, vastus lateralis and medialis, rectus femoris, sartorius, adductor group, and iliopsoas. EMG electrodes were placed in accordance to SENIAM guidelines [180]. Metabolic power was measured using indirect calorimetry (Quark CPET, Cosmed, Rome, Italy).

To warm up, participants ran without an exotendon for 5 minutes on the treadmill. Next, participants completed a series of maximum voluntary contractions (MVCs) for later normalization of EMG signals. These MVCs included five maximum height jumps and five sprints [181], in addition to one isometric and three isokinetic maximum contractions of the hamstrings, adductor group, tibialis anterior, peroneus, hip flexors (with both a flexed knee and extended knee), and hip abductors. We then recorded motion capture marker positions and ground reaction forces during a static standing trial for later scaling of a musculoskeletal model. As in Experiment 1, participants were habituated to the device through a series of over-ground walking and running trials. Participants were then instrumented with indirect calorimetry equipment and a 5-minute quiet standing trial was recorded to capture baseline metabolic energy expenditure.

Participants then completed two 7-minute runs, one 'natural running' (without an exotendon) and one 'exotendon running' (with an exotendon), with a 5-minute rest between and the order randomly assigned. Kinematic, kinetic, EMG, and metabolic data were recorded. Self-selected stride frequency was computed during the last minute of each run from the instrumented treadmill force signals with a custom Matlab script (Mathworks Inc., Natick, MA, USA). We will refer to these self-selected stride frequencies as natural self-selected stride frequency and exotendon self-selected stride frequency.

To investigate how the relationship between stride frequency and metabolic power changed when running with an exotendon, participants next completed six additional 7-minute runs during which step frequency was prescribed using an auditory metronome, along with visual cues provided by a monitor in front of the treadmill.

Participants ran at three prescribed stride frequencies during both natural and exotendon running. For the natural running conditions, the following three stride frequencies were prescribed: i. the participant's natural self-selected stride frequency; ii. the participant's exotendon self-selected stride frequency, which was higher than the natural self-selected stride frequency; and iii. a stride frequency lower than the natural self-selected stride frequency. The change from the natural self-selected stride frequency to the lower stride frequency was set to the percent difference between the natural self-selected stride frequency and the exotendon self-selected stride frequency. For the exotendon running conditions, the following three stride frequencies were prescribed: i. the participant's exotendon self-selected stride frequency; ii. the participant's natural self-selected stride frequency; and iii. a stride frequency higher than the exotendon self-selected stride frequency. The change from exotendon self-selected stride frequency to the higher stride frequency was similarly set to the percent difference between the natural self-selected stride frequency and exotendon self-selected stride frequency.

**Experiment 4 – Over-ground test**

To test whether the exotendon can safely be used in the real-world, we conducted an experiment to monitor fall risk during outdoor running. Four participants (2 females; age: 27.8±1.3 years; height: 172.6±6.1 cm; mass: 66.7±8.0 kg), who had previous experience with the exotendon through pilot testing or participation in Experiment 1, ran with a modified exotendon for 6 km on suburban streets along with the experimenter. The modified exotendon, which attached directly to the ankle via a compression brace, was reported to be more comfortable than the original exotendon, which attached directly to the shoelaces. Moving the attachment point off the shoes also reduced wear of the shoelaces caused by sliding of the carabiner. This small change in attachment point was not expected to have a significant effect on running economy. The number of tripping and falling incidents were recorded.

#### A note on device optimization

In supplementary pilot experiments (not presented here), we did attempt to perform human-in-the-loop optimization to determine the optimal exotendon length and stiffness. Four participants (two who had previously completed Experiment 1 and two naïve participants) completed a protocol similar to that described in Zhang et al. [13]. We were unable to identify length and stiffness combinations with better performance than our standard device in the four pilot participants. One possible explanation is that our chosen device parameters were indeed near optimal. Another possible explanation is that participants were more risk averse in running with our device and thus adopted control strategies that prioritized stability (not falling) over efficiency. Parsing the different effects of human-in-the-loop optimization is left for future work.

### 5.2.5 Data analysis

#### Experiment 1 – Running economy

**Metabolics.** We computed the gross metabolic power (energy expenditure) from indirect calorimetry [182] by averaging data from the last two minutes of each experimental run. Baseline metabolic power, calculated as the average metabolic power during the last two minutes of the rested standing trial, was subtracted from our gross metabolic power measures to get net metabolic power during each run. We then computed the percent change in net metabolic power, from natural running to exotendon running for each of the four trials. We then used two-tailed, one-sample t-tests, with a Holm-Šidák correction, to determine if percent changes in net metabolic power were significant.

**Stride frequency.** We manually determined average stride frequency from video recordings by counting the strides taken and dividing by the time elapsed. When foot mounted accelerometers were instead used to compute stride frequency, we band-pass filtered accelerometer data (4th order, zero-phase shift Butterworth, 2-20 Hz), summed the X, Y and Z accelerations, identified peak accelerations, and computed stride frequency as one over the average time between peaks. Average stride frequency measures were not statistically different between the two measurement methods.

### Experiment 2 – Placebo effect

**Metabolics.** We performed the same metabolic analyses as described in Experiment 1.

### Experiment 3 – Mechanism

**Metabolics.** We performed the same metabolic analyses as described in Experiment 1 to determine the average net metabolic power for each run. To determine the effect of altering stride frequency, we computed the percent change in average net metabolic power for each enforced stride frequency, both with and without an exotendon, relative to natural running (without an exotendon and with no enforced stride frequency). For each participant, we then used least squares regression to find the best-fit quadratic curves relating net metabolic power to stride frequency for both exotendon and natural running. We then calculated the stride frequencies at the minima of the natural running and exotendon running best-fit curves, which we will refer to as the natural optimal stride frequency and the exotendon optimal stride frequency, respectively. To determine if the exotendon shifted the optimal stride frequency, we performed two-tailed paired t-tests comparing exotendon optimal stride frequency to natural optimal stride frequency. Using all participant data, we also solved for best-fit quadratic curves relating net metabolic power to stride frequency for both exotendon and natural running, and calculated the 95% bootstrap confidence intervals for these across participant curves. Note that each quadratic curve is fit to only three data points. While this is an overfit to our data, we have chosen to do so because previous studies have shown that running metabolic cost varies quadratically with stride frequency [177, 183, 184]. The curve fits are only used to interpolate the stride frequency associated with the minimum metabolic cost.

**Musculoskeletal modeling.** Joint-level kinematics, kinetics, and mechanical powers were computed using a modified musculoskeletal model [185] in OpenSim 3.3 [186]. Of the original 37 model degrees of freedom, we locked 18 including ankle eversion, toe flexion, and all those associated with the arms, leaving us with a 19 degree-of-freedom model. We generated subject-specific models by scaling the generic

model to match the anthropometry of each subject during a standing static trial. For scaling, ankle and knee joint centers were calculated as the midpoint of the calcanei markers and femoral epicondyle markers, respectively, while the hip joint centers were calculated using a regression model based on the marker positions of the posterior and anterior superior iliac spines [187]. After low-pass filtering the marker positions at 15 Hz (4th order, zero-phase shift Butterworth), we computed joint angles using the OpenSim inverse kinematics tool. This tool uses a weighted least squares algorithm to pose the model in a way that minimizes the error between model and experimental marker locations. Joint moments were computed using the OpenSim inverse dynamics tool, which uses ground reaction forces and moments, joint angles from inverse kinematics, and classical equations of motion to solve for intersegmental moments. The joint angles used as input were low-pass filtered at 15 Hz (6th order, zero-phase shift Butterworth), and ground reaction forces and moments were low-pass filtered at 15 Hz (4th order, zero-phase shift Butterworth).

We modeled the exotendon in OpenSim as a linear path spring with a deadband range equal to its slack length. Though no real material behaves as a perfect linear spring, we determined in benchtop tests that the stiffness of our device is roughly linear ($R2 = 0.96$) and returns 97% of the energy stored in it. The spring forces were applied to the calcaneous body of each foot at the location of the band attachment marker from the static trial. The length and stiffness of the modeled exotendon was scaled for each participant. Inverse dynamics were first computed without the modeled exotendon to determine the total joint moments required to produce the resultant motion and ground reaction forces, referred to as exotendon running total moments. Inverse dynamics were then recomputed with the modeled exotendon for all exotendon runs to determine the moments produced solely by biological muscle and tissue, referred to as the biological moments. The moments applied by the exotendon were computed as the difference between the exotendon running total moments and biological moments, referred to as exotendon moments. Powers were then computed at each joint by multiplying moments by angular velocities.

Participants' average joint angles and moment as a function of gait cycle for the hip, knee and ankle were calculated from the last minute of each run. To do

this, we averaged across strides after normalizing each stride time to 100% gait cycle, computed as the time from heel strike to subsequent heel strike on a single leg. Strides were excluded from these average trajectories if the value of the measure exceeded 5 standard deviations from the mean at any time point in the stride. This resulted in the removal of 3% of strides on average for all runs and participants. Joint powers were then computed from the averaged joint angles and moments for each participant. Joint powers and moments were then normalized to body mass and across-participant average trajectories were computed.

We next computed the average absolute natural running and exotendon running moments and powers (both biological and exotendon) during the stance and swing phases of gait. We note that because these values are time averaged, the relative length of the stride does not affect their magnitude. We tested for differences between natural running and exotendon running (again, both biological and exotendon) using two-tailed paired t-tests with Holm-Šidák corrections.

We performed these analyses, comparing joint moment and powers during the swing and stance phases of gait both with and without the exotendon, as a means of estimating effort during each phase. Metabolic power, measured using indirect calorimetry, is our most direct measure of energy expenditure, but cannot be used to distinguish stance and swing expenditures; their effects are intermingled during the long sampling period of indirect calorimetry. Instead we analyzed the mechanical requirements of the body (joint moments) during each phase of gait. Previous studies have shown strong correlations between metabolic power and joint moment [188], but we note that reduced joint moments do not guarantee reduced metabolic rate [189].

**Electromyography.** Electromyograms from each muscle were bandpass filtered at 30-500Hz (4th order, zero-phase shift Butterworth), rectified, and then low-pass filtered at 6Hz (4th order, zero-phase shift Butterworth) to create linear envelopes. Envelopes were then normalized to the peak signal from the MVCs [181] to compute muscle activities. We then averaged muscle activities across strides from the final minute of each run, then normalized to 100% of the gait cycle. Strides in which the muscle activities exceeded 5 standard deviations from the mean for any time point were excluded from the average curve. All remaining EMG signals were visually

examined and excluded if they appeared corrupted. Overall, 8% were excluded, with no bias towards exotendon or natural running. All processing was performed using custom Matlab scripts. We also computed average muscle activities during the stance and swing phase of gait, both for natural and exotendon running. We used two-tailed paired t-tests with Holm-Šidák corrections to compare activity during natural and exotendon running, during both stance and swing.

## 5.3 Results

### 5.3.1 Experiment 1 – Running economy

We found that connecting the legs of a running human with a simple spring improved running economy by 6.4±2.8% (n=12, p=6.9x10-6, one-sample t-test, Fig. 5A). During the first trial of the first day, participants showed no metabolic savings when running with an exotendon compared to natural running. However, by the end of the second trial, participants were expending 3.8±5.4% less energy during exotendon running compared to natural running (n = 12, p = 0.034, one-sample t-test). Metabolic savings continued to increase on the second testing day, with all participants achieving savings by the end of the second trial of the second testing day. By the end of our protocol, stride frequency increased by an average of 7.7±3.5% when wearing an exotendon (n=12, p = 1.1x10-5, paired t-test, Fig. 5B).

### 5.3.2 Experiment 2 – Placebo effect

The placebo exotendon did not improve running economy (n=4, p=0.88, one-sample t-test, Fig. 5.5).

### 5.3.3 Experiment 3 – Mechanism

The exotendon significantly increased the optimal stride frequency (+8.1%, p=3.7x10$^{-3}$, n=4, paired t-test, Fig. 5.6), and all participants adapted toward the new optimum. The exotendon reduced biological hip and knee moments during

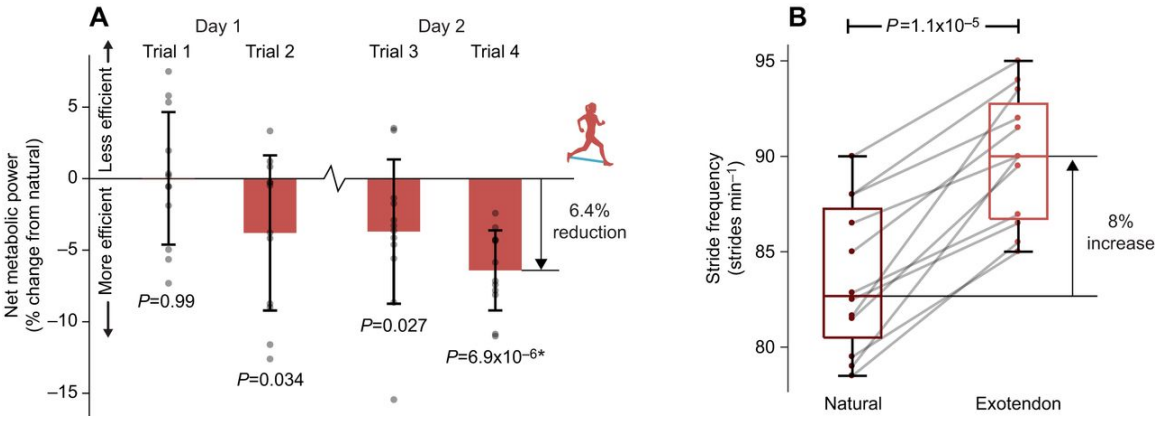


**Figure 5.4: Reduced energy expenditure during exotendon running (n=12). A.** On day 1, runners initially showed no change in energy expenditure (trial 1), yet showed reductions after running with the exotendon for 15-20 minutes (trial 2). Runners retained these savings across days (trial 3). After a total of 35-40 minutes of experience with the exotendon across both days, the greatest reductions in energy expenditure were evident (trial 4), with all runners (n=12) showing improved economy and average savings of 6.4±2.8%. Error bars represent one standard deviation. Asterisks indicate statistical significance after Holm-Šidák corrections with confidence level $\alpha$=0.05. **B.** By the final trial participants took shorter, faster strides with the exotendon, increasing stride frequency by an average of 8% above that measured during natural running (p=1.1x10$^{-5}$ two-tailed paired t-test, n=12).

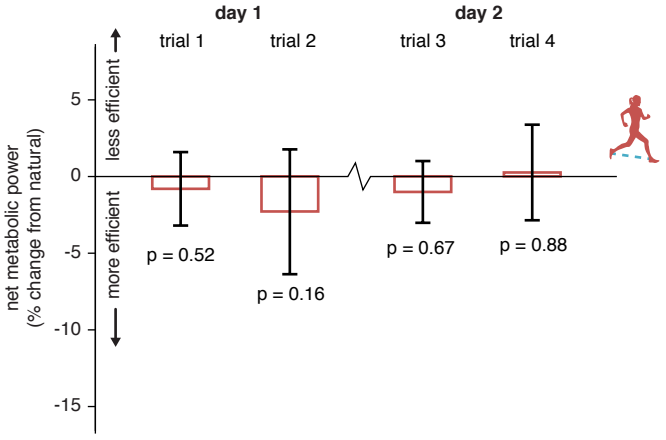


**Figure 5.5: Placebo test results (n=4).** Four participants completed the same protocol as the main experimental group, but were given an exotendon with stiffness less than 5% that of a normal exotendon. These participants showed no change in running economy, relative to natural running, with the placebo exotendon (two-tailed one-sample t-tests). Error bars represent one standard deviation.

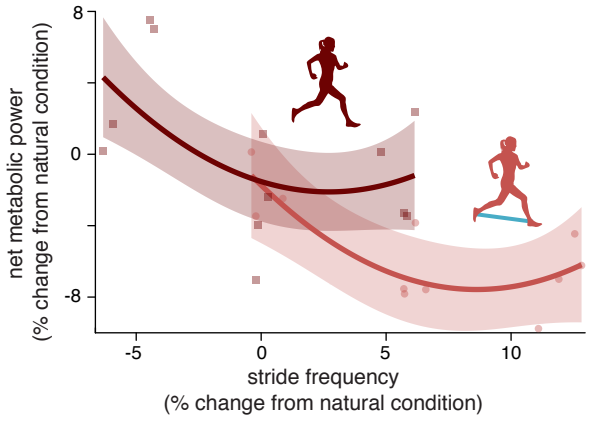


**Figure 5.6: Effect of stride frequency (n=4).**, In experiments, the exotendon increased the energetically optimal stride frequency (8.1%, p=3.7x10$^{-3}$, paired t-test, n=4). Faded regions show the 95% confidence interval of curve fits.

swing (p=2.3x10$^{-3}$, 2.5x10$^{-3}$, respectively, paired t-test) and stance (p=4.1x10$^{-3}$, 8.1x10$^{-5}$, respectively, paired t-test) (Fig. 5.7, Fig. 5.8 and Fig. 5.9). Interestingly, average knee moments during stance decreased (p=4.4x10$^{-4}$, paired t-test), even when the exotendon was applying negligible moments, likely because runners adopted a higher stride frequency, as our hypothesis suggests. In addition, biological joint powers at the knee decreased during swing and stance (p=7.7x10$^{-3}$, 1.7x10$^{-3}$, respectively, paired t-test, Fig. 5.8), as did ankle joint power during stance (p=8.4x10$^{-3}$, paired t-test, Fig. 5.8). Corresponding reductions in muscle activities were not significant, possibly due to the low signal-to-noise ratio (Figs. 5.10 and 5.11).

### 5.3.4 Experiment 4 – Over-ground test

To test the safety and potential real-world applicability of our exotendon, four participants each ran 6 km on city streets with a modified exotendon (see Materials and Methods, Experiment 4); no tripping incidents occurred.

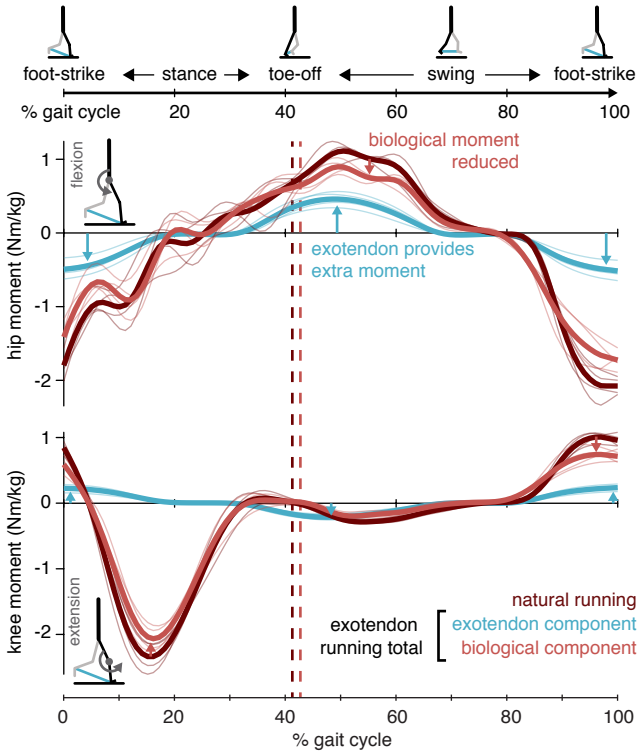


**Figure 5.7: Mechanical requirements (n=4).** Biological moments during swing were reduced, likely due to the assistance of the exotendon, and biological moments during stance were reduced, possibly due to the increased stride frequency. Note that horizontal forces applied by the exotendon to the stance foot likely do not affect the joint moments of that leg, because they are reacted by frictional forces with the ground. However, the exotendon forces applied to the swing leg may indirectly affect the joint moments of the stance leg through the hips.

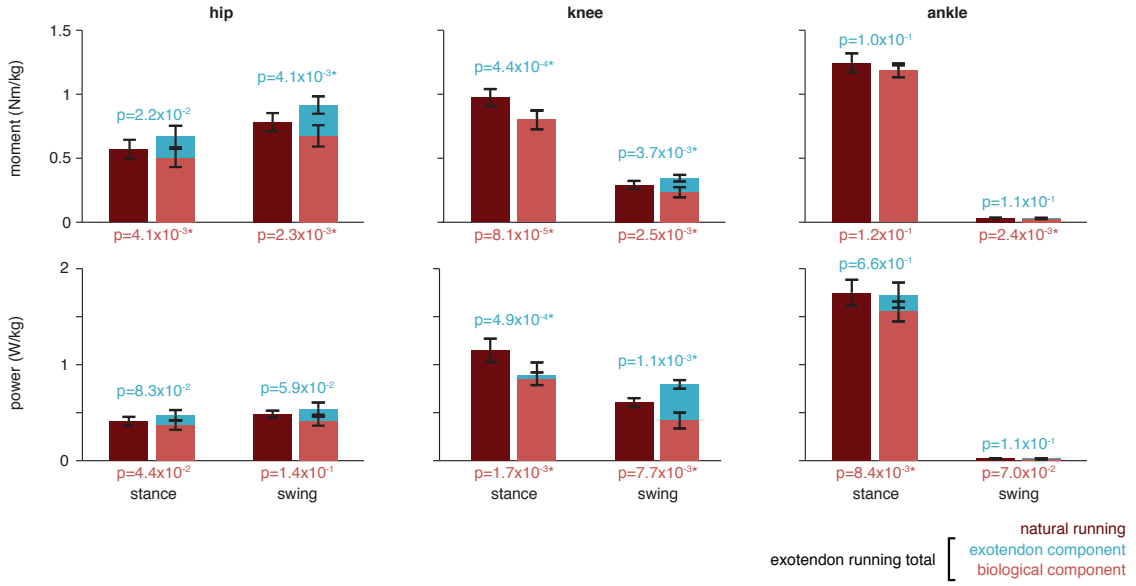


**Figure 5.8: Average joint-level kinetics (n=4).** Comparisons of average, absolute joint moments and powers across stance and swing for the four participants from Experiment 3. We compared moments and powers produced during natural running (dark red) to those produced during exotendon running. Average kinetics during exotendon runs were separated into the exotendon contribution (blue) and the biological contribution (light red). We report the p-values resulting from two-tailed paired t-tests comparing biological contributions to kinetics in natural and exotendon running below the axes (light red text) and comparing total kinetics in natural and exotendon runs above the bars (light blue). Asterisks indicate comparisons that were significant after Holm-Šidák corrections (alpha = 0.05). When running with the exotendon, during swing, hip, knee and ankle biological moments are reduced compared to natural running, as is knee power. During stance, hip and knee biological moments are reduced, along with knee and ankle powers.

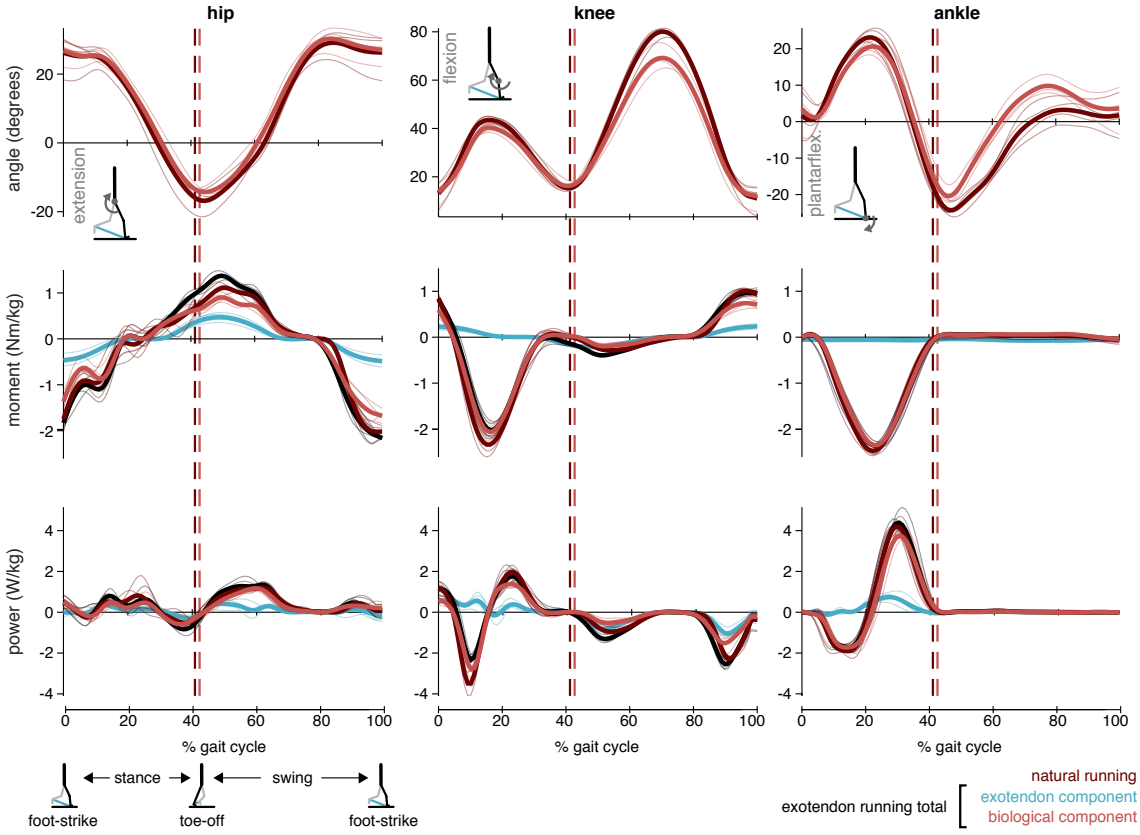


**Figure 5.9: Joint-level kinematics and kinetics (n=4).** Traces show average joint angles, moments, and powers across the gait cycle for natural running (dark red) and exotendon running. Kinetics from exotendon running are separated into exotendon contributions (blue), biological tissue (muscles, tendons, etc.) contributions (light red), and the total joint kinetics (black) for the four participants from Experiment 3. Thin traces show stride-averaged trajectories for individual participants (n=4) while the thick traces show trajectories averaged across participants. Vertical dashed lines indicate across-participant average toe-off time for exotendon running (light red) and natural running (dark red).

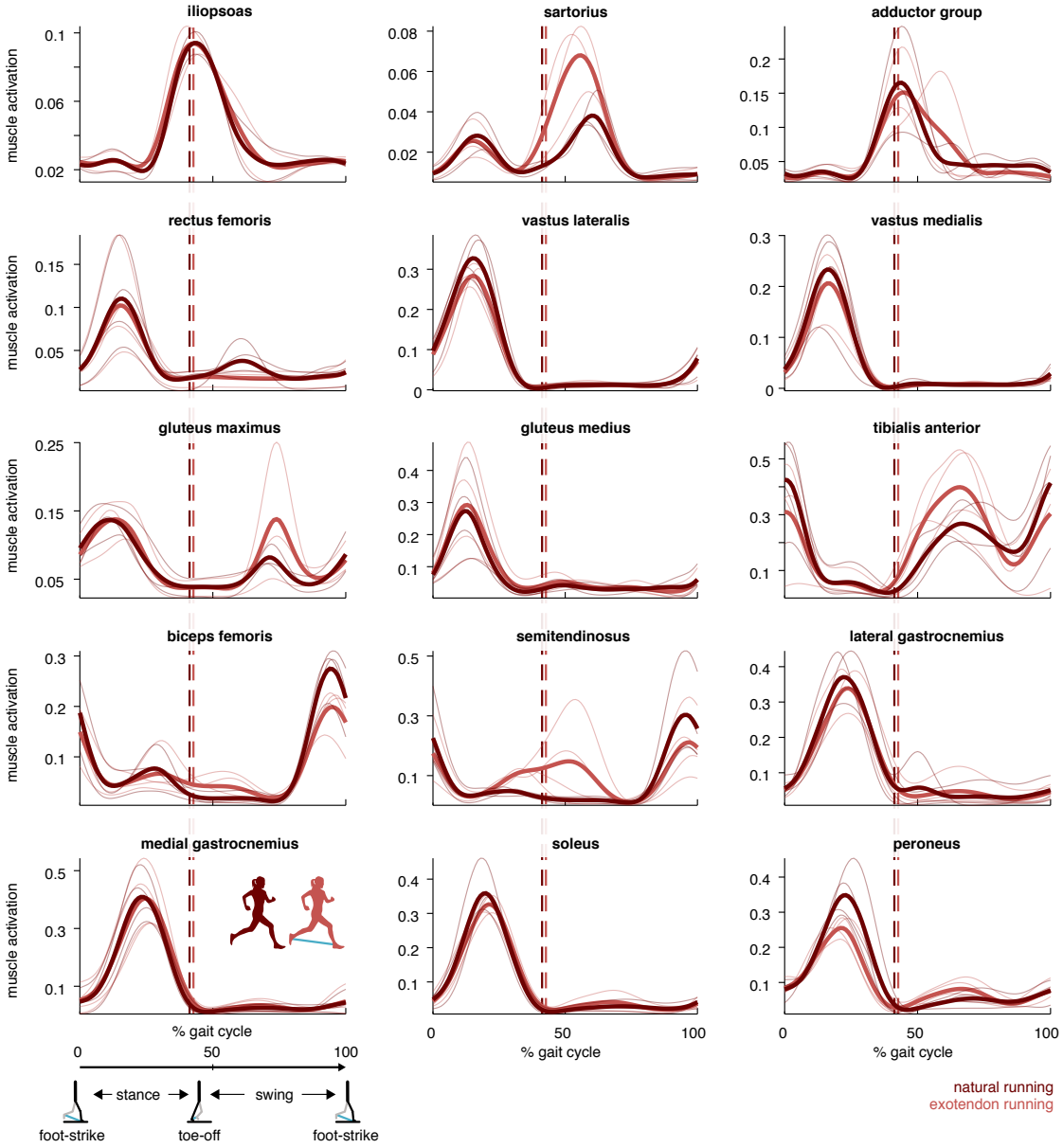


**Figure 5.10: Muscle activity (n=4).** Average muscle activity for each participant (thin traces) and across participants (solid lines) for natural running (dark red) and running with the exotendon (light red) as a function of gait cycle. The vertical dashed lines indicate the average time at which the toe lifts off the ground during exotendon running (light red) and natural running (dark red).

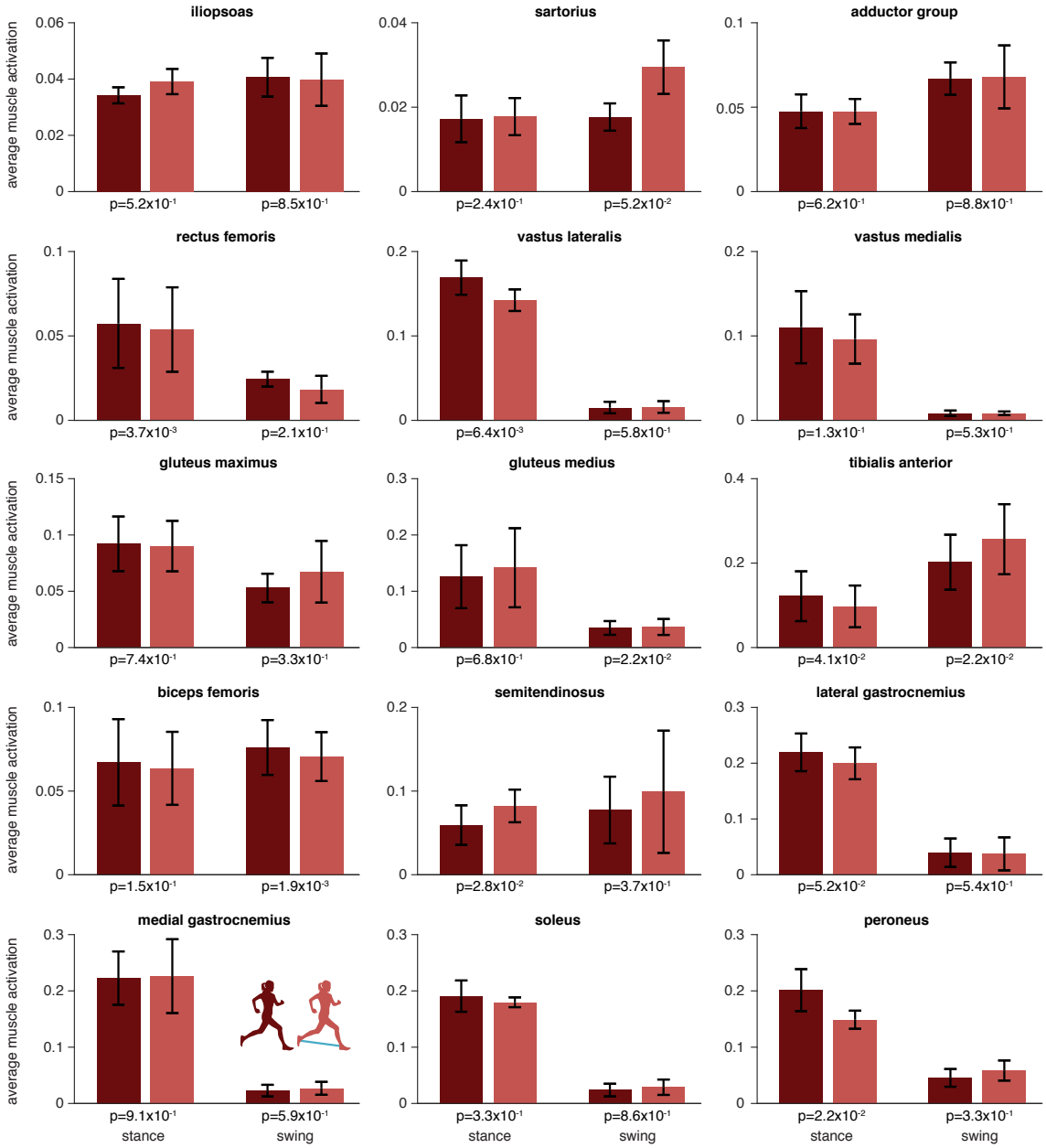


**Figure 5.11: Average muscle activity (n=4).** Comparisons of average, normalized muscle activity, computed from EMG recordings, across stance and swing phases of gait. Statistical comparison (paired t-test with Holm-Šidák corrections, $\alpha = 0.05$) revealed no significant changes in muscle activity as a result of running with the exotendon.

## 5.4 Discussion

We found that a simple spring connecting the legs of a running human can improve overall economy. Moreover, the exotendon appears to not simply reduce the cost of swinging the limbs. Instead, we found that savings are the product of a complex interaction between the mechanics of the simple device and the adaptive strategies of the runner. We show that the exotendon increases the energy optimal stride frequency, which runners then adopt. At this new stride frequency, the mechanical work of redirecting the center of mass during stance is reduced—shorter strides result in a reduction of biological joint moments and powers. This suggests that the metabolic cost associated with this mechanical work is reduced, and the overall improvement of economy is not derived solely from reducing the cost of swinging the legs. Our findings help explain why devices designed to assist the low expenditure costs of leg swing [15], yield greater improvements in overall running economy than those that directly assist the larger costs of redirecting the center of mass and supporting the bodyweight [164].

Stated more generally, during natural running, low-expenditure components can have high expenditures when a gait parameter (such as stride frequency) is changed outside of the preferred range. These sharp increases in expenditure (the marginal costs) act as a constraint, preventing adjustment to the gait parameter. During assisted running, this constraint is relaxed, freeing the runner to reduce expenditures associated with the high-expenditure components of gait (such as center of mass redirection) and achieve more efficient gait patterns overall. Critically, the associated savings can be large—much larger than would be expected from savings directly associated with a low-expenditure component of gait (Fig. 5.2).

A primary limitation of our study is the difficulty of disentangling, and quantifying, costs associated with one component of gait from another during human running. In particular we refer to two costs. One is the cost associated with performing work to re-direct the center of mass both vertically and fore-aft, which we expect to primarily occur during the stance phase of gait and expect to decrease with increasing stride frequency (or decreasing step length). The other is the cost to move the legs back and

forth during the swing phase of gait, which we expect to increase with increasing stride frequency. While there is a body of modeling and experimental evidence to broadly support the importance and tradeoff of these two competing costs [175,176,177,188], in reality they cannot be measured in isolation. For example, at higher step frequencies we also expect greater 'force rate costs.' This cost is associated with more rapidly turning muscles on and off, with the more rapid activation cycling hypothesized to require more costly calcium pumping [174, 188, 190]. This cost would be incurred by muscles involved in center of mass redirection and body weight support, as well as muscles responsible for swing. Although joint moments and powers were reduced during both stance and swing, this does not directly map to reductions in cost because of complications like force-rate costs, as well as other considerations such as biological tendon energy storage and return, or isometric force production. Notably, we do not expect force rate costs to negate our proposed mechanism of savings. Even in its presence, our results are consistent and compatible with our hypothesized mechanism of savings (Fig. 5.12).

Adding to the challenge of disentangling costs was the limitation that we did not find significant changes in muscle activity, despite reductions in metabolic and mechanical powers during exotendon running. A similar study was also unable to verify changes in muscle activity while testing an exosuit that improved running economy by 5% in 8 participants [16]. This apparent discrepancy in our study is likely due to the distribution of the exotendon's effect on metabolic power consumption across a large number of muscles. This diluted effect might be difficult to verify in EMG signals with relatively high variability. Additionally, recorded muscle activity may not have changed despite decreased joint moments if changes occurred in non-superficial muscles unmeasurable with surface EMG [191, 192, 193].

An open question is whether our device would be more or less effective at higher running speeds. Our current study was conducted at one, relatively slow, speed. At higher running speeds the amplitude and frequency of leg swing increase [194] leading to greater leg swing costs [188] that the device may help offset. However, at the same time, the marginal costs associated with the work to redirect the center of mass and force rate costs would likely change with running speed, making the net

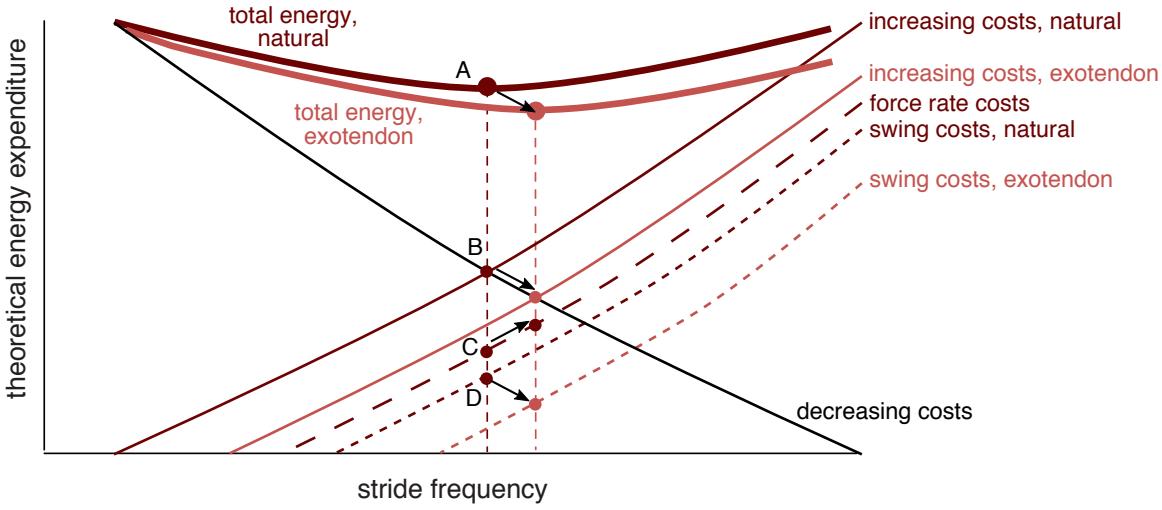


**Figure 5.12: Exotendon hypothesized mechanism of savings including 'force rate' costs.** The total energetic cost (bold, dark red line) comprises costs that increase with stride frequency (thin, dark red line), and costs that decrease with stride frequency (thin, black line). The increasing costs can be broken into subcomponents, here force rate costs (long dashed, dark red line) and swing costs (short dashed, dark red line), although others could be added as well. When the exotendon assists leg swing, the swing costs subcomponent line shifts (short dashed, light red line). This in turn shifts the net increasing costs line (thin, light red line), resulting in a new total energy curve (bold, light red line), and a new the optimal stride frequency (vertical, dashed light red line). The operating points on the curves of both the increasing costs and decreasing costs (Point B) as well as on the total energy expenditure curve (Point A) shift down and to the right with the exotendon, as does Point D (the operating point on the curve of the swing costs subcomponent of the increasing costs). The net savings in energy expenditure occurs despite Point C (operating point on the curve of the force rate costs) shifting up and to the right. Thus, even though some costs might increase with adaptation to the exotendon, decreases in other costs can result in net savings.

effect unclear. To further complicate the situation, other kinematic changes occur at high speeds. For example, during natural running at faster speeds greater knee bend is evident at the rearward extent of leg swing, reducing the leg's moment of inertia about the hip and potentially reducing swing costs. The exotendon may in fact hinder this more exaggerated knee bend at higher speeds, leaving the net effect on leg swing costs uncertain. Although the effect of our device at faster running speeds is somewhat unclear, the improvement in economy at the tested speed does imply that recreational runners may be able to run faster and further with our device. A runner, with a natural pace of 2.7 m/s and a marathon finishing time of 4:20, could expect a 6% improvement in economy with our device, theoretically leading to a decrease in their finishing time to around the 4 hour mark [20].

Our study shows how a spring designed to assist leg swing can significantly improve human running economy through a complex mechanism of savings. The device changes the relationship between stride frequency and energy expenditure, driving the runner to discover new locomotor strategies. This change in turn reduces the mechanical work the runner does to both swing the legs and redirect the center-of-mass, resulting in overall greater efficiency than anticipated. Our exotendon could serve as an affordable and low-tech assistive device to improve human running performance, or a simple and robust intervention to further explore the complexities of human gait and human-machine interactions. More broadly, our study shows that a simple device can create unexpected and complex interactions between the dynamics of the body and the adaptive strategies of the individual—an important reminder for all who seek to augment humans.

# Chapter 6

# Conclusion

In this thesis, I describe new exosuit actuators and exoskeletons that are designed to use a minimal set of inexpensive components with the aim to reduce one of the primary barriers to exoskeleton access: cost. Cost limits access to exoskeleton devices, which limits both the real-world usefulness of exoskeleton robots and research progress in developing exoskeletons for new applications or validating their usefulness in domains such as stroke recovery. Rather than attempting to design multipurpose tools that aid human operators in accomplishing a range of tasks, I use insights from human neuromechanics to assist with movement subtasks, such as supporting the arm against gravity or swinging the legs. Chapter-wise contributions are as follows:

- **Chapter 2**: We described in detail **a new type of exosuit actuator** designed specifically to actuate shoulder abduction, which is commonly associated with reduced reachable workspace in stroke survivors. This exosuit actuator lifts the arm from below using pushing forces rather than pulling from above with tensile elements or directly applying bending moments. We characterized this actuator on the benchtop and in healthy human subjects to demonstrate its effectiveness. We then performed one of the fist pilot studies in a stroke survivor of an upper extremity exosuit and **demonstrate that reachable workspace is increased with our actuator.** The material cost of our actuator is less than 20 USD. While no upper extremity exosuits are commercially available, some lower extremity offerings for walking cost approximately 30,000 USD.

- **Chapter 3**: We described in detail an **updated design for our exosuit actuator to actuate shoulder abduction,** based on a new class of growing robots [106, 107]. We demonstrated in healthy operators that the exosuit actuator provides the intended support without interfering with other joints. We then **demonstrated increased reachable workspace** in 4 out of 6 stroke survivors using this type of support, and provided data supporting the hypothesis that abnormal activation of the flexor synergy causes reduced upper extremity workspace. We repeated these assessments using a ceiling-mounted device as a positive control and found much better performance using the positive control. This inconsistency demonstrates that **two devices can show the same outcomes in healthy users but very different outcomes in the target impaired population.** Many similar studies test only in healthy users to validate their designs; we contribute data that cautions against extrapolating these results to stroke survivors.

- **Chapter 4**: We described in detail **a passive exoskeleton to assist shoulder abduction.** We characterized the new exoskeleton on the benchtop and in healthy operators, demonstrating that the exoskeleton **provides the intended assistance without impeding range of motion in any other upper extremity joint.** We also presented a protocol for assessing this exoskeleton's usefulness in aiding stroke survivors with activities of daily living, rather than specialized subtasks such as reachable workspace area. The material costs of this exoskeleton were less than 100 USD, while similar commercially available passive exoskeletons for industrial applications are typically priced between 5,000 and 8,000 USD. Because of its effectiveness, simplicity, and price point, this design could be a powerful tool for studying the effects of gravity compensation on stroke recovery with higher dosages than existing devices.

- **Chapter 5**: We described the design of **an exotendon that demonstrably improves human running economy by 6%**, exceeding the performance of many powered exoskeletal robots. We provided **a theoretical biomechanical framework that explains the mechanism of energetic savings.** This

framework predicted changes in mechanical effort required in specific phases of gait that we verified. We also performed ancillary tests to demonstrate that the benefits of our device are not due to the placebo effect and that it can be effectively used in unstructured environments, such as suburban streets. Our device is manufacturable for approximately 1 USD.

In this section, I compare the material cost of our designs to the retail price of existing devices. The retail price of existing devices encapsulates the material cost as well as logistics, labor, profit margins, marketing, legal, and other costs. The retail price might also be driven by economic considerations. For instance, many devices are designed for industrial use and a manufacturing company might be willing to pay a higher price for an assistive device than an individual consumer. Without going through the exercise of commercializing our devices, I can not accurately estimate the ultimate retail price. I made an effort to limit the number and cost of the components used in our designs for the sake of accessibility, but readers should be mindful of the differences between material cost and retail price in our comparisons.

## 6.1 Limitations

Conducting studies involving human subjects using exoskeletal robots is difficult. Exoskeletal robots are traditionally expensive to purchase, expensive to build, and typically require specialized expertise to maintain, operate, or modify. Ensuring safety of human operators in experimental devices and gathering requisite approvals from ethical review boards takes time and effort. As a result, most studies investigating exoskeletal robots or wearable assistive device studies consider small subject populations ($<$15). While this number is typically sufficient to show some device effect, it may not be sufficient to observe any side effects that might emerge with greater dosage or in uncommon cases. A few studies have made the herculean effort to examine larger subject numbers ($>$40) and comparatively large doses ($>$20 hours) without reporting any unexpected ill-effects [46, 104, 105]. The long term and potential uncommon effects of the devices studied in this thesis are not knowable without considerably more investigation.

## 6.2 Future Work

Some devices might not be recognizable as exoskeletal robot analogs, even if they perform similar functions. The exotendon described in Chapter 5 is one example of a device that applies forces to the human hip to help swing the legs similar to the exosuits developed by the Harvard Biodesign Lab [13, 78] and the passive exoskeleton presented by Nasiri et al. [15]. Because of the difference in form factor, our exotendon might not be easily recognized as belonging to the same class of assistive devices, even though it modifies the dynamics of the human body in the same way as passive exoskeletons. These simple passive devices might be the most likely form of exoskeletal robot to achieve widespread adoption. The Nike Vaporfly is one example of a device that passively improves running economy [195] and likely running performance [20, 196] through subtle changes to limb mechanics. While few are likely to think of exoskeletal robots while looking at this Nike shoe, it matches the performance of powered exosuits for running assistance [78], is commercially available, and has been used by thousands of professional athletes in competition [197]. The success of the Nike Vaporfly suggests that at present and in the near future, simple passive devices will be the most accessible and successful form of wearable assistive device.

While passive devices appear to be the answer for today, hybrid and low-power devices might be a solution for tomorrow. Passive assistive devices modify the mechanical properties of the human body to be better suited for the intended task. For example, the passive exoskeleton presented in Chapter 4 can be considered to reduce the weight of the arm, reducing the biomechanical requirements on the muscles in performing a given task. However, different mechanical properties may be desirable when the human operator changes tasks. For instance, when lying down, the forces exerted by our passive exoskeleton no longer oppose gravitational forces and may interfere with accomplishing the next task. Some features from active exoskeletal robots could be incorporated into the design of passive assistive devices to form hybrid devices that are capable of actively switching between modes or adapting the assistance provided to suit changing needs [198, 199]. Similarly, some devices can use a small amount of energy compared to the requirements of exoskeletal robots to

stimulate muscles into action in humans [200] and other primates [201]. While this approach likely would not reduce the metabolic effort required to accomplish a task as the human muscle is the element performing the mechanical work, this approach might aid certain motor impaired populations in controlling their limbs.

The use of hybrid and low-power exoskeletal robots will reintroduce the difficult control challenges that are not present in passive devices. Because passive devices are designed to mechanically alter the dynamics of the human operator, active control is not needed and the control challenges discussed in Chapter 1.2.2 do not apply. However, switching between tasks requires that the device can identify when a switch is needed. Improving systems that automatically infer human intent and can control an exoskeletal robot to work with the human will be important topics of continuing research to make future hybrid and low-power exoskeletal robots tractable.

Ultimately, only powered exoskeletal robots may be suitable for some applications, such as assisting patients with spinal cord injuries. Design iterations on complex machines in which safety is paramount, such as exoskeletal robots, can be slow and costly. To speed up the design process, high performance robot emulators are being used to model candidate exoskeletal robots and rapidly test each candidate [13, 56]. These emulators can be combined with optimization algorithms to determine optimal parameters for exoskeletal robot systems [13, 202, 203]. This approach will likely lead to the fastest advancements in exoskeletal robot design in the near future.

# Bibliography

[1] D. W. Franklin and D. M. Wolpert, "Computational mechanisms of sensorimotor control," *Neuron*, vol. 72, no. 3, pp. 425–442, 2011.

[2] J. K. Yim and R. S. Fearing, "Precision jumping limits from flight-phase control in Salto-1P," in *IEEE/RSJ International Conference on Intelligent Robots and Systems*, 2018, pp. 2229–2236.

[3] O. Khatib, X. Yeh, G. Brantner, B. Soe, B. Kim, S. Ganguly, H. Stuart, S. Wang, M. Cutkosky, A. Edsinger *et al.*, "Ocean one: A robotic avatar for oceanic discovery," *IEEE Robotics & Automation Magazine*, vol. 23, no. 4, pp. 20–29, 2016.

[4] D. Mozaffarian, E. Benjamin, A. Go, D. Arnett, M. Blaha, M. Cushman, S. De Ferranti, J. Després, H. Fullerton, V. Howard, M. Huffman, S. Judd, B. Kissela, D. Lackland, J. Lichtman, L. Lisabeth, S. Liu, R. Mackey, D. Matchar, D. McGuire, E. Mohler, C. Moy, P. Muntner, M. Mussolino, K. Nasir, R. Neumar, G. Nichol, L. Palaniappan, D. Pandey, M. Reeves, C. Rodriguez, P. Sorlie, J. Stein, A. Towfighi, T. Turan, S. Virani, J. Willey, D. Woo, R. Yeh, and M. Turner, "Executive summary: Heart disease and stroke statistics — 2015 update: A report from the American Heart Association," *Circulation*, vol. 131, no. 4, pp. 434–441, 2015.

[5] E. J. Benjamin, M. J. Blaha, S. E. Chiuve, M. Cushman, S. R. Das, R. Deo, J. Floyd, M. Fornage, C. Gillespie, C. Isasi *et al.*, "Heart disease and stroke

statistics — 2017 update: a report from the American Heart Association," *Circulation*, vol. 135, no. 10, pp. e146–e603, 2017.

[6] S. Prabhakaran, E. Zarahn, C. Riley, A. Speizer, J. Y. Chong, R. M. Lazar, R. S. Marshall, and J. W. Krakauer, "Inter-individual variability in the capacity for motor recovery after ischemic stroke," *Neurorehabilitation and Neural Repair*, vol. 22, no. 1, pp. 64–71, 2008.

[7] E. Zarahn, L. Alon, S. L. Ryan, R. M. Lazar, M.-S. Vry, C. Weiller, R. S. Marshall, and J. W. Krakauer, "Prediction of motor recovery using initial impairment and fmri 48 h poststroke," *Cerebral Cortex*, vol. 21, no. 12, pp. 2712–2721, 2011.

[8] C. Winters, E. E. van Wegen, A. Daffertshofer, and G. Kwakkel, "Generalizability of the proportional recovery model for the upper extremity after an ischemic stroke," *Neurorehabilitation and Neural Repair*, vol. 29, no. 7, pp. 614–622, 2015.

[9] P. Muntner, E. Garrett, M. J. Klag, and J. Coresh, "Trends in stroke prevalence between 1973 and 1991 in the us population 25 to 74 years of age," *Stroke*, vol. 33, no. 5, pp. 1209–1213, 2002.

[10] G. Kwakkel, B. J. Kollen, J. van der Grond, and A. J. Prevo, "Probability of regaining dexterity in the flaccid upper limb: impact of severity of paresis and time since onset in acute stroke," *Stroke*, vol. 34, no. 9, pp. 2181–2186, 2003.

[11] "Apparatus for facilitating walking, running, and jumping," U.S. Patent 420 197, 1890.

[12] S. H. Collins, M. B. Wiggin, and G. S. Sawicki, "Reducing the energy cost of human walking using an unpowered exoskeleton," *Nature*, vol. 522, no. 7555, pp. 212–215, 2015.

[13] J. Zhang, P. Fiers, K. A. Witte, R. W. Jackson, K. L. Poggensee, C. G. Atkeson, and S. H. Collins, "Human-in-the-loop optimization of exoskeleton assistance during walking," *Science*, vol. 356, no. 6344, pp. 1280–1284, 2017.

[14] L. N. Awad, J. Bae, K. O'Donnell, S. M. De Rossi, K. Hendron, L. H. Sloot, P. Kudzia, S. Allen, K. G. Holt, T. D. Ellis *et al.*, "A soft robotic exosuit improves walking in patients after stroke," *Science Translational Medicine*, vol. 9, no. 400, p. eaai9084, 2017.

[15] R. Nasiri, A. Ahmadi, and M. N. Ahmadabadi, "Reducing the energy cost of human running using an unpowered exoskeleton," *IEEE Transactions on Neural Systems and Rehabilitation Engineering*, vol. 26, no. 10, pp. 2026–2032, 2018.

[16] G. Lee, J. Kim, F. Panizzolo, Y. Zhou, L. Baker, I. Galiana, P. Malcolm, and C. Walsh, "Reducing the metabolic cost of running with a tethered soft exosuit," *Science Robotics*, vol. 2, no. 6, p. eaan6708, 2017.

[17] L. M. Mooney, E. J. Rouse, and H. M. Herr, "Autonomous exoskeleton reduces metabolic cost of walking," in *36th Annual International Conference of the IEEE Engineering in Medicine and Biology Society*, vol. 2014, 2014, pp. 3065–3068.

[18] C. J. Walsh, K. Endo, and H. Herr, "A quasi-passive leg exoskeleton for load-carrying augmentation," *International Journal of Humanoid Robotics*, vol. 4, no. 3, pp. 487–506, 2007.

[19] A. B. Zoss, H. Kazerooni, and A. Chu, "Biomechanical design of the berkeley lower extremity exoskeleton (bleex)," *IEEE/ASME Transactions on Mechatronics*, vol. 11, no. 2, pp. 128–138, 2006.

[20] W. Hoogkamer, S. Kipp, B. A. Spiering, and R. Kram, "Altered running economy directly translates to altered distance-running performance," *Medicine and Science in Sports and Exercise*, vol. 48, no. 11, pp. 2175–2180, 2016.

[21] H. Kazerooni, "The human power amplifier technology at the university of california, berkeley," *Robotics and Autonomous Systems*, vol. 19, no. 2, pp. 179–187, 1996.

[22] H. Kazerooni, E. Hacker, L.-H. Chen, W. Tung, P. Nathan, and T. Yangyuenthanasan, "Trunk supporting exoskeleton and method of use," Aug 2017, US Patent 9,744,066.

[23] S. Spada, L. Ghibaudo, S. Gilotta, L. Gastaldi, and M. P. Cavatorta, "Investigation into the applicability of a passive upper-limb exoskeleton in automotive industry," *Procedia Manufacturing*, vol. 11, pp. 1255–1262, 2017.

[24] M. D. Ellis, T. Sukal, T. DeMott, and J. P. Dewald, "ACT 3D exercise targets gravity-induced discoordination and improves reaching work area in individuals with stroke," in *IEEE International Conference on Rehabilitation Robotics*, 2007, pp. 890–895.

[25] T. G. Sugar, J. He, E. J. Koeneman, J. B. Koeneman, R. Herman, H. Huang, R. S. Schultz, D. Herring, J. Wanberg, S. Balasubramanian *et al.*, "Design and control of rupert: a device for robotic upper extremity repetitive therapy," *IEEE Transactions on Neural Systems and Rehabilitation Engineering*, vol. 15, no. 3, pp. 336–346, 2007.

[26] G. B. Prange, M. J. Jannink, C. G. Groothuis-Oudshoorn, H. J. Hermens, and M. J. IJzerman, "Systematic review of the effect of robot-aided therapy on recovery of the hemiparetic arm after stroke," *Journal of Rehabilitation Research and Development*, vol. 43, no. 2, p. 171, 2006.

[27] N. Hogan, H. I. Krebs, J. Charnnarong, P. Srikrishna, and A. Sharon, "Mitmanus: a workstation for manual therapy and training. i," in *Proceedings IEEE International Workshop on Robot and Human Communication*, 1992, pp. 161–165.

[28] A. Esquenazi, M. Talaty, A. Packel, and M. Saulino, "The rewalk powered exoskeleton to restore ambulatory function to individuals with thoracic-level motor-complete spinal cord injury," *American Journal of Physical Medicine & Rehabilitation*, vol. 91, no. 11, pp. 911–921, 2012.

[29] A. Gupta and M. K. O'Malley, "Design of a haptic arm exoskeleton for training and rehabilitation," *IEEE/ASME Transactions on Mechatronics*, vol. 11, no. 3, pp. 280–289, 2006.

[30] A. Gupta, M. K. O'Malley, V. Patoglu, and C. Burgar, "Design, control and performance of ricewrist: a force feedback wrist exoskeleton for rehabilitation and training," *The International Journal of Robotics Research*, vol. 27, no. 2, pp. 233–251, 2008.

[31] X. Gu, Y. Zhang, W. Sun, Y. Bian, D. Zhou, and P. O. Kristensson, "Dexmo: An inexpensive and lightweight mechanical exoskeleton for motion capture and force feedback in vr," in *Proceedings of the CHI Conference on Human Factors in Computing Systems*, 2016, pp. 1991–1995.

[32] C. Carignan, J. Tang, and S. Roderick, "Development of an exoskeleton haptic interface for virtual task training," in *IEEE/RSJ International Conference on Intelligent Robots and Systems*, 2009, pp. 3697–3702.

[33] A. Schiele and G. Visentin, "The esa human arm exoskeleton for space robotics telepresence," in *International Symposium on Artificial Intelligence, Robotics and Automation in Space*, 2003, pp. 19–23.

[34] S. B. Schorr and A. M. Okamura, "Three-dimensional skin deformation as force substitution: Wearable device design and performance during haptic exploration of virtual environments," *IEEE Transactions on Haptics*, vol. 10, no. 3, pp. 418–430, 2017.

[35] D. Barthélemy, S. Alain, M. J. Grey, J. B. Nielsen, and L. Bouyer, "Rapid changes in corticospinal excitability during force field adaptation of human walking," *Experimental Brain Research*, vol. 217, no. 1, pp. 99–115, 2012.

[36] G. R. Tan, M. Raitor, and S. H. Collins, "Bump'em: an open-source, bump-emulation system for studying human balance and gait," in *IEEE International Conference on Robotics and Automation*, 2020.

[37] A. R. Emmens, E. H. Van Asseldonk, and H. Van Der Kooij, "Effects of a powered ankle-foot orthosis on perturbed standing balance," *Journal of Neuroengineering and Rehabilitation*, vol. 15, no. 1, p. 50, 2018.

[38] J. C. Selinger, S. M. O'Connor, J. D. Wong, and J. M. Donelan, "Humans can continuously optimize energetic cost during walking," *Current Biology*, vol. 25, no. 18, pp. 2452–2456, 2015.

[39] K. E. Gordon and D. P. Ferris, "Learning to walk with a robotic ankle exoskeleton," *Journal of Biomechanics*, vol. 40, no. 12, pp. 2636–2644, 2007.

[40] J. C. Selinger, J. D. Wong, S. N. Simha, and J. M. Donelan, "How humans initiate energy optimization and converge on their optimal gaits," *Journal of Experimental Biology*, vol. 222, no. 19, p. jeb198234, 2019.

[41] D. M. Wolpert, R. C. Miall, and M. Kawato, "Internal models in the cerebellum," *Trends in Cognitive Sciences*, vol. 2, no. 9, pp. 338–347, 1998.

[42] A. Resulaj, R. Kiani, D. M. Wolpert, and M. N. Shadlen, "Changes of mind in decision-making," *Nature*, vol. 461, no. 7261, pp. 263–266, 2009.

[43] E. Burdet, R. Osu, D. W. Franklin, T. E. Milner, and M. Kawato, "The central nervous system stabilizes unstable dynamics by learning optimal impedance," *Nature*, vol. 414, no. 6862, pp. 446–449, 2001.

[44] Q. Li, V. Naing, J. A. Hoffer, D. J. Weber, A. D. Kuo, and J. M. Donelan, "Biomechanical energy harvesting: Apparatus and method," in *IEEE International Conference on Robotics and Automation*, 2008, pp. 3672–3677.

[45] J. M. Donelan, Q. Li, V. Naing, J. A. Hoffer, D. Weber, and A. D. Kuo, "Biomechanical energy harvesting: generating electricity during walking with minimal user effort," *Science*, vol. 319, no. 5864, pp. 807–810, 2008.

[46] S. P. Dukelow, T. M. Herter, K. D. Moore, M. J. Demers, J. I. Glasgow, S. D. Bagg, K. E. Norman, and S. H. Scott, "Quantitative assessment of limb position

sense following stroke," *Neurorehabilitation and Neural Repair*, vol. 24, no. 2, pp. 178–187, 2010.

[47] J. C. Perry, J. Rosen, and S. Burns, "Upper-limb powered exoskeleton design," *IEEE/ASME Transactions on Mechatronics*, vol. 12, no. 4, pp. 408–417, 2007.

[48] H. Kazerooni and T. J. Snyder, "Case study on haptic devices: Human-induced instability in powered hand controllers," *Journal of Guidance, Control, and Dynamics*, vol. 18, no. 1, pp. 108–113, 1995.

[49] M. Wehner, B. Quinlivan, P. M. Aubin, E. Martinez-Villalpando, M. Baumann, L. Stirling, K. Holt, R. Wood, and C. Walsh, "A lightweight soft exosuit for gait assistance," in *IEEE International Conference on Robotics and Automation*, 2013, pp. 3362–3369.

[50] A. T. Asbeck, R. J. Dyer, A. F. Larusson, and C. J. Walsh, "Biologically-inspired soft exosuit," *IEEE International Conference on Rehabilitation Robotics*, no. June, pp. 1–8, 2013.

[51] A. M. Dollar and H. Herr, "Design of a quasi-passive knee exoskeleton to assist running," in *IEEE/RSJ International Conference on Intelligent Robots and Systems*, 2008, pp. 747–754.

[52] A. J. Young, J. Foss, H. Gannon, and D. P. Ferris, "Influence of power delivery timing on the energetics and biomechanics of humans wearing a hip exoskeleton," *Frontiers in Bioengineering and Biotechnology*, vol. 5, p. 4, 2017.

[53] H. S. Lo and S. Q. Xie, "Exoskeleton robots for upper-limb rehabilitation: State of the art and future prospects," *Medical Engineering & Physics*, vol. 34, no. 3, pp. 261–268, 2012.

[54] A. Petron, J.-F. Duval, and H. Herr, "Multi-indenter device for in vivo biomechanical tissue measurement," *IEEE Transactions on Neural Systems and Rehabilitation Engineering*, vol. 25, no. 5, pp. 426–435, 2016.

[55] J. Klein, S. Spencer, J. Allington, J. E. Bobrow, and D. J. Reinkensmeyer, "Optimization of a parallel shoulder mechanism to achieve a high-force, low-mass, robotic-arm exoskeleton," *IEEE Transactions on Robotics*, vol. 26, no. 4, pp. 710–715, 2010.

[56] J. M. Caputo and S. H. Collins, "A universal ankle–foot prosthesis emulator for human locomotion experiments," *Journal of Biomechanical Engineering*, vol. 136, no. 3, 2014.

[57] S. J. Ball, I. E. Brown, and S. H. Scott, "A planar 3dof robotic exoskeleton for rehabilitation and assessment," in *Annual International Conference of the IEEE Engineering in Medicine and Biology Society*, 2007, pp. 4024–4027.

[58] A. Schiele and F. C. van der Helm, "Influence of attachment pressure and kinematic configuration on phri with wearable robots," *Applied Bionics and Biomechanics*, vol. 6, no. 2, pp. 157–173, 2009.

[59] B. Celebi, M. Yalcin, and V. Patoglu, "Assiston-knee: A self-aligning knee exoskeleton," in *IEEE/RSJ International Conference on Intelligent Robots and Systems*, 2013, pp. 996–1002.

[60] A. Otten, C. Voort, A. Stienen, R. Aarts, E. van Asseldonk, and H. van der Kooij, "Limpact: a hydraulically powered self-aligning upper limb exoskeleton," *IEEE/ASME Transactions on Mechatronics*, vol. 20, no. 5, pp. 2285–2298, 2015.

[61] A. H. Stienen, E. E. Hekman, F. C. Van Der Helm, and H. Van Der Kooij, "Self-aligning exoskeleton axes through decoupling of joint rotations and translations," *IEEE Transactions on Robotics*, vol. 25, no. 3, pp. 628–633, 2009.

[62] S. H. Collins, M. Wisse, and A. Ruina, "A three-dimensional passive-dynamic walking robot with two legs and knees," *The International Journal of Robotics Research*, vol. 20, no. 7, pp. 607–615, 2001.

[63] V. Duchaine and C. M. Gosselin, "Investigation of human-robot interaction stability using Lyapunov theory," in *IEEE International Conference on Robotics and Automation*, 2008, pp. 2189–2194.

[64] P. M. Fitts, "The information capacity of the human motor system in controlling the amplitude of movement." *Journal of Experimental Psychology*, vol. 47, no. 6, p. 381, 1954.

[65] N. Hogan, "An organizing principle for a class of voluntary movements," *Journal of Neuroscience*, vol. 4, no. 11, pp. 2745–2754, 1984.

[66] H. G. Wu, Y. R. Miyamoto, L. N. G. Castro, B. P. Ölveczky, and M. A. Smith, "Temporal structure of motor variability is dynamically regulated and predicts motor learning ability," *Nature Neuroscience*, vol. 17, no. 2, p. 312, 2014.

[67] L. E. Kahn, P. S. Lum, W. Z. Rymer, and D. J. Reinkensmeyer, "Robot-assisted movement training for the stroke-impaired arm: Does it matter what the robot does?" *Journal of Rehabilitation Research and Development*, vol. 43, no. 5, pp. 619–630, 2006.

[68] P. Nuyujukian, J. M. Fan, J. C. Kao, S. I. Ryu, and K. V. Shenoy, "A high-performance keyboard neural prosthesis enabled by task optimization," *IEEE Transactions on Biomedical Engineering*, vol. 62, no. 1, pp. 21–29, 2014.

[69] T. Lenzi, S. M. M. De Rossi, N. Vitiello, and M. C. Carrozza, "Intention-based emg control for powered exoskeletons," *IEEE Transactions on Biomedical Engineering*, vol. 59, no. 8, pp. 2180–2190, 2012.

[70] J. V. Kopke, M. D. Ellis, and L. J. Hargrove, "Determining user intent of partly dynamic shoulder tasks in individuals with chronic stroke using pattern recognition," *IEEE Transactions on Neural Systems and Rehabilitation Engineering*, vol. 28, no. 1, 2019.

[71] H. Kawamoto and Y. Sankai, "Power assist system hal-3 for gait disorder person," in *International Conference on Computers for Handicapped Persons*. Springer, 2002, pp. 196–203.

[72] J. R. Wolpaw, D. J. McFarland, G. W. Neat, and C. A. Forneris, "An eeg-based brain-computer interface for cursor control," *Electroencephalography and Clinical Neurophysiology*, vol. 78, no. 3, pp. 252–259, 1991.

[73] A. Kilicarslan, S. Prasad, R. G. Grossman, and J. L. Contreras-Vidal, "High accuracy decoding of user intentions using eeg to control a lower-body exoskeleton," in *International Conference of the IEEE Engineering in Medicine and Biology Society*, 2013, pp. 5606–5609.

[74] L. Van Engelhoven and H. Kazerooni, "Design and intended use of a passive actuation strategy for a shoulder supporting exoskeleton," in *Wearable Robotics Association Conference*, 2019, pp. 7–12.

[75] A. M. Grabowski and H. M. Herr, "Leg exoskeleton reduces the metabolic cost of human hopping," *Journal of Applied Physiology*, vol. 107, no. 3, pp. 670–678, 2009.

[76] K. N. Gregorczyk, J. P. Obusek, L. Hasselquist, J. M. S. Bensel, K. Carolyn, D. Gutekunst, and P. Frykman, "The effects of a lower body exoskeleton load carriage assistive device on oxygen consumption and kinematics during walking with loads," *Ergonomics*, vol. 53, no. 10, 2010.

[77] A. T. Asbeck, S. M. De Rossi, I. Galiana, Y. Ding, and C. J. Walsh, "Stronger, smarter, softer: next-generation wearable robots," *IEEE Robotics & Automation Magazine*, vol. 21, no. 4, pp. 22–33, 2014.

[78] J. Kim, G. Lee, R. Heimgartner, D. A. Revi, N. Karavas, D. Nathanson, I. Galiana, A. Eckert-Erdheim, P. Murphy, D. Perry, N. Menard, D. K. Choel, P. Malcom, and C. J. Walsh, "Reducing the metabolic rate of walking and running with a versatile, portable exosuit," *Science*, vol. 365, no. 6454, pp. 668–672, 2019.

[79] F. A. Panizzolo, I. Galiana, A. T. Asbeck, C. Siviy, K. Schmidt, K. G. Holt, and C. J. Walsh, "A biologically-inspired multi-joint soft exosuit that can reduce the energy cost of loaded walking," *Journal of Neuroengineering and Rehabilitation*, vol. 13, no. 1, p. 43, 2016.

[80] Y. Mao and S. K. Agrawal, "A cable driven upper arm exoskeleton for upper extremity rehabilitation," in *IEEE International Conference on Robotics and Automation*, 2011, pp. 4163–4168.

[81] E. A. Brackbill, Y. Mao, S. K. Agrawal, M. Annapragada, and V. N. Dubey, "Dynamics and control of a 4-dof wearable cable-driven upper arm exoskeleton," in *IEEE International Conference on Robotics and Automation*, 2009, pp. 2300–2305.

[82] R. Natividad and C. Yeow, "Development of a soft robotic shoulder assistive device for shoulder abduction," in *IEEE International Conference on Biomedical Robotics and Biomechatronics*, 2016, pp. 989–993.

[83] V. Oguntosin, W. S. Harwin, S. Kawamura, S. J. Nasuto, and Y. Hayashi, "Development of a wearable assistive soft robotic device for elbow rehabilitation," in *IEEE International Conference on Rehabilitation Robotics*, 2015, pp. 747–752.

[84] C. S. Simpson, A. M. Okamura, and E. W. Hawkes, "Exomuscle: An inflatable device for shoulder abduction support," in *IEEE International Conference on Robotics and Automation*, 2017, pp. 6651–6657.

[85] C. T. O'Neill, N. S. Phipps, L. Cappello, S. Paganoni, and C. J. Walsh, "A soft wearable robot for the shoulder: Design, characterization, and preliminary testing," in *IEEE International Conference on Rehabilitation Robotics*, 2017, pp. 1672–1678.

[86] S. Lessard, P. Pansodtee, A. Robbins, J. M. Trombadore, S. Kurniawan, and M. Teodorescu, "A soft exosuit for flexible upper-extremity rehabilitation," *IEEE Transactions on Neural Systems and Rehabilitation Engineering*, vol. 26, no. 8, pp. 1604–1617, 2018.

[87] R. F. Natividad, S. W. Hong, T. M. Miller-Jackson, and C.-H. Yeow, "The exosleeve: A soft robotic exoskeleton for assisting in activities of daily living,"

in *International Symposium on Wearable Robotics*. Springer, 2018, pp. 406–409.

[88] L. Tiseni, M. Xiloyannis, D. Chiaradia, N. Lotti, M. Solazzi, H. Van der Kooij, A. Frisoli, and L. Masia, "On the edge between soft and rigid: an assistive shoulder exoskeleton with hyper-redundant kinematics," in *IEEE International Conference on Rehabilitation Robotics*, 2019, pp. 618–624.

[89] P. Polygerinos, K. C. Galloway, E. Savage, M. Herman, K. O'Donnell, and C. J. Walsh, "Soft robotic glove for hand rehabilitation and task specific training," in *IEEE International Conference on Robotics and Automation*, 2015, pp. 2913–2919.

[90] B. Lenzo, M. Fontana, S. Marcheschi, F. Salsedo, A. Frisoli, and M. Bergamasco, "Trackhold: a novel passive arm-support device," *Journal of Mechanisms and Robotics*, vol. 8, no. 2, 2016.

[91] R. Altenburger, D. Scherly, and K. S. Stadler, "Design of a passive, iso-elastic upper limb exoskeleton for gravity compensation," *Robomech Journal*, vol. 3, no. 1, pp. 1–7, 2016.

[92] G. Cannella, D. Shona Laila, and C. T. Freeman, "Mechanical design of an affordable adaptive gravity balanced orthosis for upper limb stroke rehabilitation," *Mechanics Based Design of Structures and Machines*, vol. 44, no. 1-2, pp. 96–108, 2016.

[93] B. Mastenbroek, E. de Haan, M. van den Berg, and J. L. Herder, "Development of a mobile arm support (armon): Design evolution and preliminary user experience," in *IEEE International Conference on Rehabilitation Robotics*, 2007, pp. 1114–1120.

[94] I. Babik, A. B. Cunha, and M. A. Lobo, "Play with objects in children with arthrogryposis: Effects of intervention with the playskin lift$^{TM}$ exoskeletal garment," in *American Journal of Medical Genetics Part C: Seminars in Medical Genetics*, vol. 181, no. 3. Wiley Online Library, 2019, pp. 393–403.

[95] I. Babik, E. Kokkoni, A. B. Cunha, J. C. Galloway, T. Rahman, and M. A. Lobo, "Feasibility and effectiveness of a novel exoskeleton for an infant with arm movement impairments," *Pediatric Physical Therapy: the Official Publication of the Section on Pediatrics of the American Physical Therapy Association*, vol. 28, no. 3, p. 338, 2016.

[96] M. L. Hall and M. A. Lobo, "Design and development of the first exoskeletal garment to enhance arm mobility for children with movement impairments," *Assistive Technology*, vol. 30, no. 5, pp. 251–258, 2018.

[97] C. G. Welker, C. S. Simpson, and E. W. Hawkes, "Simulation of a passive assistive device to reduce running effort," in *Proceedings of the XXVI Congress of the International Society of Biomechanics*, 2017.

[98] M. Gunn, T. M. Shank, M. Eppes, J. Hossain, and T. Rahman, "User evaluation of a dynamic arm orthosis for people with neuromuscular disorders," *IEEE Transactions on Neural Systems and Rehabilitation Engineering*, vol. 24, no. 12, pp. 1277–1283, 2015.

[99] A. J. Van den Bogert, "Exotendons for assistance of human locomotion," *BioMedical Engineering OnLine*, vol. 2, no. 1, p. 17, 2003.

[100] E. Frederick, J. Daniels, and J. Hayes, "The effect of shoe weight on the aerobic demands of running," in *Current Topics in Sports Medicine, Proceedings of the World Congress of Sports Medicine*, vol. 198. Urban & Schwarzenberg, 1984, pp. 616–625.

[101] J. McCabe, M. Monkiewicz, J. Holcomb, S. Pundik, and J. J. Daly, "Comparison of robotics, functional electrical stimulation, and motor learning methods for treatment of persistent upper extremity dysfunction after stroke: a randomized controlled trial," *Archives of Physical Medicine and Rehabilitation*, vol. 96, no. 6, pp. 981–990, 2015.

[102] C. E. Lang, K. R. Lohse, and R. L. Birkenmeier, "Dose and timing in neurorehabilitation: prescribing motor therapy after stroke," *Current Opinion in Neurology*, vol. 28, no. 6, p. 549, 2015.

[103] "Cigna medical coverage policy: Prosthetic devices," https://cignaforhcp.cigna.com/public/content/pdf/coveragePolicies/medical/mm_0536_coveragepositioncriteria_prosthetic_devices.pdf, Jan 2020.

[104] J. M. Veerbeek, A. C. Langbroek-Amersfoort, E. E. Van Wegen, C. G. Meskers, and G. Kwakkel, "Effects of robot-assisted therapy for the upper limb after stroke: a systematic review and meta-analysis," *Neurorehabilitation and Neural Repair*, vol. 31, no. 2, pp. 107–121, 2017.

[105] A. C. Lo, P. D. Guarino, L. G. Richards, J. K. Haselkorn, G. F. Wittenberg, D. G. Federman, R. J. Ringer, T. H. Wagner, H. I. Krebs, B. T. Volpe, C. T. Bever, D. M. Bravata, P. W. Duncan, B. H. Corn, A. D. Maffucci, S. E. Nadeau, S. S. Conroy, J. M. Powell, G. D. Huang, and P. Peduzzi, "Robot-assisted therapy for long-term upper-limb impairment after stroke," *New England Journal of Medicine*, vol. 362, no. 19, pp. 1772–1783, 2010.

[106] E. W. Hawkes, L. H. Blumenschein, J. D. Greer, and A. M. Okamura, "A soft robot that navigates its environment through growth," *Science Robotics*, vol. 2, no. 8, p. eaan3028, 2017.

[107] Z. M. Hammond, N. S. Usevitch, E. W. Hawkes, and S. Follmer, "Pneumatic reel actuator: Design, modeling, and implementation," in *IEEE International Conference on Robotics and Automation*, 2017, pp. 626–633.

[108] J. P. A. Dewald, V. Sheshadri, M. L. Dawson, and R. F. Beer, "Upper-Limb Discoordination in Hemiparetic Stroke: Implications for Neurorehabilitation," *Topics in Stroke Rehabilitation*, 2001.

[109] J. P. A. Dewald, P. S. Pope, J. D. Given, T. S. Buchanan, and W. Z. Rymer, "Abnormal muscle coactivation patterns during isometric torque generation at

the elbow and shoulder in hemiparetic subjects," *Brain*, vol. 118, no. 2, pp. 495–510, 1995.

[110] V. C. Cheung, A. Turolla, M. Agostini, S. Silvoni, C. Bennis, P. Kasi, S. Paganoni, P. Bonato, and E. Bizzi, "Muscle synergy patterns as physiological markers of motor cortical damage," *Proceedings of the National Academy of Sciences*, vol. 109, no. 36, pp. 14 652–14 656, 2012.

[111] D. J. Clark, L. H. Ting, F. E. Zajac, R. R. Neptune, and S. A. Kautz, "Merging of healthy motor modules predicts reduced locomotor performance and muscle coordination complexity post-stroke," *Journal of Neurophysiology*, vol. 103, no. 2, pp. 844–857, 2010.

[112] J. P. Dewald and R. F. Beer, "Abnormal joint torque patterns in the paretic upper limb of subjects with hemiparesis," *Muscle & Nerve: Official Journal of the American Association of Electrodiagnostic Medicine*, vol. 24, no. 2, pp. 273–283, 2001.

[113] R. F. Beer, M. D. Ellis, B. G. Holubar, and J. P. Dewald, "Impact of gravity loading on post-stroke reaching and its relationship to weakness," *Muscle & Nerve: Official Journal of the American Association of Electrodiagnostic Medicine*, vol. 36, no. 2, pp. 242–250, 2007.

[114] L. E. Kahn, P. S. Lum, W. Z. Rymer, and D. J. Reinkensmeyer, "Robot-assisted movement training for the stroke-impaired arm: Does it matter what the robot does?" *Journal of Rehabilitation Research and Development*, vol. 43, no. 5, pp. 619–630, 2014.

[115] M. D. Ellis, T. Sukal-Moulton, and J. P. Dewald, "Progressive shoulder abduction loading is a crucial element of arm rehabilitation in chronic stroke," *Neurorehabilitation and Neural Repair*, vol. 23, no. 8, pp. 862–869, 2009.

[116] T. M. Sukal, M. D. Ellis, and J. P. Dewald, "Shoulder abduction-induced reductions in reaching work area following hemiparetic stroke: neuroscientific implications," *Experimental Brain Research*, vol. 183, no. 2, pp. 215–223, 2007.

[117] J. Roh, W. Z. Rymer, and R. F. Beer, "Evidence for altered upper extremity muscle synergies in chronic stroke survivors with mild and moderate impairment," *Frontiers in Human Neuroscience*, vol. 9, 2015.

[118] M. Mulas, M. Folgheraiter, and G. Gini, "An EMG-controlled exoskeleton for hand rehabilitation," in *IEEE International Conference on Rehabilitation Robotics*. IEEE, 2005, pp. 371–374.

[119] L. H. Ting and J. M. Macpherson, "A limited set of muscle synergies for force control during a postural task," *Journal of Neurophysiology*, vol. 93, no. 1, pp. 609–613, 2005.

[120] C. Simpson, B. Huerta, S. Sketch, M. Lansberg, E. Hawkes, and A. Okamura, "Upper extremity exomuscle for shoulder abduction support," *bioRxiv*, 2020.

[121] B. Ovbiagele and M. N. Nguyen-Huynh, "Stroke epidemiology: advancing our understanding of disease mechanism and therapy," *Neurotherapeutics*, vol. 8, no. 3, p. 319, 2011.

[122] P. Polygerinos, S. Lyne, Z. Wang, L. F. Nicolini, B. Mosadegh, G. M. Whitesides, and C. J. Walsh, "Towards a soft pneumatic glove for hand rehabilitation," in *IEEE/RSJ International Conference on Intelligent Robots and Systems*, 2013, pp. 1512–1517.

[123] J. Realmuto and T. Sanger, "A robotic forearm orthosis using soft fabric-based helical actuators," in *2nd IEEE International Conference on Soft Robotics*, 2019, pp. 591–596.

[124] C. T. O'Neill, T. Proietti, K. Nuckols, M. E. Clarke, C. J. Hohimer, A. Cloutier, D. J. Lin, and C. J. Walsh, "Inflatable soft wearable robot for reducing therapist fatigue during upper extremity rehabilitation in severe stroke," *IEEE Robotics and Automation Letters*, 2020.

[125] A. H. Stienen, E. E. Hekman, G. B. Prange, M. J. Jannink, F. C. van der Helm, and H. van der Kooij, "Freebal: design of a dedicated weight-support system

for upper-extremity rehabilitation," *Journal of Medical Devices*, vol. 3, no. 4, 2009.

[126] J. Essers, A. Murgia, A. Bergsma, P. Verstegen, and K. Meijer, "An inverse dynamic analysis on the influence of upper limb gravity compensation during reaching," in *IEEE International Conference on Rehabilitation Robotics*, 2013, pp. 1–5.

[127] J.-B. Mignardot, C. G. Le Goff, R. Van Den Brand, M. Capogrosso, N. Fumeaux, H. Vallery, S. Anil, J. Lanini, I. Fodor, G. Eberle, A. Ijspeert, B. Schurch, A. Curt, S. Carda, J. Bloch, J. von Zitzewitz, and G. Courtine, "A multidirectional gravity-assist algorithm that enhances locomotor control in patients with stroke or spinal cord injury," *Science Translational Medicine*, vol. 9, no. 399, 2017.

[128] F. C. Huang and J. L. Patton, "Augmented dynamics and motor exploration as training for stroke," *IEEE Transactions on Biomedical Engineering*, vol. 60, no. 3, pp. 838–844, 2012.

[129] M. D. Ellis, I. Schut, and J. P. Dewald, "Flexion synergy overshadows flexor spasticity during reaching in chronic moderate to severe hemiparetic stroke," *Clinical Neurophysiology*, vol. 128, no. 7, pp. 1308–1314, 2017.

[130] I. Cusmano, I. Sterpi, A. Mazzone, S. Ramat, C. Delconte, F. Pisano, and R. Colombo, "Evaluation of upper limb sense of position in healthy individuals and patients after stroke," *Journal of Healthcare Engineering*, vol. 5, no. 2, pp. 145–162, 2014.

[131] D. Bourbonnais and S. V. Noven, "Weakness in patients with hemiparesis," *American Journal of Occupational Therapy*, vol. 43, no. 5, pp. 313–319, 1989.

[132] C. L. Watkins, M. J. Leathley, J. M. Gregson, A. P. Moore, T. L. Smith, and A. K. Sharma, "Prevalence of spasticity post stroke," *Clinical Rehabilitation*, vol. 16, no. 5, pp. 515–522, 2002.

[133] J. Duysens, F. De Groote, and I. Jonkers, "The flexion synergy, mother of all synergies and father of new models of gait," *Frontiers in Computational Neuroscience*, vol. 7, p. 14, 2013.

[134] S. M. Sketch, C. S. Simpson, F. Crevecoeur, and A. M. Okamura, "Simulating the impact of sensorimotor deficits on reaching performance," in *IEEE International Conference on Rehabilitation Robotics*, 2017, pp. 31–37.

[135] J. L. Herder, "Development of a statically balanced arm support: Armon," in *IEEE International Conference on Rehabilitation Robotics*, 2005, pp. 281–286.

[136] L. F. Cardoso, J. L. Herder *et al.*, "Conceptual design of a passive arm orthosis," in *International Design Engineering Technical Conferences and Computers and Information in Engineering Conference*. American Society of Mechanical Engineers Digital Collection, 2002, pp. 747–756.

[137] S. M. El-Shamy, "Efficacy of armeo® robotic therapy versus conventional therapy on upper limb function in children with hemiplegic cerebral palsy," *American Journal of Physical Medicine & Rehabilitation*, vol. 97, no. 3, pp. 164–169, 2018.

[138] P. N. Kooren, A. G. Dunning, M. M. Janssen, J. Lobo-Prat, B. F. Koopman, M. I. Paalman, I. J. de Groot, and J. L. Herder, "Design and pilot validation of a-gear: a novel wearable dynamic arm support," *Journal of Neuroengineering and Rehabilitation*, vol. 12, no. 1, p. 83, 2015.

[139] M. D. Ellis, T. M. Sukal-Moulton, and J. P. Dewald, "Impairment-based 3-D robotic intervention improves upper extremity work area in chronic stroke: targeting abnormal joint torque coupling with progressive shoulder abduction loading," *IEEE Transactions on Robotics*, vol. 25, no. 3, pp. 549–555, 2009.

[140] A. R. Fugl-Meyer, L. Jääskö, I. Leyman, S. Olsson, and S. Steglind, "The post-stroke hemiplegic patient. 1. a method for evaluation of physical performance." *Scandinavian Journal of Rehabilitation Medicine*, vol. 7, no. 1, pp. 13–31, 1975.

[141] R. C. Lyle, "A performance test for assessment of upper limb function in physical rehabilitation treatment and research," *International Journal of Rehabilitation Research*, vol. 4, no. 4, pp. 483–492, 1981.

[142] N. Yozbatiran, L. Der-Yeghiaian, and S. C. Cramer, "A standardized approach to performing the action research arm test," *Neurorehabilitation and Neural Repair*, vol. 22, no. 1, pp. 78–90, 2008.

[143] J. W. Krakauer and S. T. Carmichael, *Broken movement: The neurobiology of motor recovery after stroke*. MIT Press, 2017.

[144] R. Nijland, E. van Wegen, J. Verbunt, R. van Wijk, J. van Kordelaar, and G. Kwakkel, "A comparison of two validated tests for upper limb function after stroke: The wolf motor function test and the action research arm test," *Journal of Rehabilitation Medicine*, vol. 42, no. 7, pp. 694–696, 2010.

[145] J. H. Van Der Lee, H. Beckerman, G. J. Lankhorst, L. M. Bouter *et al.*, "The responsiveness of the action research arm test and the fugl-meyer assessment scale in chronic stroke patients," *Journal of Rehabilitation Medicine*, vol. 33, no. 3, pp. 110–113, 2001.

[146] E. Taub, G. Uswatte, R. Pidikiti *et al.*, "Constraint-induced movement therapy: a new family of techniques with broad application to physical rehabilitation-a clinical review," *Journal of Rehabilitation Research and Development*, vol. 36, no. 3, pp. 237–251, 1999.

[147] T. Stevenson, L. Thalman, H. Christie, and W. Poluha, "Constraint-induced movement therapy compared to dose-matched interventions for upper-limb dysfunction in adult survivors of stroke: a systematic review with meta-analysis," *Physiotherapy Canada*, vol. 64, no. 4, pp. 397–413, 2012.

[148] C. S. Simpson, C. G. Welker, S. D. Uhlrich, S. M. Sketch, R. W. Jackson, S. L. Delp, S. H. Collins, J. C. Selinger, and E. W. Hawkes, "Connecting the legs with a spring improves human running economy," *Journal of Experimental Biology*, vol. 222, no. 17, p. jeb202895, 2019.

[149] R. M. Alexander, "Models and the scaling of energy costs for locomotion," *Journal of Experimental Biology*, vol. 208, no. 9, pp. 1645–1652, 2005.

[150] P. J. Butler, "The physiological basis of bird flight," *Philosophical Transactions of the Royal Society B: Biological Sciences*, vol. 371, no. 1704, p. 20150384, 2016.

[151] K. Schmidt-Nielsen, "Locomotion: Energy Cost of Swimming, Flying, and Running," *Science*, vol. 177, no. 4045, pp. 222–228, 1972.

[152] C. T. Davies, "Effects of wind assistance and resistance on the forward motion of a runner," *Journal of Applied Physiology*, vol. 48, no. 4, pp. 702–709, 1980.

[153] L. G. C. E. Pugh, "Oxygen intake in track and treadmill running with observations on the effect of air resistance," *The Journal of Physiology*, vol. 207, no. 3, pp. 823–835, 1970.

[154] C. J. Arellano and R. Kram, "Partitioning the metabolic cost of human running: A task-by-task approach," in *Integrative and Comparative Biology*, vol. 54, no. 6. Oxford University Press, dec 2014, pp. 1084–1098.

[155] R. L. Marsh, D. J. Ellerby, J. A. Carr, H. T. Henry, and C. I. Buchanan, "Partitioning the Energetics of Walking and Running: Swinging the Limbs Is Expensive," *Science*, vol. 303, no. 5654, pp. 80–83, 2004.

[156] J. R. Modica and R. Kram, "Metabolic energy and muscular activity required for leg swing in running," *Journal of Applied Physiology*, vol. 98, no. 6, pp. 2126–2131, 2005.

[157] R. Full, "Mechanics and energetics of terrestrial locomotion: bipeds to polypeds," in *Energy Transformation in Cells and Animals*, 1989, pp. 175–182.

[158] A. E. Minetti, P. Gaudino, E. Seminati, and D. Cazzola, "The cost of transport of human running is not affected, as in walking, by wide acceleration/deceleration cycles," *Journal of Applied Physiology*, vol. 114, no. 4, pp. 498–503, 2013.

[159] T. G. Sugar, A. Bates, M. Holgate, J. Kerestes, M. Mignolet, P. New, R. K. Ramachandran, S. Redkar, and C. Wheeler, "Limit Cycles to Enhance Human Performance Based on Phase Oscillators," *Journal of Mechanisms and Robotics*, vol. 7, no. 1, p. 011001, 2015.

[160] J. Kerestes and T. G. Sugar, "Enhanced Running Using a Jet Pack," in *International Design Engineering Technical Conferences and Computers and Information in Engineering Conference*. ASME, Aug 2015, p. V05AT08A006.

[161] A. E. Kerdok, A. A. Biewener, T. A. McMahon, P. G. Weyand, and H. M. Herr, "Energetics and mechanics of human running on surfaces of different stiffnesses," *Journal of Applied Physiology*, vol. 92, no. 2, pp. 469–478, 2002.

[162] T. A. McMahon and P. R. Greene, "The influence of track compliance on running," *Journal of Biomechanics*, vol. 12, no. 12, pp. 893–904, 1979.

[163] W. Hoogkamer, S. Kipp, and R. Kram, "The Biomechanics of Competitive Male Runners in Three Marathon Racing Shoes: A Randomized Crossover Study," *Sports Medicine*, vol. 49, no. 1, pp. 133–143, 2019.

[164] W. Hoogkamer, S. Kipp, J. H. Frank, E. Farina, G. Luo, and R. Kram, "New Running Shoe Reduces the Energetic Cost of Running," *Medicine & Science in Sports & Exercise*, vol. 49, p. 195, 2017.

[165] R. M. Alexander, N. J. Dimery, and R. F. Ker, "Elastic structures in the back and their role in galloping in some mammals," *Journal of Zoology*, vol. 207, pp. 467–482, 1985.

[166] M. B. Bennett, "A possible energy-saving role for the major fascia of the thigh in running quadrupedal mammals," *Journal of Zoology*, vol. 219, no. 2, pp. 221–230, 1989.

[167] D. A. Pabst, "Springs in Swimming Animals," *American Zoologist*, vol. 36, no. 6, pp. 723–735, dec 2007.

[168] R. M. Alexander and H. C. Bennet-Clark, "Storage of elastic strain energy in muscle and other tissues," *Nature*, vol. 265, no. 5590, pp. 114–117, 1977.

[169] D. J. Wells, "Muscle performance in hovering hummingbirds," *Journal of Experimental Biology*, vol. 178, pp. 39–57, 1993.

[170] M. W. Craib, V. A. Mitchell, K. B. Fields, T. R. Cooper, R. Hopewell, and D. W. Morgan, "The association between flexibility and running economy in sub-elite male distance runners," *Medicine and Science in Sports and Exercise*, vol. 28, no. 6, pp. 737–743, 1996.

[171] G. W. Gleim, N. S. Stachenfeld, and J. A. Nicholas, "The influence of flexibility on the economy of walking and jogging," *Journal of Orthopaedic Research*, vol. 8, no. 6, pp. 814–823, 1990.

[172] A. M. Jones, "Running economy is negatively related to sit-and-reach test performance in international-standard distance runners. / L ' economie de course est en relation negative avec la performance au test de souplesse 'sit and reach' chez des coureurs de fond de niv," *International Journal of Sports Medicine*, vol. 23, pp. 40–43, 2002.

[173] M. H. Dickinson and J. R. B. Lighton, "Muscle Efficiency and Elastic Storage in the Flight Motor of Drosophila," *Science*, vol. 268, no. 5207, pp. 87–90, 1995.

[174] J. Doke, J. M. Donelan, and A. D. Kuo, "Mechanics and energetics of swinging the human leg," *Journal of Experimental Biology*, vol. 208, no. 3, pp. 439–445, 2005.

[175] A. D. Kuo, "A Simple Model of Bipedal Walking Predicts the Preferred Speed–Step Length Relationship," *Journal of Biomechanical Engineering*, vol. 123, no. 3, pp. 264–269, 2001.

[176] A. D. Kuo, J. M. Donelan, and A. Ruina, "Energetic consequences of walking like an inverted pendulum: step-to-step transitions." *Exercise and Sport Sciences Reviews*, vol. 33, no. 2, pp. 88–97, 2005.

[177] K. L. Snyder and C. T. Farley, "Energetically optimal stride frequency in running: the effects of incline and decline," *Journal of Experimental Biology*, vol. 214, no. 12, pp. 2089–2095, jun 2011.

[178] A. Schiele and F. C. van der Helm, "Influence of attachment pressure and kinematic configuration on pHRI with wearable robots," *Applied Bionics and Biomechanics*, vol. 6, no. 2, pp. 157–173, 2009.

[179] D. M. Sengeh and H. Herr, "A variable-impedance prosthetic socket for a transtibial amputee designed from magnetic resonance imaging data," *Journal of Prosthetics and Orthotics*, vol. 25, no. 3, pp. 129–137, 2013.

[180] H. J. Hermens, B. Freriks, R. Merletti, D. Stegeman, J. Blok, G. Rau, C. Disselhorst-Klug, and G. Hägg, "European recommendations for surface electromyography," *Roessingh Research and Development*, vol. 8, no. 2, pp. 13–54, 1999.

[181] S. M. Suydam, K. Manal, and T. S. Buchanan, "The Advantages of Normalizing Electromyography to Ballistic Rather than Isometric or Isokinetic Tasks," *Journal of Applied Biomechanics*, vol. 33, no. 3, pp. 189–196, jun 2017.

[182] J. M. Brockway, "Derivation of formulae used to calculate energy expenditure in man." *Human nutrition: Clinical nutrition*, vol. 41, no. 6, pp. 463–71, 1987.

[183] P. Högberg, "How do stride length and stride frequency influence the energy-output during running?" *Arbeitsphysiologie*, vol. 14, no. 6, pp. 437–441, 1952.

[184] I. Hunter and G. A. Smith, "Preferred and optimal stride frequency, stiffness and economy: Changes with fatigue during a 1-h high-intensity run," *European Journal of Applied Physiology*, vol. 100, no. 6, pp. 653–661, 2007.

[185] A. Rajagopal, C. L. Dembia, M. S. DeMers, D. D. Delp, J. L. Hicks, and S. L. Delp, "Full-Body Musculoskeletal Model for Muscle-Driven Simulation of Human Gait," *IEEE Transactions on Biomedical Engineering*, vol. 63, no. 10, pp. 2068–2079, 2016.

[186] S. L. Delp, F. C. Anderson, A. S. Arnold, P. Loan, A. Habib, C. T. John, E. Guendelman, and D. G. Thelen, "Opensim: open-source software to create and analyze dynamic simulations of movement," *IEEE Transactions on Biomedical Engineering*, vol. 54, no. 11, pp. 1940–1950, 2007.

[187] M. E. Harrington, A. B. Zavatsky, S. E. Lawson, Z. Yuan, and T. N. Theologis, "Prediction of the hip joint centre in adults, children, and patients with cerebral palsy based on magnetic resonance imaging," *Journal of Biomechanics*, vol. 40, no. 3, pp. 595–602, jan 2007.

[188] J. Doke and A. D. Kuo, "Energetic cost of producing cyclic muscle force, rather than work, to swing the human leg," *Journal of Experimental Biology*, vol. 210, no. 13, pp. 2390–2398, 2007.

[189] B. D. Robertson, D. J. Farris, and G. S. Sawicki, "More is not always better: Modeling the effects of elastic exoskeleton compliance on underlying ankle muscle-tendon dynamics," *Bioinspiration and Biomimetics*, vol. 9, no. 4, p. 46018, 2014.

[190] H. Pontzer, "Predicting the energy cost of terrestrial locomotion: a test of the LiMb model in humans and quadrupeds," *Journal of Experimental Biology*, vol. 210, no. 3, pp. 484–494, 2007.

[191] N. A. Bernstein, *The Co-ordination and regulation of movements*. Pergamon Press Ltd., 1967.

[192] S. Martelli, D. Calvetti, E. Somersalo, and M. Viceconti, "Stochastic modelling of muscle recruitment during activity," *Interface Focus*, vol. 5, no. 2, p. 20140094, 2015.

[193] C. S. Simpson, M. Hongchul Sohn, J. L. Allen, and L. H. Ting, "Feasible Muscle Activation Ranges Based on Inverse Dynamics Analyses of Human Walking," *Journal of Biomechanics*, p. BMD1401187, 2015.

[194] A. G. Schache, T. W. Dorn, G. P. Williams, N. A. Brown, and M. G. Pandy, "Lower-Limb Muscular Strategies for Increasing Running Speed," *Journal of Orthopaedic & Sports Physical Therapy*, vol. 44, no. 10, pp. 813–824, 2014.

[195] W. Hoogkamer, S. Kipp, J. H. Frank, E. M. Farina, G. Luo, and R. Kram, "A Comparison of the Energetic Cost of Running in Marathon Racing Shoes," *Sports Medicine*, vol. 48, no. 6, pp. 1521–1522, 2018.

[196] S. Kipp, R. Kram, and W. Hoogkamer, "Extrapolating Metabolic Savings in Running: Implications for Performance Predictions," *Frontiers in Physiology*, vol. 10, no. February, pp. 1–8, 2019.

[197] "Strava year in sport," https://blog.strava.com/press/strava-releases-2019-year-in-sport-data-report/, Jan 2020.

[198] D. J. Braun, V. Chalvet, T.-H. Chong, S. S. Apte, and N. Hogan, "Variable stiffness spring actuators for low-energy-cost human augmentation," *IEEE Transactions on Robotics*, vol. 35, no. 6, pp. 1435–1449, 2019.

[199] S. Diller, C. Majidi, and S. H. Collins, "A lightweight, low-power electroadhesive clutch and spring for exoskeleton actuation," in *IEEE International Conference on Robotics and Automation*, 2016, pp. 682–689.

[200] G. Pfurtscheller, G. R. Müller, J. Pfurtscheller, H. J. Gerner, and R. Rupp, "'Thought'–control of functional electrical stimulation to restore hand grasp in a patient with tetraplegia," *Neuroscience Letters*, vol. 351, no. 1, pp. 33–36, 2003.

[201] M. Capogrosso, T. Milekovic, D. Borton, F. Wagner, E. M. Moraud, J.-B. Mignardot, N. Buse, J. Gandar, Q. Barraud, D. Xing *et al.*, "A brain–spine interface alleviating gait deficits after spinal cord injury in primates," *Nature*, vol. 539, no. 7628, pp. 284–288, 2016.

[202] Y. Ding, M. Kim, S. Kuindersma, and C. J. Walsh, "Human-in-the-loop optimization of hip assistance with a soft exosuit during walking," *Science Robotics*, vol. 3, no. 15, p. eaar5438, 2018.

[203] W. Felt, J. C. Selinger, J. M. Donelan, and C. D. Remy, ""Body-in-the-loop": Optimizing device parameters using measures of instantaneous energetic cost," *PloS one*, vol. 10, no. 8, 2015.